
[All ETDs from UAB](#)

[UAB Theses & Dissertations](#)

2005

A comprehensive study of woven carbon fiber -reinforced nylon 6 composites.

Selvum Pillay
University of Alabama at Birmingham

Follow this and additional works at: <https://digitalcommons.library.uab.edu/etd-collection>

Recommended Citation

Pillay, Selvum, "A comprehensive study of woven carbon fiber -reinforced nylon 6 composites." (2005). *All ETDs from UAB*. 5468.
<https://digitalcommons.library.uab.edu/etd-collection/5468>

This content has been accepted for inclusion by an authorized administrator of the UAB Digital Commons, and is provided as a free open access item. All inquiries regarding this item or the UAB Digital Commons should be directed to the [UAB Libraries Office of Scholarly Communication](#).

A COMPREHENSIVE STUDY OF WOVEN CARBON FIBER-REINFORCED
NYLON 6 COMPOSITES

by

SELVUM PILLAY

A DISSERTATION

Submitted to the graduate faculty of The University of Alabama at Birmingham,
in partial fulfillment of the requirements for the degree of
Doctor of Philosophy

BIRMINGHAM, ALABAMA

2005

UMI Number: 3201175

Copyright 2005 by
Pillay, Selvum

All rights reserved.

INFORMATION TO USERS

The quality of this reproduction is dependent upon the quality of the copy submitted. Broken or indistinct print, colored or poor quality illustrations and photographs, print bleed-through, substandard margins, and improper alignment can adversely affect reproduction.

In the unlikely event that the author did not send a complete manuscript and there are missing pages, these will be noted. Also, if unauthorized copyright material had to be removed, a note will indicate the deletion.

UMI[®]

UMI Microform 3201175

Copyright 2006 by ProQuest Information and Learning Company.

All rights reserved. This microform edition is protected against unauthorized copying under Title 17, United States Code.

ProQuest Information and Learning Company
300 North Zeeb Road
P.O. Box 1346
Ann Arbor, MI 48106-1346

Copyright by
Selvum Pillay
2005

ABSTRACT OF DISSERTATION
GRADUATE SCHOOL, UNIVERSITY OF ALABAMA AT BIRMINGHAM

Degree Ph.D. Program Materials Engineering

Name of Candidate Selvum Pillay

Committee Chairs Gregg M. Janowski and Uday K. Vaidya

Title A Comprehensive Study of Woven Carbon Fiber-Reinforced Nylon 6 Composites

Liquid molding of thermoset composites has become very popular in all industry sectors, including aerospace, automotive, mass transit, and sporting goods, but the cost of materials and processing has limited the use to high-end applications. Thermoplastic composites are relatively cheap; however, the use has been limited to components with short fiber reinforcing. The high melt viscosity and short processing window precludes their use in the liquid molding of large structures and applications with continuous fiber reinforcement.

The current research addresses the processing parameters, methodology, and limitations of vacuum assisted resin transfer molding (VARTM) of carbon fabric-reinforced, thermoplastic polyamide 6 (PA6). The material used is casting grade PA6. The process developed for using VARTM to produce carbon fabric-reinforced PA6 composites is explained in detail. The effects of infusion temperature and flow distance on the fiber weight fraction and crystallinity of the PA6 resin are presented. The degree of conversion from monomer to polymer was determined. Microscopic studies to show the wet-out of the fibers at the filament level are also presented.

Tensile, flexural, short beam shear strength (SBSS), and low-velocity impact test results are presented and compared to a equivalent thermoset matrix composite. The rub-

ber toughened epoxy system (SC-15) was chosen for the comparative study because the system has been especially developed to overcome the brittle nature of epoxy composites.

The environmental effects of moisture and ultraviolet (UV) radiation on the carbon/nylon 6 composite were investigated. The samples were immersed in boiling water for 100 hr, and mechanical tests were conducted. Results showed that moisture causes plasticization of the matrix and attacks the fiber matrix interface. This leads to deterioration of the mechanical properties. The samples were also exposed to UV for up to 600 hr, and post exposure tests were conducted. The exposure to UV caused an increase in the degree of crystallinity of the PA6. The mechanical properties were not affected by the exposure to UV for 600 hr.

DEDICATION

This work is dedicated to my mother for her unconditional love, my late father for tattooing the phrase “they can take everything but not your education” on my brain, and my late brother Joe for his belief in me.

To my wife, Thirumanie, and daughters Thamendrie and Huvanya who had to survive four years of hardship with me, this work is a testament of your love.

ACKNOWLEDGEMENTS

There are many people without whom this dissertation would not have been completed, and I could never properly thank each and every one for their assistance. First, I thank my research mentors, Dr. Gregg M. Janowski and Uday K. Vaidya. Their constant support, guidance, and willingness to take on the challenges presented by this research kept me motivated throughout. Many thanks go also to the remaining members of my committee – Drs. Derrick Dean, Mark Weaver, Nasim Uddin, and Mr. George Husman – for their time, support, and input as the project progressed.

The financial support by the Federal Transit Administration (FTA), Project AL-26-7001 and Southern Research Institute, Birmingham, Alabama, is graciously acknowledged. I am thankful to Bruggemann Chemicals, Airtech, and General Sealants for all of the supplies they provided at no charge.

I thank the Durban Institute of Technology, my employers in South Africa, for granting me study leave so that I could pursue this work. I would also like to thank the National Research Foundation (NRF-SA) and Kentron for their financial support during my stay in the USA.

The support of Drs. Andrews, Chawla, Griffin, Patterson, and Eberhardt is greatly appreciated. I thank Ms. Cheri Moss and Dr. Jonathan Sullivan for their help with the SEM imaging.

To my fellow graduate students – Rebecca O Davis, Haibin Ning, Shane Bartus, Chad Ulven, and the rest of the composites and polymers group – without your help this long journey would have been impossible.

To all of the other faculty, staff, and students of the MSE department who have not been mentioned, your friendship, help, and support is also appreciated. To my family and friends in South Africa, thank you for your love and encouragement through this endeavor.

To my mother, who has loved me unconditionally and has always believed in my abilities to succeed, I cannot thank you enough. It is your love and belief in me, even through very trying times that has taken me to this point. I would like to thank my children Tammy and Huvanya for their patience, understanding and love during this very trying period. Finally I would like to thank my dear wife, Thiru. It is your love, support, patience, and friendship over the years that have resulted in the successful completion of this work.

TABLE OF CONTENTS

	<i>Page</i>
ABSTRACT.....	iii
DEDICATION.....	v
ACKNOWLEDGEMENTS.....	vi
LIST OF TABLES.....	x
LIST OF FIGURES.....	xi
LIST OF ABBREVIATIONS.....	xv
INTRODUCTION.....	1
Anionically Polymerized Nylon 6.....	2
Vacuum Assisted Resin Transfer Molding (VARTM).....	4
Effects of Moisture and Ultra-Violet Irradiation on Nylon 6.....	5
Objectives.....	6
Experimental Approach.....	7
Processing and Materials.....	7
Microscopy and Thermal Characterization.....	9
Static and Dynamic Mechanical Testing.....	10
Moisture Absorption.....	12
UV Exposure.....	13
Organization of the Work.....	13
LIQUID MOLDING OF CARBON FABRIC-REINFORCED NYLON MATRIX COMPOSITE LAMINATES.....	15
MECHANICAL CHARACTERIZATION AND CRYSTALLIZATION STUDY OF LIQUID MOLDED CARBON FABRIC-REINFORCED NYLON MATRIX COMPOSITE LAMINATES.....	48
EFFECTS OF MOISTURE AND UV EXPOSURE ON LIQUID MOLDED CARBON FABRIC-REINFORCED NYLON 6 MATRIX COMPOSITE LAMINATES.....	76
GENERAL SUMMARY.....	116
FUTURE WORK.....	119

TABLE OF CONTENTS (Continued)

GENERAL LIST OF REFERENCES 120

LIST OF TABLES

<i>Table</i>	<i>Page</i>
MECHANICAL CHARACTERIZATION AND CRYSTALLIZATION STUDY OF LIQUID MOLDED CARBON FABRIC REINFORCED NYLON MATRIX COMPOSITE LAMINATES	
1 Average results of tensile tests performed for C/PA6 and C/SC-15 composite systems.	58
2 Average results of flexure tests performed for carbon/nylon 6 and carbon/SC-15 composite systems.	59
3 Average results of short beam shear tests performed for carbon/nylon 6 and carbon/SC-15 composite systems.	60
4 Average results of impact tests performed for C/PA6 and C/SC-15 composite systems.	62
EFFECTS OF MOISTURE AND UV EXPOSURE ON LIQUID MOLDED CARBON FABRIC REINFORCED NYLON 6 MATRIX COMPOSITE LAMINATES	
1 Sample sizes prepared for different tests.	85
2 Average results of flexure tests performed for carbon/nylon 6 samples; M – samples exposed to moisture; MD- samples exposed to moisture, then dried; D- samples processed and then dried to remove any moisture.	93
3 Average results of flexure tests performed for carbon/nylon 6 samples, for various number hours of UV exposure.	93
4 Average results of SBSS tests performed for carbon/nylon 6 samples; M – samples exposed to moisture; MD- samples exposed to moisture, then dried; D- samples processed and then dried to remove any moisture.	95
5 Average results of SBSS tests performed for carbon/nylon 6 samples, at various number hours of UV exposure.	95

LIST OF FIGURES

<i>Figure</i>	<i>Page</i>
LIQUID MOLDING OF CARBON FABRIC REINFORCED NYLON MATRIX COMPOSITE LAMINATES	
1	Reaction mechanism of anionic polymerization (AP) of caprolactam.....33
2	Time – viscosity curves at different temperatures (adapted from Sibal et al. [23]).34
3	Time–temperature profile of the tool; thermocouple positioned on surface of the carbon fabric preform and measurement conducted under 91.4 kPa of vacuum.35
4	Schematic of the processing system.36
5	Optical micrographs showing wet-out of the fiber tows.37
6	SEM image showing a cross section of fiber filaments fully impregnated by the nylon 6 resin.38
7	SEM image showing impregnation of the filaments along the length.39
8	Time – temperature profile of a typical carbon/nylon 6 process.....40
9	Typical TGA scan of the caprolactam monomer, neat polymer, and carbon/nylon6 composite sample.41
10	Flow distance versus percentage fiber weight fraction of panels processed at 150°C and panels infused at 100°C and ramped to 150°C.....42
11	DSC scan of neat polymer reacted at 150°C under a nitrogen environment.....43
12	DSC thermogram of panel infused at 150°C with samples taken along the flow length.....44
13	DSC thermogram of panel infused at 100°C and ramped to 150°C with samples taken along the flow length.45
14	Flow distance versus melt temperature for samples from both processing conditions and the neat polymer processed at 150°C.....46

LIST OF FIGURES (Continued)

<i>Figure</i>	<i>Page</i>
15 Flow distance versus degree of crystallinity for samples from both processing conditions and the neat polymer processed at 150°C.....	47

MECHANICAL CHARACTERIZATION AND CRYSTALLIZATION STUDY OF
LIQUID MOLDED CARBON FABRIC REINFORCED NYLON MATRIX
COMPOSITE LAMINATES

1 DSC thermograms of sections taken from the top, middle, and bottom (tool face) of carbon/nylon 6 composite panels.	67
2 XRD scans of neat anionically polymerized nylon 6 and sections taken from the top, middle, and bottom (tool face) of carbon/nylon 6 composite panels	68
3 Typical failed sample in tension of carbon/PA6 composite sample. Failure occurred within the gage	69
4 Typical failed sample in flexure of carbon/nylon 6 composite sample.....	70
5 Load – deflection curve from flexure test, comparing carbon/nylon 6 to carbon/SC-15 composites.....	71
6 Typical failed sample after short beam shear test	72
7 Typical force/energy – time curve for carbon/PA6 composite samples for various energy levels	73
8 Typical force/energy – time curve for carbon/SC-15 composite samples for various energy levels	74
9 Force/energy – time curve for carbon/nylon 6 and carbon/SC-15 composite samples at maximum energy level.	75

LIST OF FIGURES (Continued)

<i>Figure</i>	<i>Page</i>
EFFECTS OF MOISTURE AND UV EXPOSURE ON LIQUID MOLDED CARBON FABRIC REINFORCED NYLON 6 MATRIX COMPOSITE LAMINATES	
1	SEM image of carbon/nylon 6 composite surface cracks after exposure to water at 100°C for 100 h101
2	SEM image of carbon/nylon 6 composite showing fiber matrix interface degradation after exposure to water at 100°C for 100 h.....102
3	SEM image of carbon/nylon 6 composite showing the fiber matrix interface after processing.....103
4	Curve showing percentage water absorption against the square root of time for the different types of samples immersed in water at 100°C.104
5	Curve showing percentage water absorption against the square root of time for the ASTM D 570 samples immersed in water at 100°C compared to the dual diffusivity and Fickian models.105
6	DSC thermograms for samples immersed in water at 100°C for 100 h, after recovery and dry samples.106
7	DSC thermograms for samples exposed to UV for 100, 200, 300, 420, and 600 h107
8	Typical failed carbon/nylon 6 sample tested in flexure after immersion in water at 100°C for 100 h.108
9	Typical failed carbon/nylon 6 sample tested in flexure after exposure to UV for 100 h.109
10	Typical failed SBSS sample, with initial failure crack at the midsection, as highlighted in the image.110
11	Typical force/energy – time curves for carbon/nylon 6 composite material exposed to moisture at 100°C; M- exposed to moisture, MD- exposed to moisture then dried, D- as processed and dried.....111
12	SEM image of moisture exposed sample after low velocity impact test.....112

LIST OF FIGURES (Continued)

<i>Figure</i>	<i>Page</i>
13 SEM image of as processed, dry sample after low velocity impact test.	113
14 SEM image of sample exposed to 600 h of UV and then tested under low velocity impact conditions.....	114
15 Typical force/energy – time curves for carbon/nylon 6 composite material exposed to UV for 600 h.	115

LIST OF ABBREVIATIONS

AP	Anionic Polymerization
APA	Anionic Polyamide
ASTM	American Society for Testing and Materials
ATHAS	Advanced Thermal Analysis Laboratory
C/PA6	Carbon/Polyamide 6
DSC	Differential Scanning Calorimeter
ILSS	Interlaminar Shear Strength
LVI	Low Velocity Impact
PA6	Polyamide 6
PBT	Polybutylene Therephthalate
RIM	Reaction Injection Molding
RTM	Resin Transfer Molding
SBS	Short Beam Shear
SBSS	Short Beam Shear Strength
SEM	Scanning Electron Microscopy
TGA	Thermal Gravimetric Analysis
UTS	Ultimate Tensile Strength
UV	Ultra Violet
VARTM	Vacuum Assisted Resin Transfer Molding

LIST OF ABBREVIATIONS (Continued)

VOC Volatile Organic Compound

XRD X-ray Diffraction

INTRODUCTION

The use of polymer matrix composite materials in commercial applications, namely aerospace, automotive, and sporting goods, has become common practice today. The main drivers have always been weight savings and improved performance. The majority of developments in thermoset matrix composites have been pioneered by the aerospace industry, as the costs were initially very high and could be justified by the potential weight savings and improved performance. The production requirements of the aerospace industry are also very low and can justify the long processing times required for thermoset resin composites.

The automotive industry has pioneered most of the developments in thermoplastic matrix composites, as very low costs and high-volume production are a requirement of this sector. The annual United States market for thermoplastic matrix composites is currently in excess of one billion pounds, half of which is consumed by the automotive industry [1,2]. By adapting and developing liquid molding processes for thermoplastic composites, the use of these materials can be expanded into structural and semi-structural applications.

Thermoplastic composites have been limited to products that can be manufactured using processes like injection molding, compression molding, and extrusion. These techniques accommodate short fiber lengths but are incompatible with continuous woven fabrics and long fibers. However, the mechanical properties, especially the impact resistance, of thermoplastic composites improve with an increase in fiber length [3,4]. Woven

fabric can be combined with thermoplastic resins, such as polyetheretherketone and polyetherketone, using an autoclave under high temperatures ($>400^{\circ}\text{C}$) and pressures (>850 kPa), which is a very expensive processing approach. Vacuum assisted resin transfer molding (VARTM) has been very well developed and is now a proven, low-cost manufacturing technique for thermoset resin composites [5,6]. Unfortunately, the high melt viscosity of thermoplastic resins generally precludes the use of VARTM due to poor impregnation or mold fill, which can only be overcome by either significantly lowering the viscosity of the resin or reducing the flow distance. Furthermore, VARTM utilizes a closed mold system that allows zero volatile organic compounds (VOCs) and uses a single-sided tool, which reduces part cost.

Anionically Polymerized Nylon 6

Schlack [7] (1938) first reported the conversion of dry ϵ -caprolactam to ϵ -aminocaproic acid polymer by heating it in a sealed tube in the absence of air at 220 - 250°C for a prolonged period of time. He reported that the reaction is very slow, and heating periods of 200 h are required to achieve appreciable polymerization of the dry ϵ -caprolactam.

The process of anionic polymerization of ϵ -caprolactam was first developed by Joyce et al. [8,9] in 1941. It is a base catalyzed reaction that requires anhydrous conditions and is characterized by high rates of conversion and molecular weights. Equilibrium conversions are achieved within a few minutes.

The anionically polymerized nylon 6 properties compare favorably with the properties of nylon 6 produced by the conventional hydrolytic polymerization process [10].

An excellent review of the chemistry, mechanisms, properties, and processes of nylon 6 is presented by Reimschuessel [10].

A process for using the anionically polymerized polyamide 6 (APA) 6 systems for the liquid molding or, more specifically, reaction injection molding (RIM) of composites, was investigated in the early 1980s by Sibal and coworkers [11]. The following criteria were listed as conditions for successful implementation in RIM applications:

1. The reaction must proceed at reasonable rates without the uncontrolled formation of by products.
2. The initial viscosities of the reactants must be low enough to allow for good impingement mixing.
3. The viscosity must increase slowly enough to permit filling of the entire mold cavity without turbulence.
4. The material, once in the mold, must build modulus and strength rapidly to reduce demolding times.
5. The part must release easily from the mold.
6. There must be minimal shrinkage.
7. The reactants must have reasonable stability of reactants in storage tanks.
8. The reactants must be compatible with typical materials of construction.

Sibal investigated and reported on the reaction kinetics of APA6 for use in RIM.

Nylon block copolymers for RIM (NYRIM)TM were developed by Mooij [12]. The nylon block copolymer is formed by the reaction of anionically polymerized (AP)-caprolactam with a prepolymer (NYRIM), which is an activated impact modifier (rubber). The amount of the prepolymer can be between 10 and 40%, depending on the de-

sired properties of the composite. Extensive research has also been carried out by Gabbert and coworkers [13-16] using nylon 6 and nylon 6 block copolymers for resin transfer molding (RTM) and RIM.

The interest in nylon 6 for liquid molding of composites dwindled after the mid 1980s. A renewed interest in the capabilities of nylon 6 and other thermoplastics for liquid molding of composites has recently been driven by environmental regulations, economics, and improved performance requirements of components and structures. This has led to substantial investigations recently into the liquid molding of thermoplastic resin composites using the matrices anionic polyamide 12 (APA12) [17,18], cyclic polybutylene terephthalate (PBT) [19,20], and anionic polyamide 6 (APA6) [21,22]. Anionic ring opening polymerization of lactams has been studied extensively by many researchers in both academia [23-25] and industry [26-29].

Thermoset infusion techniques can be used for thermoplastics by either significantly lowering the viscosity of the resin or reducing the flow distance. By accomplishing this, the advantages of thermoplastics over thermosets of cost, faster cycle times, superior impact properties, and recyclability can be brought to composite materials and structures.

Vacuum Assisted Resin Transfer Molding (VARTM)

Resin infusion techniques have been extensively developed and studied over the years for the efficient manufacture of composite parts and structures [5,6]. The Marco method [30] was developed and patented in the USA in 1950. This was a closed mold method developed for the manufacture of boat hulls. Dry reinforcement was placed onto a male tool and a semi-flexible/splash female tool was used for consolidation and to pro-

vide a seal for the application of vacuum. In 1978, Gotch [31] detailed the use of vacuum impregnation using one solid tool and a silicone rubber diaphragm bag. Liquid resin was poured onto the preform, which was then bagged by the silicone rubber. The vacuum was applied to evenly distribute the resin into the preform. He later developed the process further by first bagging the preform and then applying vacuum pressure to draw the resin into the fiber bed [32,33]. Many variations of the process have since been developed and extensively used in composites manufacture.

Effects of Moisture and UltraViolet Irradiation on Nylon 6

The main limitation of using nylon 6 matrix composite structures, especially in exterior components or in high humidity applications, is the propensity of the material to absorb moisture. The absorbed moisture not only plasticizes the matrix as in the unreinforced system but also attacks the fiber matrix interface [34]. The combined effects of temperature and moisture, known as hygrothermal aging, are more damaging to the composite than either effect alone and have a detrimental effect on the composite [35-37]. Hygrothermal swelling causes a change in the residual stresses within the composite and could lead to micro-crack formation. The micro-cracks provide a fast diffusion path and may alter the moisture absorption characteristics of the laminate [38]

The effect of ultraviolet (UV) light irradiation on the composite is also an area that needs to be investigated, especially for components for exterior applications. The ultraviolet spectrum from intense sunlight may break the bonds of the molecules, resulting in the structural capacity degradation of the material [39]. The effects of ultraviolet radiation on polymers has been investigated by other researchers and depending on the expo-

sure time and intensity, can cause mere discoloration or complete breakdown of the polymer by chain scission [40,41].

Objectives

1. Processing – Develop the processing parameters and methodology of using VARTM for nylon 6 matrix composites.
2. Characterization – Optical microscopy and scanning electron microscopy (SEM) to establish effective fiber impregnation. Differential scanning calorimeter (DSC) tests for polymerization and degree of crystallinity, Soxhlet extraction to determine degree of polymerization.
3. Mechanical testing – Tensile, three-point bend, interlaminar shear strength, low-velocity impact. Data to be compared to identical panels produced using SC-15 resin (rubber toughened thermoset resin).
4. Environmental effects on woven carbon – nylon 6 composite panels. Studies to be conducted on the effects of temperature, moisture, and UV radiation on carbon – nylon post exposure mechanical tests (as above) to be conducted to establish the effects of the environmental exposure on these composites.
5. Diffusion models – Apply and/or modify existing diffusion models for moisture absorption of carbon/nylon 6 composites and compare to experimental data.

Experimental Approach

The experimental approach for this study is divided into the following subsections: (1) processing of carbon/nylon 6 composite panels, (2) optical and thermal characterization, (3) static and dynamic mechanical testing, namely tensile, flexure, short beam shear strength, and low-velocity impact tests, (4) moisture exposure, and (5) UV exposure. The relevant constituent materials, processing and test methods are discussed.

PROCESSING AND MATERIALS

There are several different techniques that can be used for the processing of polymer matrix composites, including hand lay-up, liquid infusion, autoclave molding, and filament winding. This study focused on developing an inexpensive method of liquid molding of carbon fabric-reinforced nylon 6 resin composite panels. VARTM was chosen as the system to explore because it uses very low-cost tooling and produces composites with low void content and high volume fractions of fiber.

Resin system

The current study will use polyamide 6 (PA6), a well-known commodity thermoplastic resin that has been used extensively for nylon casting applications. AP grade caprolactam monomer was used and has low levels of moisture (<0.0015% by mass), a low melting point ($T_M = 69^\circ\text{C}$), and low viscosity (4.87 mPa·s at 100°C). Bruggolen C20, hexamethylene dicarbamoyl dicaprolactam, and Bruggolen C10, sodium caprolactamate, both especially developed for AP of caprolactam, were used as the activator and catalyst,

respectively. The melt temperature of both C10 and C20 is 60°C. The catalyst and activator are used to control the speed and quality of the AP process. The monomer, catalyst, and activator were supplied by Bruggemann Chemical U.S., Inc., and were used without any further processing or purification. Due to the sensitivity to moisture of the catalyst and activator, they were stored and handled in a dry box with the relative humidity maintained at 8%.

The anionic ring opening polymerization of caprolactam follows an activated monomer mechanism. The chain growth reaction proceeds by the interaction of an activated monomer with the growing chain end.

A rubber toughened SC-15 resin was chosen for comparative studies, as this resin has been specially developed to improve the toughness of thermoset matrix composites. The SC-15 resin was supplied by Applied Polymeric, Inc. The resin was a two-part system, a base resin and a catalyst, with a manufacturer-specified ratio of 70:30. The ambient viscosity of the resin is 400 mPa•s, which allows for a working time of approximately 4 h at 20°C.

Reinforcements

Carbon fabric was chosen as the reinforcement in this study because of its superior mechanical properties. The fabric used in this study was supplied by US Composites and was a 4 harness satin weave, with a 3K tow size and an areal density and thickness of 0.02 g/cm² and 0.254 mm, respectively. The fabric was washed in acetone to remove lubricants and sizing, then was placed in a recirculating oven at 100°C for 1 h to remove

residual moisture and/or acetone. The fabric was used as supplied for infusion of the rubber toughened SC-15 resin.

MICROSCOPY AND THERMAL CHARACTERIZATION

Microscopy

Optical and scanning electron microscopes were used to assess the level of fiber impregnation on both the tow and filament level. They were also used to characterize the damage due to moisture ingress and UV exposure. Failure modes after mechanical testing were assessed using OM and SEM. A thorough visual observation were made of the specimens, and typical images were captured.

Thermal Gravimetric Analysis (TGA)

Thermal gravimetric analysis was performed to study the mass loss of the resin from the composite and to establish the degradation temperature of the resins. A TA Instruments TGA 2950 was used for this study. Measurements were done under nitrogen to prevent oxidation of the carbon fiber. A scan rate of 10°C/min was used, and the samples were run to 700°C.

Differential Scanning Calorimeter

The thermal behavior of the processed composite was evaluated by using a TA Instruments Q100 DSC. The heat flow as a function of time was established. The samples were heated from 40 to 250°C at rate of 10°C/min. The melt temperatures were obtained from these curves, and single peaks versus multiple peaks were used as an early indica-

tion of the success of polymerization of the nylon 6. The crystallinity calculations were done by integrating the area under the peaks of the DSC thermograms to obtain the heat of fusion, ΔH . These values were compared to the theoretical heat of fusion for a 100% crystalline structure.

STATIC AND DYNAMIC MECHANICAL TESTING

Tensile

Tensile tests were conducted according to ASTM D 3039M using samples of dimensions 12.5 x 250 mm cut from the panel. The sample ends were tabbed with an epoxy/glass material, dimensions 12.5 x 63 x 0.85 mm, with the tab ends tapered to 5°. The tabs were bonded to the sample using a Three Bond™ thermoplastic adhesive. Samples were tested in a servo-hydraulic tensile test machine at a displacement rate of 2 mm/min. with a gage length of 120 mm. The change in length of the sample was measured using a clip-on extensometer, which was detached prior to failure.

Flexure

Three-point bend tests were conducted according to ASTM D 790M. Samples of the dimensions 10 x 80 x 4 mm were prepared from the panel. The support span was set at 64 mm, and the rate of cross-head motion was 1.7 mm/min. The load as a function of displacement was recorded.

Interlaminar Shear Stress

Short beam shear (SBS) tests were conducted according to ASTM D2344 to measure the interlaminar shear stress of the composites. Samples of the dimensions 10 x 24 x 4 mm were prepared from the panel. The support span was set at 16 mm, and the rate of cross-head motion was 1 mm/min. The beams were loaded in three-point bending such that the dominant failure was shear. A variety of failure modes (bending, plastic indentation, and compressive) can occur that can skew the results, and care must be taken to examine the failed specimen to ensure that failure occurs at the midsection or neutral axis of the beam, which is indicative of shear failure. The tests do not purport to be absolute; however, they are a good indication of the interlaminar shear strength of the composite.

Impact

Low-velocity impact (LVI) tests were conducted to study the resistance to impact and damage initiation and propagation of the composite panels. An instrumented drop weight tower equipped with a load cell of capacity 1590 kg was used to conduct the tests. A hemispherical shaped tup of diameter 19.5 mm and mass 0.12 kg was used as the impactor. The total impactor mass, including the tup, was 6.15 kg. The samples were clamped using a pneumatic assist mechanism, such that a 76.2 mm (3") diameter of the sample face was exposed to the impactor. Three impact heights, 0.46 m, 0.71 m, and 1.15 m, were chosen in order to capture the dominant failure modes of the plates from incipient to total failure and to analyze the energy absorption mechanism and damage progres-

sion. The force-time, energy-time, and load-deflection responses of the samples were measured. Damage initiation and progression was monitored.

MOISTURE ABSORPTION

Since the focus of this study was to evaluate the deterioration in mechanical properties of the carbon fabric-nylon 6 matrix composite, it was decided to expose the material to the most aggressive moisture condition, i.e., immersed in water at 100° C. The specimens were cut from the panels using a diamond blade saw and then polished with 600 grit silicon carbide paper to minimize any cracking or debonding on the edges. The following sizes of specimens were prepared for the different tests:

100 x 100 mm	LVI
10 x 80 mm	Flexure
9 x 25 mm	Short beam shear strength (SBSS)
25 x 75 mm	Moisture absorption (ASTM D-570)

The specimens were then dried in an air-recirculating oven at 70°C and periodically weighed on a high precision balance with a 0.1 mg resolution, until the weight had stabilized. The dry weight (W_d) of all the specimens was then recorded. The samples were then placed on a rack and fully submerged in boiling water. The temperature of the water was maintained at 100°C using a hotplate and oil bath to maintain even heating. The specimens were taken out at periodic intervals and weighed after excess moisture was removed. The percentage weight gain (equation below) was monitored as a function of the square root of time.

$$M = \frac{W_i - W_d}{W_d} \times 100$$

Where M = percentage weight gain; W_i = weight of moist material at a specific time; and W_d = dry weight.

The weight gain was plotted against the square root of time until the equilibrium weight gain (M_∞) was reached. The samples were then removed from the chamber, and 50% were put into a container with water at ambient temperature and taken for testing and evaluation, while the rest were placed in the recirculating oven at 70° C to dry. The same process as the preconditioning was used to remove the moisture. After the weight stabilized, the samples were placed in a desiccator and taken for testing and evaluation.

UV EXPOSURE

Specimens were cut and prepared for the LVI, flexure, and SBSS tests. The specimens were then placed in RTR 200 UV exposure chamber with 12 fluorescent bulbs that provide UV radiation at wavelengths of 200 to 400 nm within the chamber. The intensity was not measured because the chamber and bulbs was relatively new, and it was assumed that the manufacturer's specifications were still valid. The specimens were removed at 100, 200, 300, 420, and 600 h of exposure and tested and evaluated.

Organization of the Work

The focus of this study was to develop an affordable manufacturing system to process nylon 6 matrix composite structures using woven carbon fabric as the reinforcement. The thermal, static, and dynamic mechanical properties and degradation due to moisture and UV exposure of the material are also established.

The experimental and analytical results accompanied by discussions for each aspect of this study are organized into three interconnected manuscripts. Each manuscript builds from the other and is consistent with the objectives for the entire study.

Manuscript 1 reports on the processing parameters, methodology, and limitations of VARTM of carbon fabric-reinforced nylon 6 matrix composite panels. Microscopy studies to evaluate wet-out at both the tow and filament levels are presented. The degree of monomer conversion to polymer and the effects of infusion temperature and flow distance on fiber weight fraction and crystallinity are presented.

Manuscript 2 reports on the through-the-thickness crystallinity of carbon/nylon 6 composites using both DSC and X-ray diffraction (XRD). The degree of crystallinity of nylon 6 has a significant effect on the mechanical properties. The mechanical properties, including tensile strength, flexural strength, SBSS, and impact resistance, are evaluated. The static and dynamic mechanical properties of the carbon/nylon 6 are compared to equivalent carbon/SC-15 (rubber toughened) composite panels.

Manuscript 3 reports on the moisture absorption characteristics of the carbon/nylon 6 composite and compares the experimental results to a mathematical model. The samples were immersed in boiling water for 100 h. The effects of exposure to ultraviolet radiation for 600 h are also reported. The degradation of mechanical properties due to exposure to moisture and UV are evaluated and presented.

LIQUID MOLDING OF CARBON FABRIC-REINFORCED NYLON MATRIX
COMPOSITE LAMINATES

by

SELVUM PILLAY, UDAY K. VAIDYA, AND GREGG M. JANOWSKI

Journal of Thermoplastic Composite Materials, Vol. 18: 509-527

Copyright

2005

by

Sage Publications

Used by permission

Format adapted for dissertation

ABSTRACT

The present work addresses the processing parameters, methodology, and limitations of vacuum assisted resin transfer molding (VARTM) of carbon fabric-reinforced, thermoplastic polyamide 6 (PA6) matrix panels on the laboratory scale. VARTM is a mature technology for producing large-scale thermoset composite parts/structures but has not been used for thermoplastic composites, which are manufactured primarily by compression molding, extrusion, and/or injection molding. In general, liquid molding of thermoplastics has limitations, such as high resin viscosity, high temperature processing requirements, and a short processing window. The material used in this study are casting grade polyamide 6, ϵ -Caprolactam with a sodium-based catalyst, and an initiator. This system allows the resin to maintain a very low viscosity ($<1 \text{ Pa}\cdot\text{s}$) for a reasonable period of time at relatively low temperatures (100°C). The carbon fabric preform is infused using VARTM, after which the resin is fully polymerized in situ. The process developed for using VARTM to produce carbon fabric-reinforced, PA6 matrix composites is explained in detail. Microscopy studies are presented to evaluate wet-out of the fibers at both the tow and filament levels. The effects of infusion temperature and flow distance on the fiber weight fraction and crystallinity of the PA6 resin are investigated. The degree of monomer conversion to polymer was determined.

INTRODUCTION

Thermoplastic composites have gained steady favor over traditional materials such as steel in structural and semi-structural applications due to their specific strength, damping capacity, corrosion resistance, recyclability, and impact resistance. The annual

market for such materials in the United States is currently in excess of one billion pounds, half of which is consumed by the automotive industry [1, 2]. By adapting and developing liquid molding processes to thermoplastic composites, its use in structural and semi-structural applications can be expanded.

Thermoplastic composites have been limited to products that can be manufactured using processes like injection molding, compression molding, and extrusion. These techniques accommodate short fiber lengths but are incompatible with continuous woven fabrics and long fibers. However, mechanical properties, especially impact resistance, of thermoplastic composites improve with an increase in fiber length [3,4]. Woven fabric can be combined with some thermoplastic resins, such as polyetheretherketone and polyetherketone, using an autoclave under high temperatures ($>400^{\circ}\text{C}$) and pressures (>850 kPa), which is a very expensive processing approach. Vacuum assisted resin transfer molding (VARTM) has been very well developed and is now a proven, low-cost manufacturing technique for thermoset resin composites [5,6]. Unfortunately, the high melt viscosity of thermoplastic resins generally precludes the use of VARTM due to poor impregnation or mold fill, which can be overcome by either significantly lowering the viscosity of the resin or reducing the flow distance. Furthermore, VARTM utilizes a closed mold system that allows zero volatile organic compounds (VOCs) and uses a single-sided tool, which reduces part cost.

Recently, there has been substantial interest in liquid molding of thermoplastic resin composites using the matrices anionic polyamide 12 (APA12) [7,8], cyclic polybutylene terephthalate (PBT) [9,10], and anionic polyamide 6 (APA6) [11,12]. Anionic ring opening polymerization of lactams has been studied extensively by many researchers

in both academia [13-15] and industry [16-19]. The anionic polymerization (AP) of ϵ -caprolactam was first reported by Joyce and coworkers [20,21]. Caprolactam is the most popular type of lactam used commercially for the production of APA6 (also referred to as nylon 6 and PA6 in this paper). The properties of APA6 compare favorably with the properties of nylon 6 produced by the conventional hydrolytic polymerization process [22]. An excellent review of the different chemistry, mechanisms, properties, and processes of nylon 6 is presented by Reimschuessel [22].

A process for using the APA 6 systems for the liquid molding, or, more specifically, reaction injection molding (RIM) of composites, was investigated in the early 1980s by Sibal and coworkers [23]. Nylon block copolymers for RIM (NYRIM)TM were developed by Mooij [24]. The nylon block copolymer is formed by the reaction of AP-caprolactam with a prepolymer (NYRIM), which is an activated impact modifier (rubber). The amount of the prepolymer can be varied between 10 and 40%, depending on the desired properties of the composite. Extensive research has also been carried out by Gabbert and coworkers [25-28] using nylon 6 and nylon 6 block copolymers for resin transfer molding (RTM) and RIM.

The interest in nylon 6 for liquid molding of composites has dwindled since the mid 1980s. Renewed interest in the capabilities of nylon 6 and other thermoplastics for liquid molding of composites has recently been driven by environmental regulations (especially in Europe), economics, and improved performance requirements of components and structures.

This paper presents the processing parameters, methodology, and limitations of using VARTM for PA6 matrix composites. The current study will utilize APA6, a well-

known commodity thermoplastic resin that has been used extensively for nylon 6 casting applications. Microscopic studies that evaluate wet-out of the fibers at both the tow and filament levels are presented. The effects of infusion (temperature, flow distance) on the fiber weight fraction, and crystallinity of the PA6 resin are investigated. The degree of conversion of monomer to polymer was studied as a function of processing conditions.

MATERIALS

Carbon Fabric

The carbon fabric used in this study was supplied by US Composites and was a 4 harness satin weave, with a 3K tow size, and an areal density and thickness of 0.02 g/cm² and 0.254 mm, respectively. The fabric was washed in acetone to remove lubricants and sizing and then placed in a recirculating oven at 100°C for 1 h to remove residual moisture and/or acetone.

Monomer, Activator, and Catalyst

AP grade caprolactam monomer was used in this study. The monomer has low levels of moisture (<0.0015% by mass), low melting point ($T_M = 69^\circ\text{C}$), and low viscosity (4.87 mPa·s at 100°C). Bruggolen C20, hexamethylene dicarbamoyl dicaprolactam, and Bruggolen C10, sodium caprolactamate, both especially developed for the anionic polymerization of caprolactam, were used as the activator and catalyst, respectively. The melt temperature of both C10 and C20 was 60°C. The catalyst and the activator were used to control the speed and quality of the AP process. The monomer, catalyst, and activator were supplied by Bruggemann Chemical U.S., Inc., and were used without any fur-

ther processing or purification. Due to the moisture sensitivity of the catalyst and the activator, they were stored and handled in a dry box with the relative humidity maintained at 8%.

Reaction Mechanism

The anionic ring opening polymerization of caprolactam follows an activated monomer mechanism. The chain growth reaction proceeds by the interaction of an activated monomer with the growing chain end. The reaction path for polymerization is shown in Figure 1.

The anionic catalyst, C10, reacts with the lactam monomer to first form the salt, which in turn dissociates to the active species, namely, the lactam anion. Accordingly, a strongly dissociating catalyst in low concentrations is always preferable to a weakly dissociating catalyst in higher concentrations, which results in the probability of achieving a higher molecular weight polymer. It also speeds the polymerization process and results in a lower concentration of catalyst in the fully polymerized material. The catalytic activity of the various alkali metal and quaternary salts of lactam generally follow the extent of their ion dissociation, which in turn depends on the cation. Activity of a salt decreases with increasing size of the cation due to restricted mobility and decreased ionization potential.

PROCESSING

The kinetics of AP of caprolactam have been extensively reported in the literature, with various catalysts and activators, and at different temperatures. The majority of

the studies reported that a polymerization temperature of 130°C results in acceptable conversion from monomer to polymer. Magill [29] has reported that the temperature for maximum crystallization is about 140-145°C. Above this, the nucleation rate is low; viscous effects hinder crystal growth at low temperatures. Low temperatures also lead to premature crystallization and incomplete polymerization, as the reactive sites become trapped in the crystals. At 140-145°C, heterogeneous reaction conditions are encountered if there is simultaneous polymerization of caprolactam and crystallization of the nylon 6 formed during polymerization. It is not the scope of this study to conduct kinetic or rheological studies on the AP of caprolactam, but rather to use the available data and develop a practical process for use of APA 6 as an effective matrix for carbon fiber-reinforced composites. Most of the studies considered adiabatic and isothermal conditions, which are not practical for the VARTM process. The information, however, has been used as a guide for determining processing conditions.

The time-temperature-viscosity data developed by Sibal et al. [23] is shown in Figure 2. This study was repeated by van Rijswijk and coworkers [30], and the results were similar. These curves were used as a basis for the infusion and processing of the PA6 resin using VARTM. The viscosity change was very minimal for a substantial period of time at 100°C. This was ideal for VARTM since low viscosity is required to get full impregnation of the fibers. The hypothesis was to infuse at 100°C to obtain full wet-out in minimal time and then increase the temperature to accelerate the process of polymerization and minimize premature crystallization. Various temperatures between 130 and 160°C were used as the final set points for polymerization. 150°C was the minimum temperature that allowed acceptable conversion, visually, and was therefore used as the set

point for polymerization. The manufacturer's guide with respect to the amount of the catalyst and activator was used: 1.5 % activator (C20) to 3% catalyst (C10).

A 400 x 400 x 50 mm aluminum block was used as the tool for the preform lay-up. The aluminum block was fitted with heaters to achieve the required rate of temperature increase for effective polymerization. The heating profile of the tool is shown in Figure 3. The heating rate from 100 to 150°C is of particular importance in the process that was used in this work, as this was the required temperature ramp for polymerization.

Four 300 x 300 mm layers of carbon fabric were placed between two layers of porous TeflonTM cloth and then laid onto the tool surface. A thermocouple was positioned at the surface of the top layer of the carbon to record the temperature. The preform was then bagged and sealed using high temperature film and tacky tape. The tool temperature was then raised to 100°C, and a continuous vacuum of 98 kPa was applied to the system. The system was periodically purged with nitrogen to maintain a dry, inert atmosphere in the layup. A schematic of the processing system is shown in Figure 4.

The caprolactam was weighed in the dry chamber (<10% relative humidity) and put into a reaction kettle. The temperature was raised to 100°C, and the caprolactam was brought to a molten state. The catalyst and activator were then added to the reaction kettle. A mechanical stirrer was used to mix the system under a dry nitrogen environment since the catalyst is sensitive to moisture, and the caprolactam oxidizes rapidly at these temperatures. As soon as the entire solution was completely liquid, the resin was infused into the preform via a silicone rubber tube. When the preform was fully infused, the resin supply was cut off, and the tool temperature was raised to 150°C. The tool was held at this temperature until polymerization and crystallization were complete, which was de-

terminated by the observation of an exotherm. The heaters were then shut off, the tool was air cooled to 40°C, and the part was removed.

The process was also repeated with the tool temperature at 150°C at the onset, and the APA6 system was heated, maintained, and infused at 150°C. In this case, the viscosity of the resin increased too rapidly in the tool, and complete infusion of the preform did not occur. The resin flow was up to approximately 75% of the length of the preform and further flow was not possible. The tool was maintained at this temperature (150°C) until the exotherm was observed. The same process was repeated. The latter process was conducted to establish the differences in volume fraction, crystallinity, and conversion, if any.

Note that when the tool set points of 100 and 150°C are mentioned, this refers to the controller setting for the tool, which corresponds to the tool surface temperature. The actual temperature on the carbon surface was also measured, as shown in Figure 3.

RESULTS AND DISCUSSION

The composite panel was examined visually, and it appeared to have good consolidation, with full wet-out of the preform for the panel infused at 100°C and ramped to 150°C. The surface of the nylon appeared to be fully polymerized. The panel infused at 150°C did not fully wet-out the preform. However, the section that was wet-out seemed to also have good consolidation and fully polymerized resin.

Microscopy

Cross sections of the sample were cut, mounted, and polished for optical and scanning electron microscopy (SEM). The optical micrographs, shown in Figure 5, show very good wet-out of the fiber tows. The SEM images shown in Figures 6 and 7 illustrate good impregnation at the filament level. The resin around the fiber filament is clearly seen in the cross section, and the length of the fiber is also uniformly coated with resin. Wet-out at the filament level is due largely to capillary action, which is a function of resin viscosity. Low viscosity is one of the main factors that generally lead to very good wet-out at the filament level. There was no discernable difference in the wet-out of the fibers of the two processing conditions.

Processing

The time–temperature profiles of the tool and the part are shown in Figure 8. Note that the rate of increase of temperature of the tool only is constant up to 150°C. The infused system shows that the rate increases slightly at approximately 140°C, which is due to the exotherm of the PA6 system undergoing polymerization. The net increase in temperature is 5°C. A temperature increase due to crystallization is not observed. Literature reports values of 30°C increase in temperature due to the exotherm of the system. However, most of these studies were conducted with bulk polymerization of nylon 6. We attribute the low increase in temperature (5°C) to the polymerization of the low resin content within the composite panel and a panel thickness of only 0.85 mm. This is also the reason for the nonobservance of the onset of crystallization.

Thermal Gravimetric Analysis (TGA)

The weight fraction of carbon reinforcement as a function of flow distance from the infusion point was determined. Samples were taken from the point of infusion and every 50 mm thereof for both composite panels. Thermal gravimetric analysis (TGA) was performed using a TA Instruments TGA 2950. Measurements were done under nitrogen to prevent oxidation of the carbon fiber. A scan rate of 10°C/min was used, and the samples were run to 700°C. A typical TGA scan of the monomer, neat polymer, and composite sample is shown in Figure 9. The onset of degradation of the caprolactam monomer and neat polymer was 151.91 and 312.89°C, respectively. The onset of degradation of the polymer in the composite sample was 360.53°C; an increase of approximately 48°C in the degradation temperature of the polymer results from the composite structure. The increase in degradation temperature is attributed to the increase in crystallinity of the PA6 in the composite, which is covered in greater detail in the subsection titled 'Analysis of crystallization behavior.'

Figure 10 shows the results of the flow distance versus percentage fiber weight fraction of panels processed at 150°C and panels infused at 100°C and ramped to 150°C. The average weight fractions of the panels infused at 150 and 100°C were 52% and 64%, respectively. The fiber weight fraction at the infusion point of both panels is substantially lower than at the other positions. This is to be expected as most liquid molded composites are resin-rich at the point of infusion. However, the fiber weight fraction of the panel infused at 100°C is much more uniform compared to the panel infused at 150°C. The average fiber weight fraction is also 12% higher. This observation can be attributed to the high resin viscosity preventing excess resin from leaving the preform during infusion at

150°C. In the first condition (infusion at 100°C and ramp to 150°C), the resin has a low-enough viscosity for a long period of time, and the excess resin is evacuated.

Differential Scanning Calorimeter (DSC)

A TA Instruments Q100 differential scanning calorimeter (DSC) was used to characterize the thermal behavior of the neat polymer and the composite sample. The samples were heated from 40 to 250°C at the rate of 10°C/min. Figure 11 shows the DSC thermogram for the neat polymer processed at 150°C. Only one peak at the melt temperature of 220.06°C is observed. This implies that the amount of monomer present in the sample is negligible. Integration of the peak yields a heat of fusion (ΔH) value of 74.56 J/g.

Figures 12 and 13 illustrate the DSC thermograms for the samples from both the panels taken at the different flow distances. The scans show that the peaks are sharper and have more variation in the panels infused at 100°C and then ramped to 150°C than the panels infused at 150°C. However, the melt temperature appears to be more uniform.

Figure 14 shows the melt temperature with respect to the flow distance for both processing conditions and the melt temperature of the neat nylon processed at 150°C. The average melt temperature for the panels infused at 150°C and 100°C is 214.9°C and 218.2°C, respectively. The panel infused at 100°C and ramped to 150°C had a higher melt temperature, which was closer to the melt temperature of the neat polymer. The difference in the melt temperature of the panels is attributed to the higher degree of crystallinity of the samples infused at 100°C; this is explained in the following section. The melt

temperature across the flow distance is also a lot more stable with this panel (100°-150°C).

Analysis of Crystallization Behavior

Upon cooling, nylon 6 macromolecules exist partially in a disordered amorphous state and partially in an ordered crystalline state. The structure actually realized and the degree of crystallinity is influenced by a number of factors, which include applied stress, thermal conditions, and moisture. However, the temperature of polymerization has the largest influence on the degree of crystallinity in AP.

The crystallinity calculations were done by integrating the area under the peaks of the DSC thermograms to obtain the heat of fusion, ΔH . The average ΔH values for the panels infused at 150 and 100°C were 85.2 and 98.8 J/g, respectively. These values were compared to the theoretical heat of fusion for a 100% crystalline structure. Although various values have been reported in the literature for the theoretical ΔH , the value of 230 J/g, referenced from the ATHAS data bank [31], was used since it is the accepted value [32].

Figure 15 illustrates the flow distance versus the degree of crystallinity of the samples obtained from panels infused at 150°C and panels infused at 100°C and ramped to 150°C. The degree of crystallinity of the neat polymer (31.9%), processed at 150°C, is also shown. The average value for the panel processed at 150°C is 36% and that for the panel infused at 100°C is 40%. The infusion at a lower temperature and then ramping leads to an increase in the degree of crystallinity of 4%. The degree of crystallization was more consistent for the panel infused at 150°C. The polymerization for the panel infused

at 100°C is a function of time and the temperature gradient of the tool. The processing at 150°C is a function of time only; therefore, it exhibits more uniform crystallinity.

The increase in the degree of crystallinity results in an increase in modulus, abrasion resistance, heat distortion temperature, and resistance to moisture absorption. The trade off, however, is that both the resistance to impact damage and elastic strain decreases [22].

Conversion

The conversion from monomer to polymer is an important consideration in the VARTM process, as a poor degree of conversion leads to high levels of monomer in the composite panel, which in turn lead to inferior mechanical properties.

The panels were cut up into 20 x 20 mm pieces and ground into a powder using a Poly-Art micro mill. The chamber was cooled to 0°C while the samples were being ground to prevent heating of the samples, and hence, post processing conversion. The powdered samples were then weighed and 6-10 g of the powder were put into cellulose thimbles. A Soxhlet extraction was conducted using heated acetone for 36 h. The thimble containing the powder was then removed and left to dry under an extraction hood for 3 h. The thimbles were dried in an oven at 60°C for an additional 12 h, cooled, and weighed. TGA analysis was conducted on a part of each of the samples to establish the weight of the carbon fiber. The percent conversion was then calculated using Equation (1):

$$X = \frac{m_{ext} - m_{car}}{m_{tot} - m_{car}} * 100 \quad (1)$$

where X is the degree of conversion, m_{tot} is the total mass of powder before extraction, m_{car} is the mass of carbon, and m_{ext} is the mass of powder after extraction.

Samples could not be taken relative to the flow distance due to the low thickness of the panel (0.85 mm). Large sections had to be ground to get sufficient amounts of powder for the Soxhlet extraction. The conversion to polymer ranged between 97.5 and 98.5% for both panels, with the average conversion on the panels infused at 150 and 100°C being 97.98 and 98.01%, respectively.

CONCLUSIONS

Vacuum assisted resin transfer molding (VARTM), a method that is well established for thermosets, has been effectively used to infuse carbon fabric preforms with polyamide 6 resin. A process (resin/catalyst/activator, moisture minimization, infusion technique, and temperature control) was developed to (1) maintain a low resin viscosity for sufficient time for full wet-out of the preform, (2) attain good fiber impregnation, and (3) optimize polymerization of the resin. The VARTM method was significantly modified to accommodate the differences of the thermoplastic resin, especially with regard to temperature and moisture control. The method of infusing the resin at 100°C and ramping the temperature to 150°C, compared to infusing the resin at 150°C proved effective in achieving flow of the resin through the entire preform. The optical and scanning electron microscope images show that macroscopic and microscopic fiber impregnation was achieved.

The fiber weight percentage was fairly uniform in the panel infused at 100°C, which also had a higher fiber weight percent than the panel infused at 150°C. The differential scanning calorimetry data show an average melt temperature for the neat polymer and the panels infused at 150 and 100°C of 220.6, 214.9, and 218.2°C, respectively. The

panel infused at 100°C has a crystallinity that is about 5% higher than the panel infused at 150°C. The increase in crystallinity is a reasonable trade-off for the longer infusion time and effectiveness of the process, and also can be a benefit with respect to modulus and moisture absorption. The process also yields a relatively high degree of conversion from monomer to polymer, approximately 98% for both processing conditions.

ACKNOWLEDGEMENTS

The authors are grateful for the financial support for this work provided by the Federal Transit Administration (FTA), Project AL-26-7001 and Southern Research Institute, Birmingham, Alabama. We acknowledge the technical contributions of Dr. Derrick R. Dean, Mr. Haibin Ning, and Mr. Chad Ulven. The donation of materials by Bruggemann Chemical U.S., Inc., is also appreciated.

REFERENCES

1. Hartness, T., Husman, G., Koenig J., and Dyksterhouse, J. (2001). The Characterization of Low Cost Fiber Reinforced Thermoplastic Composites Produced by the Drift Process, *Composites: Part A*, **32**: 1155-1160.
2. Composites Manufacturers Association, www.acmanet.org.
3. Thomason, J.L. and Vlug, M.A. (1996). Influence of Fiber Length and Concentration on the Properties of Glass Fibre-reinforced Polypropylene: 1. Tensile and Flexural Modulus, *Composites: Part A*, **27A**: 477-484.
4. Bush, S.F., Torres, F. G. and Methven, J. M. (2000). Rheological Characterization of Discrete Long Glass Fibre (LGF) Reinforced Thermoplastics, *Composites: Part A*, **31**: 1421-1431.
5. Brouwer W.D., van Herpt E.C.F.C. and Labordus, M. (2003). Vacuum Injection Molding for Large Structural Applications, *Composites: Part A*, **34**: 551-558.
6. Williams, C., Summerscales, J. and Grove, S. (1996). Resin Infusion under Flexible Tooling (RIFT): A Review, *Composites: Part A*, **27A**: 517-524.

7. Zingraff, L., Bourban, P.E., Wakeman, M.D., Kohler, M. and Manson, J.A.E. (2002). Reactive Processing and Forming of Polyamide 12 Thermoplastic Composites, In: *23rd Europe SAMPE Conference Proceedings*, pp. 237-248.
8. Luiser, A., Bourban, P.E. and Manson, J.A.E. (1999). *In Situ Polymerization of Polyamide 12 for Thermoplastic Composites*, ICCM-12, Paris.
9. Ciovacco, J. and Winckler, S.J. (2000). Cyclic Thermoplastic Properties and Processing, In: *45th International SAMPE Symposium*, Long Beach, CA.
10. Parton, Hilde and Verpoest, Ignass (2003). *Reactive Processing of Textile Reinforced Thermoplastics*, ICCM 14, San Diego, CA.
11. van Rijswijk, K., Vlasveld, D.P.N., Bersee, H.E.N. and Picken, S.J. (2003). Vacuum injection of anionic polyamide 6, In: *Proceeding of ICCST 4*, Durban, South Africa.
12. Vlasveld, D.P.N., Van Rijswijk, K., Bersee, H.E.N., Beukers A. and Picken, S.J.N. (2003). *Process Considerations for Liquid Molding of Composites Based on Anionic Polyamide 6*, ICCM 14, San Diego, CA.
13. Sebenda, J. (1978). Recent Progress in the Polymerization of Lactams; Review, *Progress in Polymer Science*, **6**: 123-167,
14. Kim K.J., Hong, D.S., and Tripathy, A.R. (1997). Kinetics of Adiabatic Copolymerization of ϵ -Caprolactam in the presence of Various Activators, *Journal of Applied Polymer Science*, **66**: 1195-1207,
15. Petrov, P., Jankova, K. and Mateva, R. (2003). Polyamide-6-b-Polybutadiene Block Copolymers: Synthesis and Properties, *Journal of Applied Polymer Science*, **89**: 711-717.
16. Murthy, N.S., Kagan, V.A. and Bray, R.G. (2003). Optimizing the Mechanical Performance in Semi-Crystalline Polymers: Roles of Melt Temperature and Sin-Core Crystalline Morphology of Nylon, *Journal of Reinforced Plastics and Composites*, **22**: 685-693.
17. Udipi, K., Dave, R.S., Kruse, R.L. and Stebbins, L.R. (1997). Polyamides From Lactams Via Anionic Ring-opening Polymerization: 1. Chemistry and Some Recent Findings, *Polymer*, **38**: 927-938.
18. Udipi, K., Dave, R.S., Kruse, R.L. and Stebbins, L.R. (1997). Polyamides From Lactams Via Anionic Ring-opening Polymerization: 1. Kinetics, *Polymer*, **38**: 939-947.
19. Udipi, K., Dave, R.S., Kruse, R.L. and Stebbins, L.R. (1997). Polyamides From Lactams Via Anionic Ring-opening Polymerization: 1. Rheology, *Polymer*, **38**: 949-954.

20. Joyce, R.M. and Ritter, D.M. (1941). U.S. Patent 2,251,519.
21. Hanford, W.E. and Joyce, R.M. (1948). Polymeric Amides from Epsilon-Caprolactam, *Journal of Polymer Science*, **3**: 167-172.
22. Reimschuessel, H.K. (1977). Nylon 6 Chemistry and Mechanisms, *Journal of Polymer Science: Macromolecular Reviews*, **12**: 65-139.
23. Sibal, P.W., Camargo, R.E. and Macosko, C.W. (1982). Designing Nylon 6 Polymerization for RIM, In: *Proceedings of the Second International Conference on Reactive Processing of Polymers*, pp. 97-125, Pittsburgh, Pennsylvania.
24. Mooij, H. (1991). *SRIM Nylon Composites, Advanced Materials: Cost Effectiveness, Quality Control, Health and Environment*, SAMPE/Elsevier Science Publishers, BV.
25. Gabbert, J.D. and Hedrick, R.M. (1984). Advances in Systems Utilizing NYRIM Nylon Block Copolymers for Reaction Injection Molding, *Polymer Process Engineering*, **4**: 359-373.
26. Hedrick, R.M., Gabbert, J.D. and Wohl, M.H. (1985), Nylon 6 RIM, 186th meeting of the American Chemical Society, ACS Symposium Series, pp. 135-162, Washington, DC, USA.
27. Dupre, C.R., Gabbert, J.D. and Hedrick, R.M. (1984). *Review of Properties and Processing Characteristics for Nylon Block Copolymer RIM*, Vol. 25, p. 296, Polymer Preprints, Division of Polymer Chemistry, American Chemical Society.
28. Gabbert, J.D., Garner, A.Y. and Hedrick, R.M. (1983). Reinforced Nylon 6 Block Copolymers, *Polymer Composites*, **4**: 196-199.
29. Magill, J.H. (1962). Crystallization Kinetics Study of Nylon 6, *Polymer*, **3**: 655-664.
30. van Rijswijk, I.K., Koppes, I.K., Bersee, H.E.N. and Beukers, A. (2004). *Processing Window for Vacuum Infusion of Fiber-reinforced anionic polyamide-6, FPCM-7*, pp. 71-76.
31. Pyda, M. (ed.) (1994). ATHAS Data Bank, <http://web.utk.edu/~athas/databank/>
32. Fornes, T.D. and Paul, D.R. (2003). Crystallization Behavior of Nylon 6 Nanocomposites, *Polymer*, **44**: 3945-3961.

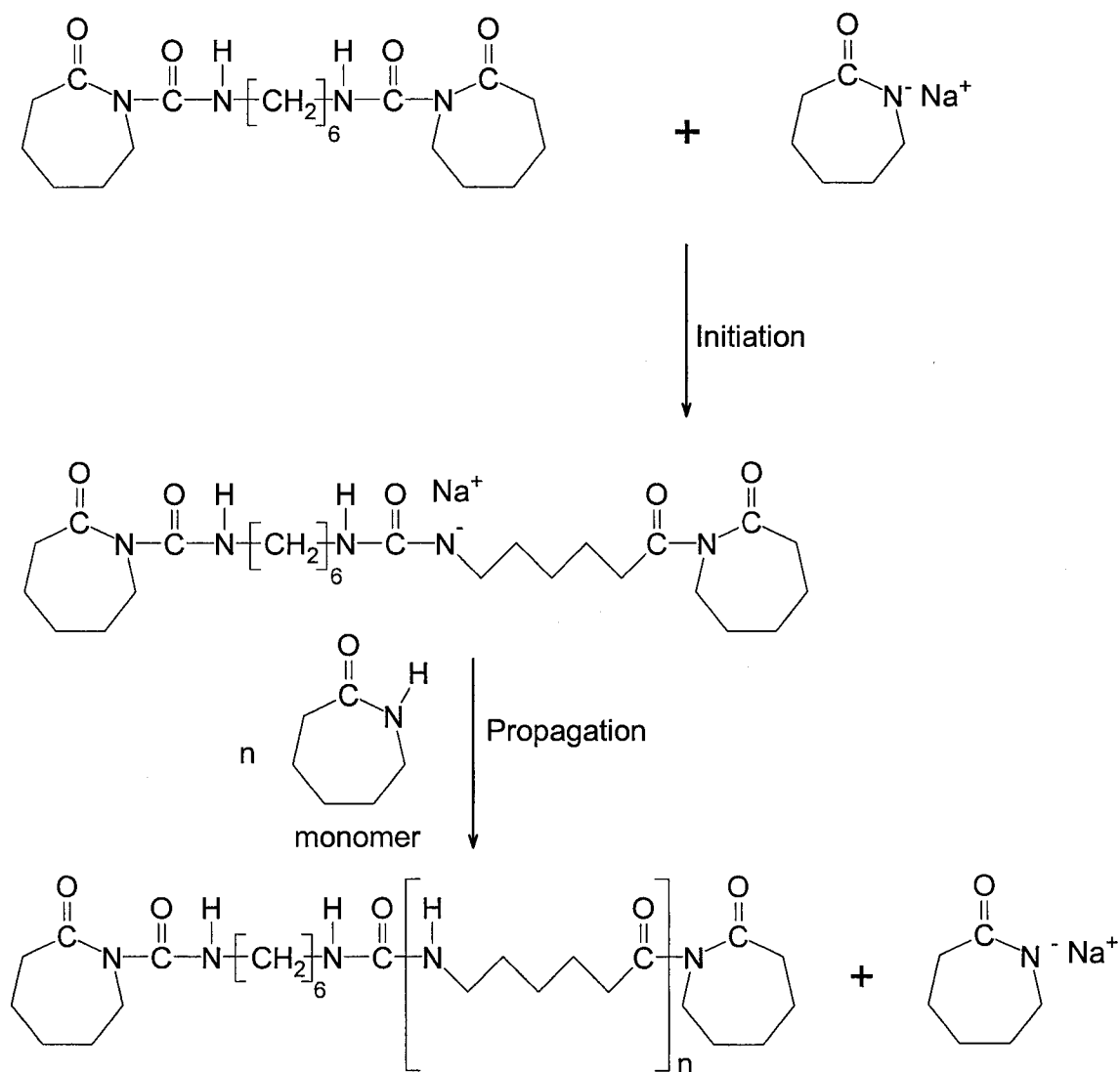


Figure 1. Reaction mechanism of anionic polymerization (AP) of caprolactam.

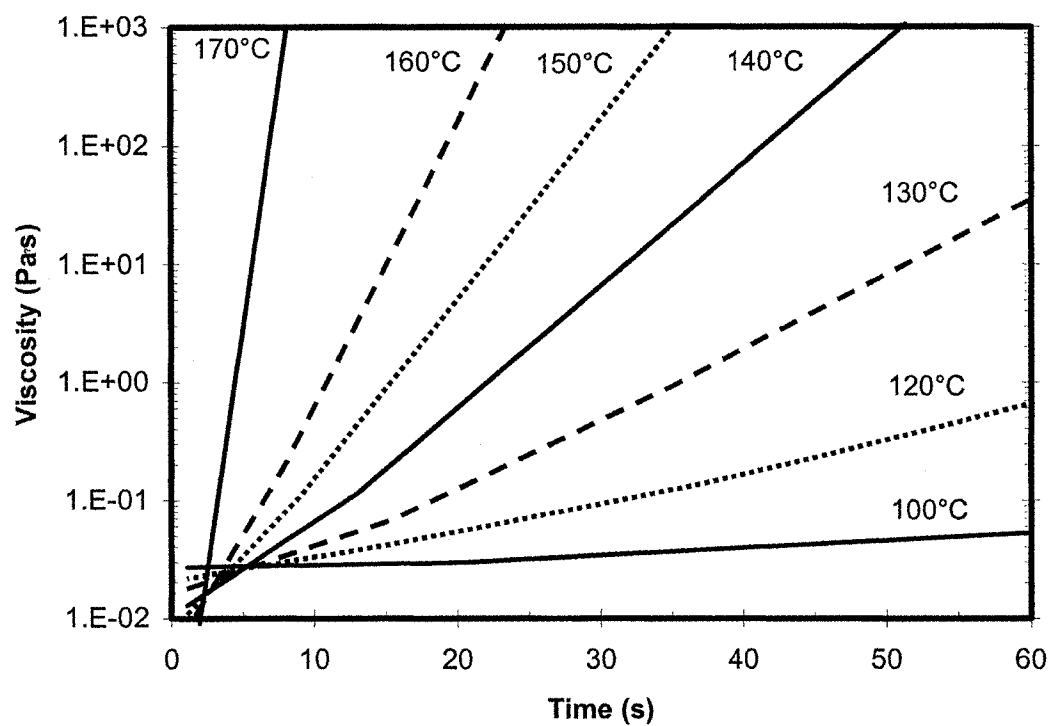


Figure 2. Time – viscosity curves at different temperatures (adapted from Sibal et al. [23]).

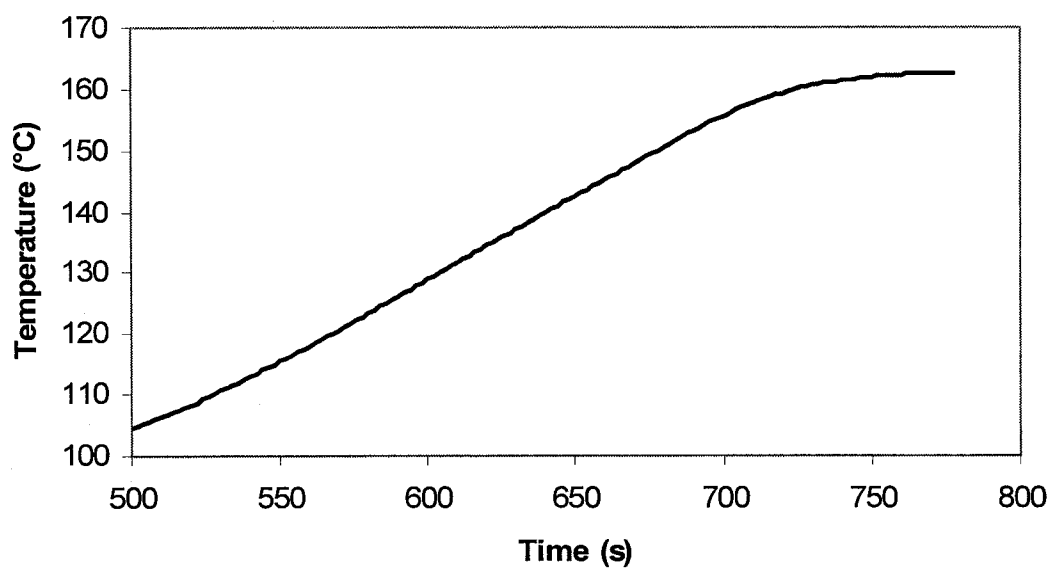


Figure 3. Time – temperature profile of the tool; thermocouple positioned on surface of the carbon fabric preform and measurement conducted under 91.4 kPa of vacuum.

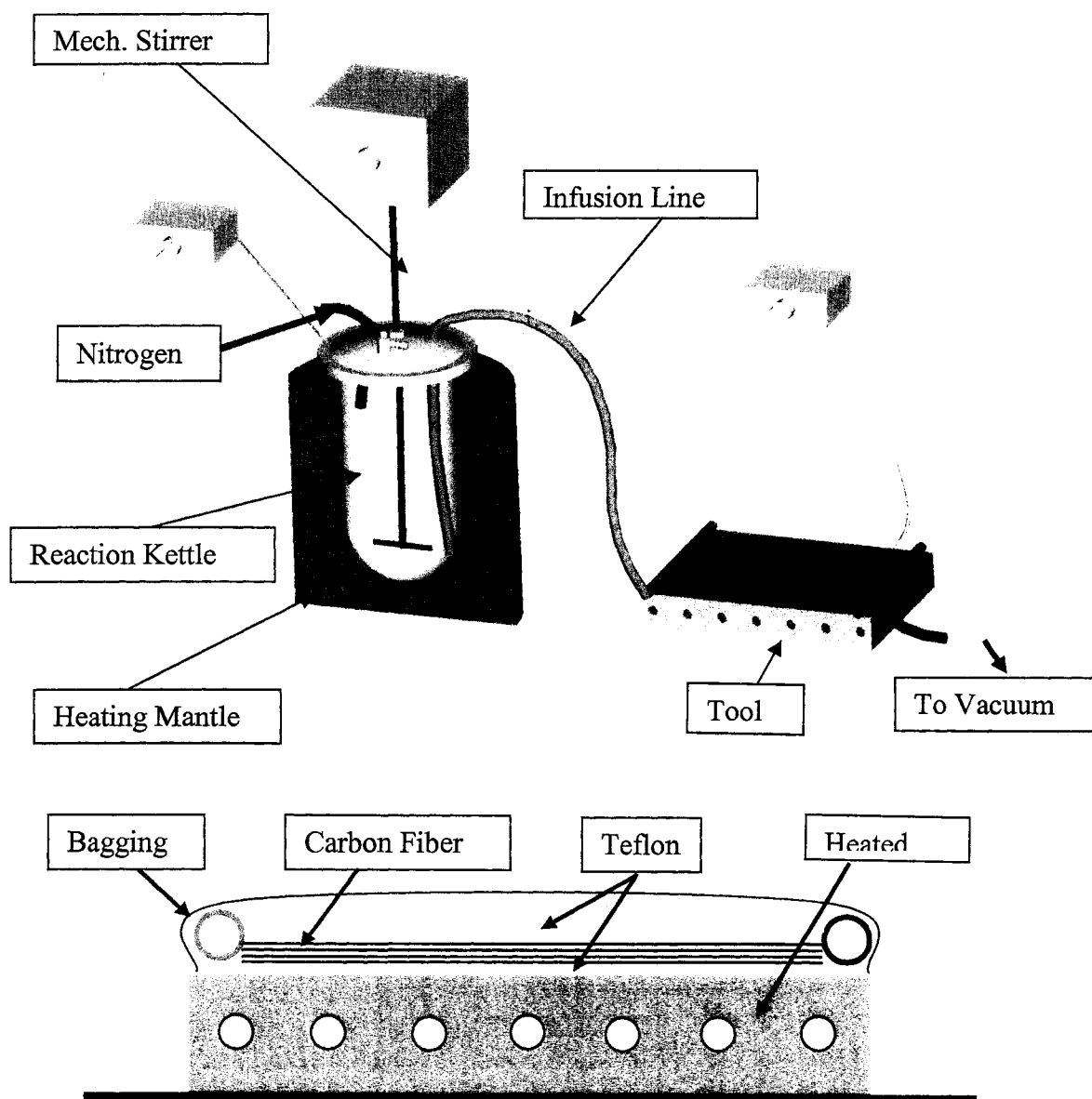


Figure 4. Schematic of the processing system.

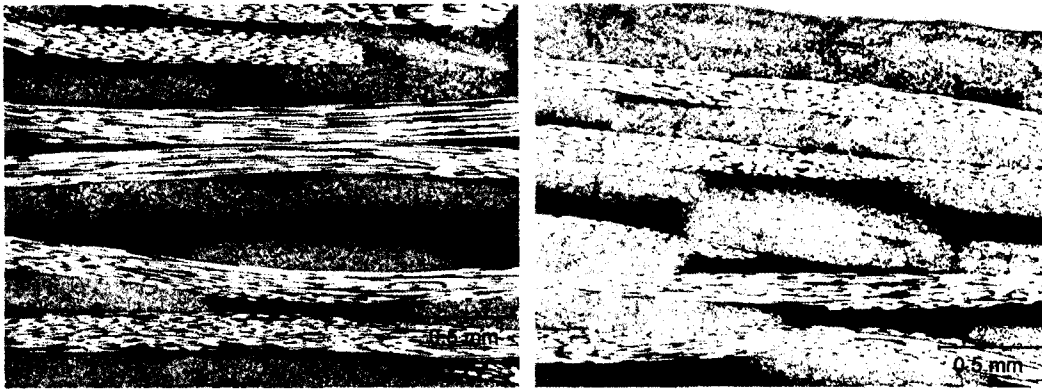


Figure 5. Optical micrographs showing wet-out of the fiber tows.

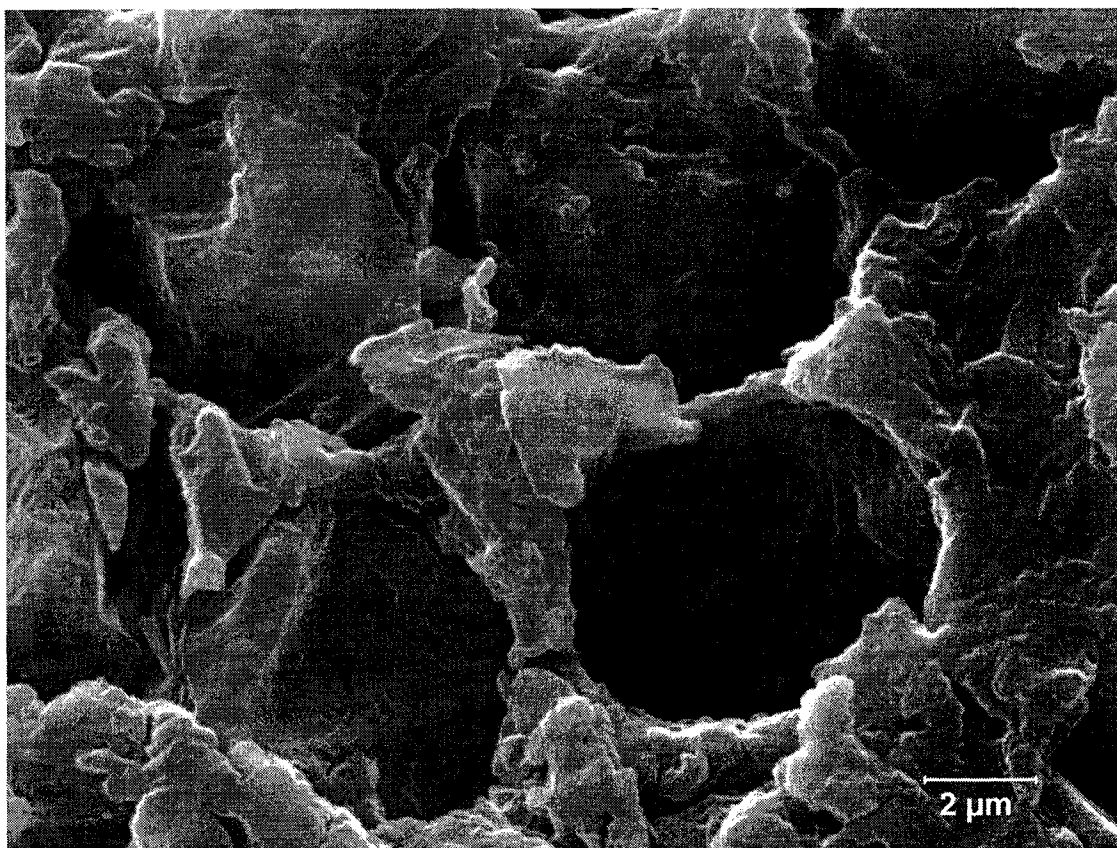


Figure 6. Scanning electron microscopy image showing a cross section of fiber filaments fully impregnated by the nylon 6 resin.

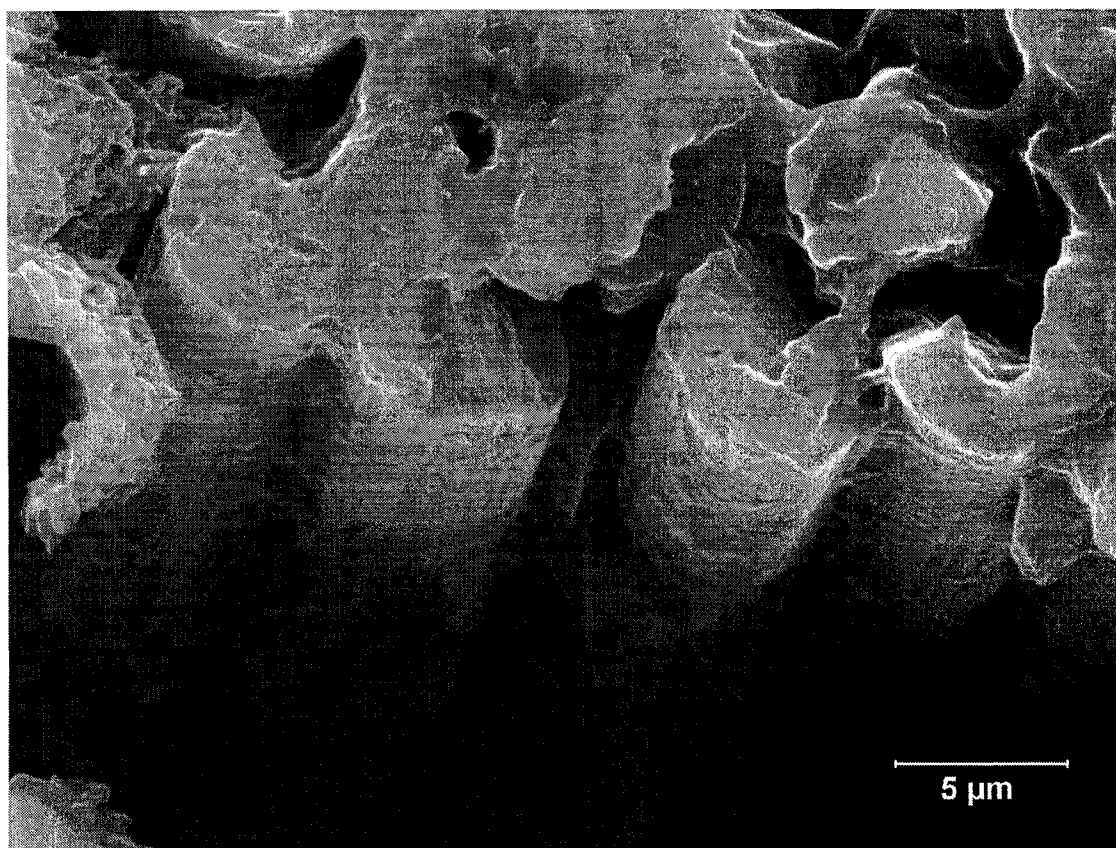


Figure 7. Scanning electron microscopy image showing impregnation of the filaments along the length.

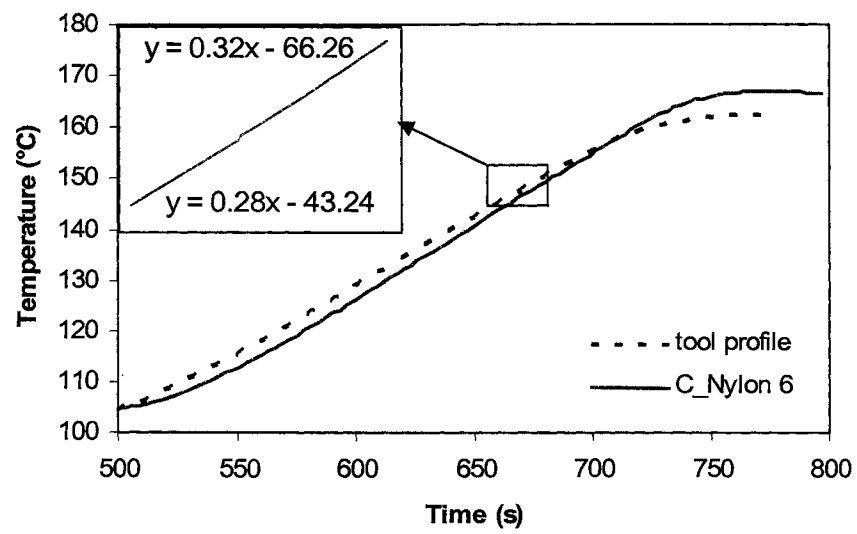


Figure 8. Time – temperature profile of a typical carbon/nylon 6 process.

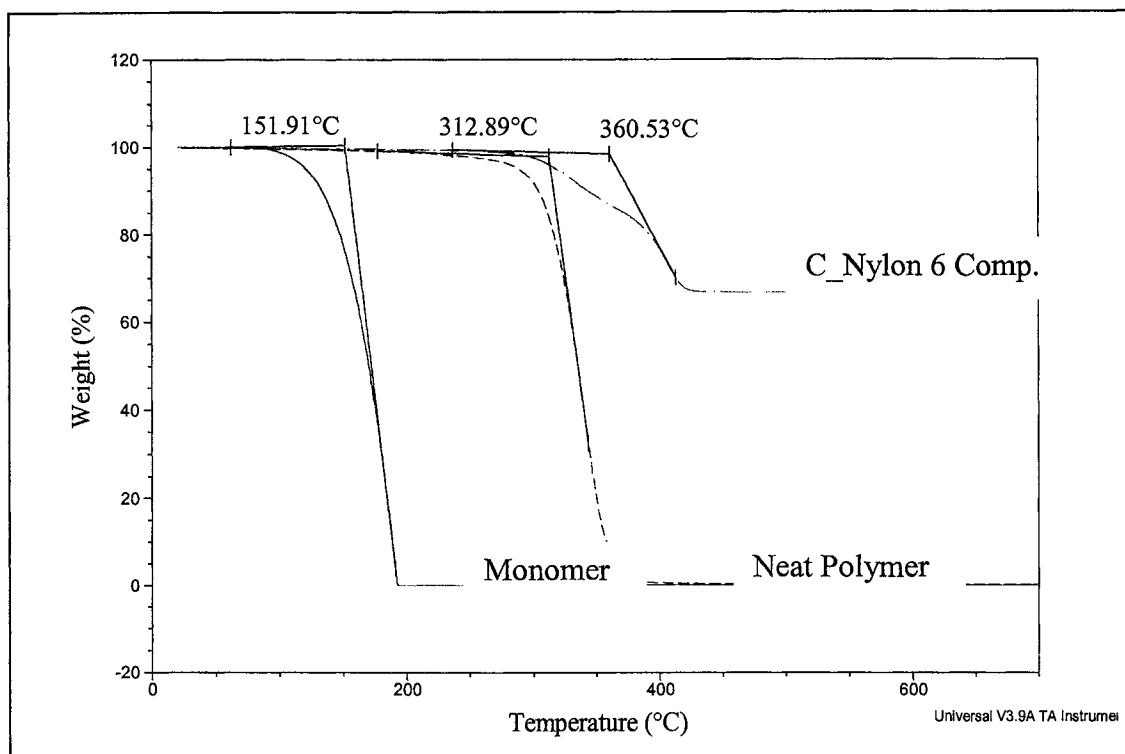


Figure 9. Typical TGA scan of the caprolactam monomer, neat polymer, and carbon/nylon6 composite sample.

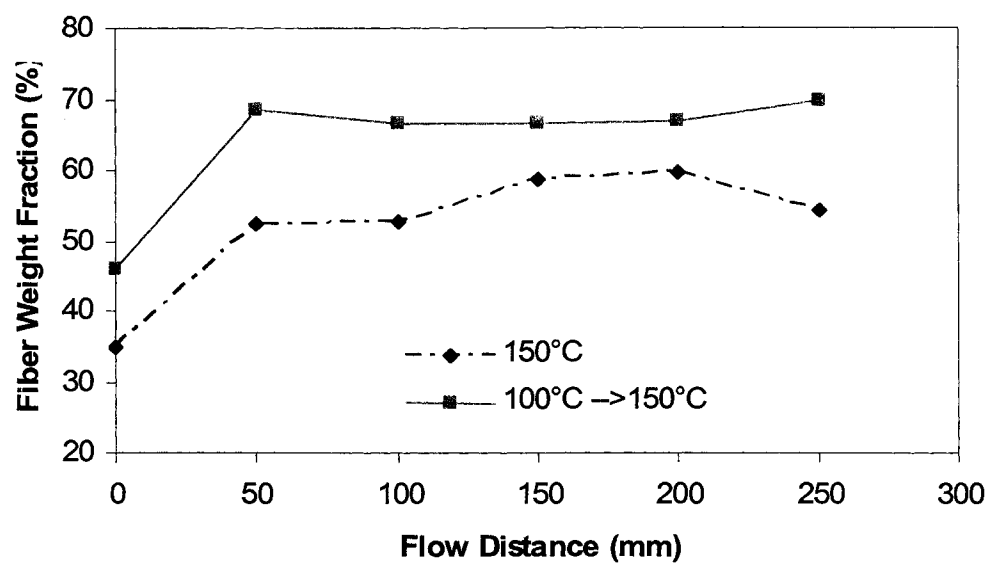


Figure 10. Flow distance vs percentage fiber weight fraction of panels processed at 150°C and panels infused at 100°C and ramped to 150°C.

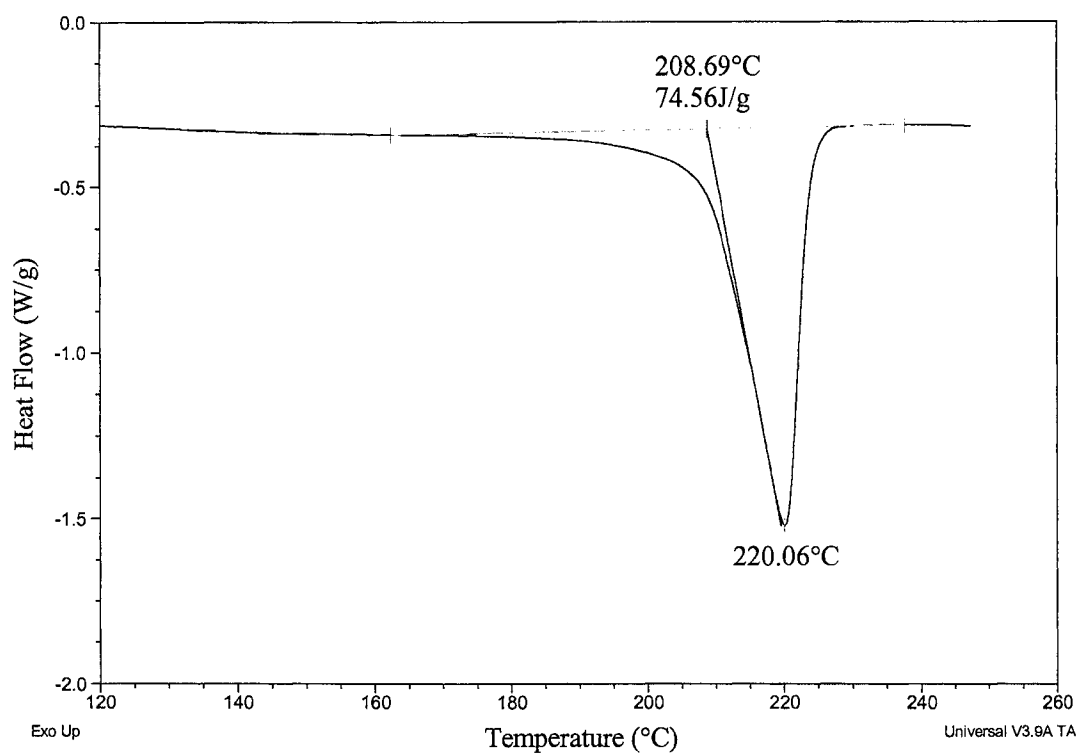


Figure 11. DSC scan of neat polymer reacted at 150°C under a nitrogen environment.

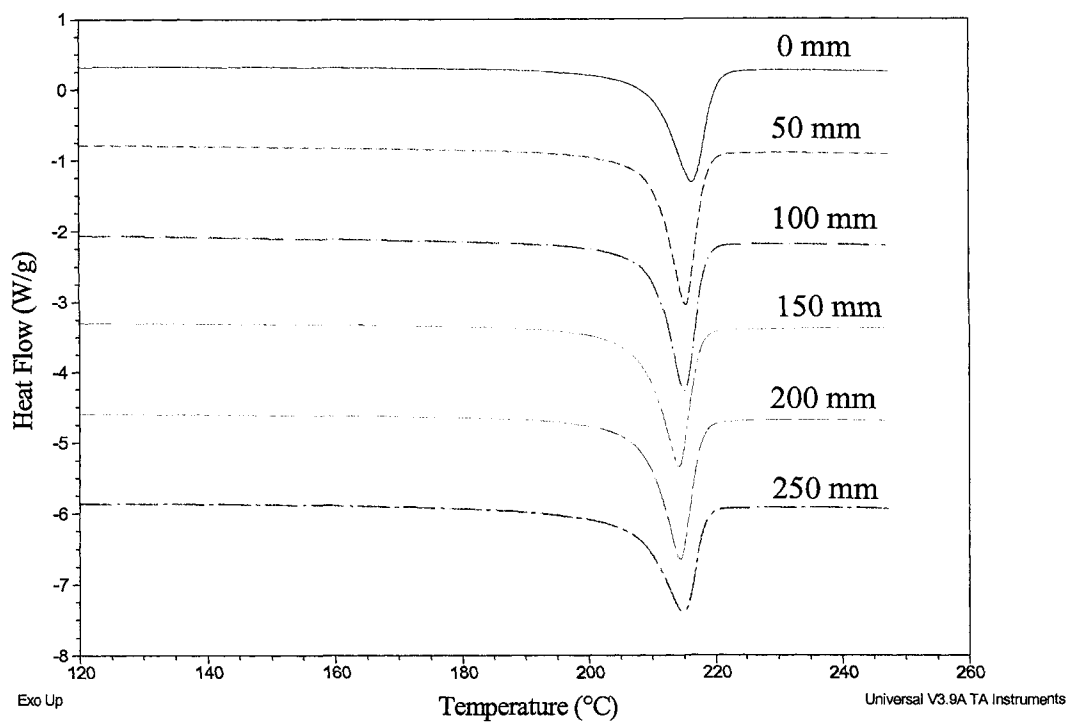


Figure 12. DSC thermogram of panel infused at 150°C with samples taken along the flow length.

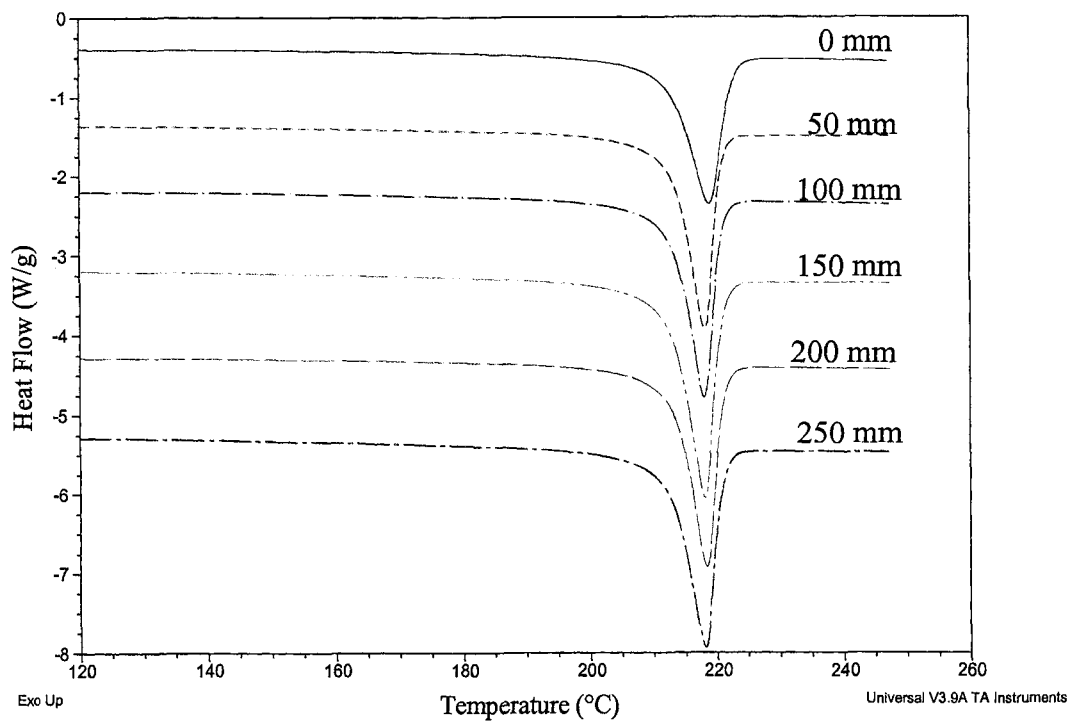


Figure 13. DSC thermogram of panel infused at 100°C and ramped to 150°C with samples taken along the flow length.

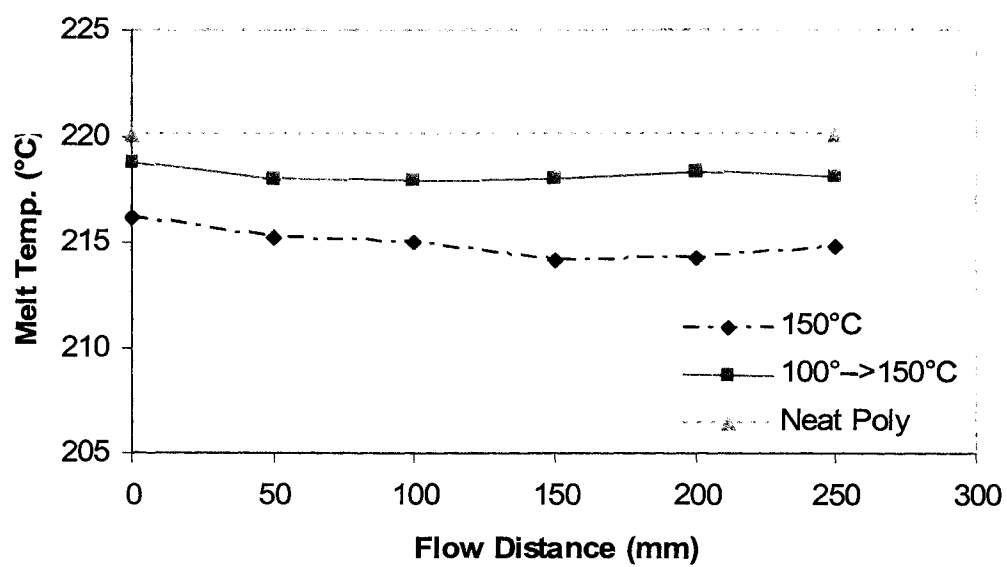


Figure 14. Flow distance versus melt temperature for samples from both processing conditions and the neat polymer processed at 150°C.

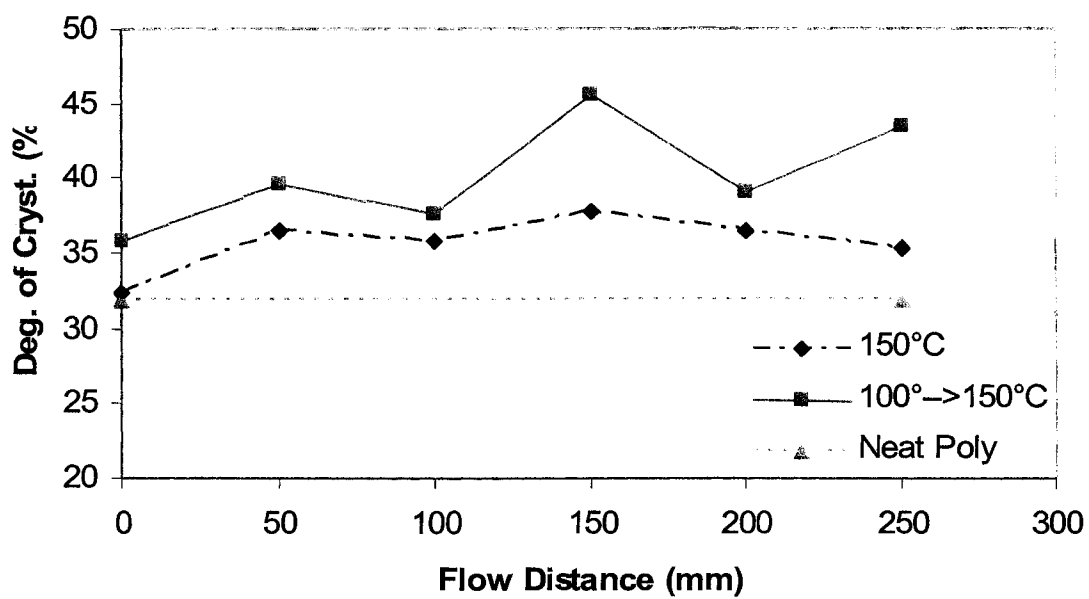


Figure 15. Flow distance vs degree of crystallinity for samples from both processing conditions and the neat polymer processed at 150°C.

MECHANICAL CHARACTERIZATION AND CRYSTALLIZATION STUDY OF
LIQUID MOLDED CARBON FABRIC-REINFORCED NYLON MATRIX
COMPOSITE LAMINATES

by

SELVUM PILLAY, UDAY K. VAIDYA, AND GREGG M. JANOWSKI

In preparation for *Journal of Thermoplastic Composite Materials*

Format adapted for dissertation

ABSTRACT

The present work addresses the thermal, static, and dynamic mechanical properties of carbon fabric-reinforced, thermoplastic polyamide 6 (also referred to as nylon 6 and/or PA6) matrix panels processed using vacuum assisted resin transfer molding (VARTM). Liquid molding of thermoplastics has been limited by high resin viscosity, high temperature processing requirements, and a short processing window. The processing parameters developed by the authors and previously reported [1] have been used to process carbon/nylon 6 composite panels. This study includes through-the-thickness crystallinity evaluation using DSC (differential scanning calorimetry) and XRD (X-ray diffraction). The material used in this study was casting grade polyamide 6, ϵ -Caprolactam with a sodium-based catalyst, and an initiator. The crystallinity was found to be marginally higher (3%) at the midsection of the panels compared to the surfaces. The static and dynamic mechanical properties are compared to equivalent panels processed using a rubber toughened SC-15 epoxy (thermoset) resin. The study showed that carbon/PA6 composite panels were equivalent in modulus and superior with respect to ultimate tensile strength (11%), short beam shear (37%), and impact resistance of the carbon/SC-15 panels. However, the carbon/SC-15 composite panels had superior (21%) flexure properties.

INTRODUCTION

Recent advances in the development and processing techniques of thermoplastic composites have increased their use in structural and semi-structural applications, the traditional domain of metal alloys or thermoset composites. The high specific strength, high damping capacity, corrosion resistance, recyclability, comparatively low cost, and impact

resistance make these materials attractive choices. However, their use has been limited to products that can be manufactured using such processes as injection molding, compression molding, and extrusion. These techniques are amenable to short fiber lengths but are incompatible with continuous woven fabrics and long fibers. However, the mechanical properties of thermoplastic composites, especially impact resistance, improve with an increase in fiber length [2,3].

Vacuum assisted resin transfer molding (VARTM) is very well developed and is now a proven, low-cost manufacturing technique for thermoset resin composites [4,5]. The high melt viscosity of thermoplastic resins generally precludes the use of VARTM due to poor impregnation or mold fill, which can be overcome by either significantly lowering the viscosity of the resin or reducing the flow distance.

An interest in the liquid molding of thermoplastic-matrix composites has recently increased due to restrictive environmental regulations (especially in Europe), economics, and higher performance requirements of components and structures. Substantial work in liquid molding of thermoplastic resin composites has recently been reported using the matrices anionic polyamide 12 (APA12) [6,7], cyclic polybutylene terephthalate (PBT) [8,9], and anionic polyamide 6 (APA6) [10,11]. Anionic ring opening polymerization of lactams has been studied extensively by many researchers in both academia [12-14] and industry [15-18]. The anionic polymerization (AP) of ϵ -caprolactam was first reported by Joyce et al. [19,20]. Caprolactam is the most popular type of lactam used commercially for the production of APA6 (also referred to as nylon 6 and PA6 in this paper). The APA6 properties compare favorably with the properties of nylon 6 produced by the conventional hydrolytic polymerization process [21].

A process for using the APA 6 systems for liquid molding or, more specifically, reaction injection molding (RIM) of composites, was investigated in the early 1980s by Sibal and coworkers [22]. Nylon block copolymers for RIM (NYRIM)TM were developed by Mooij [23]. The nylon block copolymer is formed by the reaction of AP-caprolactam with a prepolymer (NYRIM), which is an activated impact modifier (rubber). The amount of the prepolymer can range between 10 and 40%, depending on the desired properties of the composite. Extensive research has also been carried out by Gabbert and coworkers [24-27] using nylon 6 and nylon 6 block copolymers for Resin Transfer Molding (RTM) and RIM. Interest in nylon 6 for liquid molding dwindled in the mid 1980s, but now a fresh look is warranted.

A method for using VARTM to infuse carbon fabric preforms with polyamide 6 resin, a well-known thermoplastic resin that has been used extensively for nylon 6 casting applications, has been developed. The processing parameters, methodology, and limitations of using VARTM for PA6 matrix composites have been reported [1] The current study evaluates the mechanical properties (tensile, flexure, interlaminar shear strength, and low velocity impact) of these laminates and compares them to equivalent laminates manufactured using rubber toughened SC-15 epoxy (thermoset) resin (referred to as SC-15 throughout this manuscript).

MATERIALS

Carbon Fabric

The carbon fabric used in this study was supplied by US Composites and was a 4 harness satin weave, with a 3K tow size, and an areal density and thickness of 0.02 g/cm²

and 0.254 mm, respectively. The fabric was washed in acetone to remove lubricants and sizing, then placed in a recirculating oven at 100°C for 1 h to remove residual moisture and/or acetone. The fabric was used as supplied for the panels infused with rubber toughened SC-15 resin.

Monomer, Activator, and Catalyst (PA6)

AP grade caprolactam monomer was used in this study. The monomer has low levels of moisture (<0.0015% by mass), a low melting point ($T_M = 69^\circ\text{C}$), and low viscosity (4.87 mPa•s at 100°C). Bruggolen C20, hexamethylene dicarbamoyl dicaprolactam, and Bruggolen C10, sodium caprolactamate, both especially developed for AP of caprolactam, were used as the activator and catalyst, respectively. The melt temperatures of both C10 and C20 are 60°C. The monomer, catalyst, and activator were supplied by Bruggemann Chemical U.S., Inc., and were used without any further processing or purification. Due to the moisture sensitivity of the catalyst and activator, they were stored and handled in a dry box with the relative humidity maintained at 8%.

Rubber Toughened SC-15 Epoxy Resin

The rubber toughened SC-15 resin was supplied by Applied Polymeric, Inc. The resin was a two-part system, a base resin and a catalyst, with a manufacturer-specified ratio of 70:30. The ambient viscosity of the resin is 400 mPa•s and allows for a working time of approximately 4 h at 20°C.

PROCESSING

Carbon/PA6 Panels

Twenty 300 x 300 mm layers of the carbon fabric were laid onto the tool surface, then bagged and sealed using high temperature film and tacky tape. A thermocouple was positioned at the surface of the top layer of the carbon fabric to record and monitor the temperature. The tool temperature was then raised to 100°C, and a continuous vacuum of 1 atmosphere was applied to the system.

The viscosity of the resin is a function of the levels of the catalyst and initiator, temperature, and time. Various combinations were investigated to achieve both full wet-out of the preform and full polymerization. The caprolactam was heated to 100°C until it was converted to a liquid. The catalyst and activator were then added, and the solution was brought to a molten state. The catalyst is sensitive to moisture, and the caprolactam oxidizes rapidly at these temperatures. Therefore, storage and processing was done in a dry nitrogen environment. The resin was then introduced into the preform via an infusion line. Once the resin reached the end of the preform, the infusion line was clamped off, and the temperature was raised to 150°C to polymerize the PA6. For further details on the process the reader is referred to the authors' previously published work [1].

Carbon/SC-15A

The VARTM process was used to infuse 20 layers of carbon fabric with SC-15A resin at room temperature. The system was allowed to cure overnight (approximately 20 h) at room temperature and under continuous vacuum. The panel was then debagged and

placed into a recirculating oven at 82°C and post cured for 5 h, as per manufacturer's recommendations.

RESULTS AND DISCUSSION

Processing

The panels were examined visually and appeared to have good consolidation with full wet-out of the preform, for both the nylon 6 and SC-15 resins. The surface of the carbon/nylon 6 panels seemed fully polymerized. Burn-out studies were conducted to find the weight fraction of the carbon fibers and the resin in both sets of panels. 25 x 25 mm specimens were cut and dried in an air-recirculating oven at 600°C for 4 h to remove any moisture. The specimens were then weighed on a high precision balance with a 0.1 mg resolution. The specimens were then placed in preweighed aluminum pans which were then placed in a tube furnace. The furnace was heated to 600°C, held for 8 h, and then cooled, all under a nitrogen atmosphere. The pans were removed, and the carbon fibers were found visually to be free of any trace of resin. The pans were weighed again, and the weight fraction of the fibers was computed for both the SC-15 and nylon 6 resin panels. The SC-15 resin panels had an average weight fraction of 59% carbon and the nylon 6 resin panels 66%. The higher weight fraction of fiber in the nylon 6 resin panels can be attributed to the lower viscosity of the resin during the infusion process, as better flow and removal of excess resin is achieved by the vacuum system.

Crystallinity Studies of Carbon/Nylon 6 Panels

Upon cooling, nylon 6 macromolecules exist partially in a disordered amorphous state and partially in an ordered crystalline state. The structure actually realized and the degree of crystallinity is influenced by a number of factors, which include applied stress, thermal conditions, and moisture. However, the temperature of polymerization and the cooling characteristics have the largest influence on the degree of crystallinity in AP. The crystallinity has an effect on the mechanical properties of the polymer and composite. An increase in crystallinity results in an increase in tensile modulus and strength; however, the impact properties are lowered.

In our previous work, four layers of fabric were used to process panels for thermal and crystallinity studies [1]. This resulted in panels that were less than one millimeter thick, and nonuniformity of the degree of crystallinity through the thickness was a not a concern. However, 20 layers of fabric were used with the current panels which resulted in panels 3.84 mm thick for the nylon 6 resin and 3.90 mm for the SC-15 resin. The crystallinity through the thickness is influenced by the heating profile in that direction and the cooling characteristics of the panel and system [28-30]. Specimens were taken from the top, middle, and bottom (tool face) of the panel for crystallinity studies.

A TA Instruments Q100 differential scanning calorimeter (DSC) was used to characterize the thermal behavior. The samples were heated from 40 to 250°C at a rate of 10°C/min. Figure 1 shows the DSC thermograms for the specimens from the different sections (i.e., top, middle, and bottom). A single peak at the melt temperature of 220.9°C for the top and bottom specimens and 221.49°C for the middle specimen was observed. There were no peaks observed between 69°C, the melt temperature of the monomer, and

the melt temperature of each section. The single peak is an indication that high levels of conversion from monomer to polymer were achieved.

The crystallinity was determined by comparing the experimental heat of fusion (ΔH) to the theoretical value for a 100% crystalline sample. ΔH was measured by integrating the area under the peaks of the DSC thermograms. The average ΔH values for the specimens taken from the top, middle, and bottom of the panels were 94 J/g, 99 J/g, and 94 J/g, respectively. Although various values have been reported in the literature for the theoretical ΔH , the value of 230 J/g, referenced from the Advanced Thermal Analysis Laboratory (ATHAS) data bank [31] based at the Oak Ridge National Laboratory, was used, as it is the accepted value used by other researchers [32]. The degree of crystallinity of the top, middle, and bottom sections was 40, 43, and 40 %, respectively. The highest degree of crystallinity was expected in the middle section due to the cooling characteristics of the system; i.e., the top and bottom sections cool down faster than the middle. Closer examination of Figure 1 shows that the curve for the middle section has a slight linear portion at the onset of melting. The presence of both α and γ phases is generally indicated by a double peak, the γ peak being at a slightly lower temperature than the α . As the γ phase fraction decreases, the distinct peak blends into the base of the α peak. Presence of the lower melting temperature γ crystalline phase was queried, although there was not a distinct double melting peak

X-ray diffraction studies were conducted on the samples from the top, middle, and bottom sections to establish the identity of the crystalline phases. Figure 2 shows the XRD patterns for the sections from the composite and also a section of neat polymer. It is clearly evident that the only peaks that exist for both the composite and neat polymer are

α form, i.e., (200) and (002 and 220) reflections at $2\theta = 20$ and 23.7 . There were no peaks at $2\theta = 21.4$, which corresponds to the reflections of γ , i.e., (001 and 200) [32]. Therefore, it can be concluded that only the more stable form of crystal structure is present in both the neat polymer and composite.

Tensile

Tensile tests were conducted according to ASTM D 3039M using 5 samples of dimensions 12.5 mm x 250 mm cut from the panels. The sample ends were tabbed with an epoxy/glass material, dimensions 12.5 mm x 63 mm x 0.85 mm, with the tab ends tapered to 5° . The tabs were bonded to the sample using a Three Bond™ thermoplastic adhesive. Samples were tested in a servo hydraulic tensile test machine at a displacement rate of 2 mm/min with a gage length of 120 mm. The change in length of the sample was measured using a clip-on extensometer, which was detached prior to failure.

The average modulus and ultimate tensile strength (UTS) values were 69.8 GPa and 808.6 MPa for the carbon/PA6 (C/PA6) and 68.1 GPa and 730.2 MPa for the C/SC-15, respectively. The results are summarized in Table 1. The tensile properties, as expected, are similar for both the SC-15 and PA6 resins; these are generally fiber dominated properties. However, an 11% increase was found in the UTS for the C/PA6. The marginal increase in the UTS can be attributed to the slightly higher weight fraction of fibers in the C/PA6 samples. The sample failed within the gage, and failure was mainly fiber dominated. Figure 3 shows a typical failed sample; the failure pattern was typical for a laminate section.

Table 1. Average results of tensile tests performed for C/PA6 and C/SC-15 composite systems.

	Modulus (GPa)		UTS (MPa)	
	C/PA6	C/SC-15	C/PA6	C/SC-15
Mean	70	68	809	730
Standard Dev.	7.7	9.4	44.5	70.2
Minimum	62	61	729	609
Maximum	82	81	829	786

Flexure

Three-point bend tests were conducted according to ASTM D 790M. Five samples of dimension 10 mm x 80 mm x 4 mm were prepared from the panels. The support span was set at 64 mm, and the rate of cross-head motion was 1.7 mm/min. The average flexural modulus and flexural strength were 46.78 GPa and 524.66 MPa for the C/PA6 resin and 47.92 and 663 MPa for the C/SC-15 system, respectively. The results are summarized in Table 2. The C/PA6 composite showed a reduction of flexural strength of 21% compared to the C/SC-15 composite. A more ductile failure was observed with the C/PA6 composite as compared to the C/SC-15 composite.

The mode of failure was a combination of tensile face fracture and fiber wrinkling and delamination on the compressive face the C/PA6, as shown in Figure 4. The mode of failure for C/SC-15 system was tensile face fracture and subsequent delamination. The mode of failure for the C/SC-15 resin was as expected; however, the C/PA6 was not expected to fail on the tensile face as this is not typical for a thermoplastic composite. The failure mode can be attributed to the high degree of crystallinity of the nylon 6 due to the in situ anionic polymerization of the nylon 6 [1]

The load deflection curve shown in Figure 5 is a comparison of the C/PA6 and C/SC-15 composites. The ductile failure of the C/PA6 composite is clearly evident from the curves.

Table 2. Average results of flexure tests performed for carbon/nylon 6 and carbon/SC-15 composite systems.

	Modulus (GPa)		UTS (MPa)	
	C/PA6	C/SC-15	C/PA6	C/SC-15
Mean	46.78	47.92	524.66	663.00
Standard Error	2.78	0.68	71.11	11.68
Minimum	42.60	47.92	426.86	646.47
Maximum	50.29	0.34	622.94	673.98

Interlaminar Shear Stress

Short beam shear (SBS) tests were conducted according to ASTM D2344 to measure the interlaminar shear stress of the composites. The beams were loaded in three-point bending such that the dominant failure is shear. A variety of failure modes (bending, plastic indentation, and compressive) can occur that can skew the results, and care must be taken to examine the failed specimen to ensure that failure occurs at the midsection or neutral axis of the beam, which is indicative of shear failure. The tests do not purport to be absolute; however, they are a good indication for comparative analyses.

The support span for the SBS test was 16 mm (4 x thickness), and the rate of cross-head motion was 1.0 mm/min. The results are summarized in Table 3. The average short beam shear strength (SBSS) of the carbon/PA6 and carbon/SC-15 specimens was 66.4 MPa and 48.56MPa, respectively. The SBSS of the C/PA6 is 6% lower than the values for C/SC-15.

A typical photomicrograph of the tested samples is shown in Figure 6. It can be seen that the failure is at the mid section of the composite where the shear stress is at a maximum, and it can be assumed that the value of the SBSS is valid according to the ASTM D2344. Also the failure mode shows that the SBSS can be interpreted as an indication of the interlaminar shear strength of both materials, especially for comparative purposes.

Table 3. Average results of short beam shear tests performed for carbon/nylon 6 and carbon/SC-15 composite systems.

	Peak load (kN)		Short Beam Shear Strength (MPa)	
	C/PA6	C/SC-15	C/PA6	C/SC-15
Mean	2523	1938.2	46.0	48.56
Standard Dev.	741	46.7	3.72	1.06
Minimum	2886	1882	36.26	47.13
Maximum	1811	1995	52.54	49.63

Impact

Low-velocity impact (LVI) tests were conducted to study the resistance to impact and damage initiation and propagation of the C/PA6 and C/SC-15 composite panels. An instrumented drop weight tower equipped with a load cell of capacity of 1590 kg (3500 lbs) was used to conduct the tests. A hemispherical shaped tup of diameter 19.5 mm and mass 0.12 kg was used as the impactor. The total impactor mass, including the tup, was 6.15 kg. The samples were clamped using a pneumatic assist mechanism, such that 76.2 mm (3") diameter of the sample face was exposed to the impactor. Three impact heights, 0.46 m, 0.71 m, and 1.15 m, were chosen in order to capture the dominant failure modes

of the plates from incipient to total failure and to analyze the energy absorption mechanism and damage progression. The force-time, energy-time and load-deflection response of the samples were measured. Damage initiation and progression was monitored.

The results are summarized in Table 4 for composites produced from both of the resin systems showing the peak force and energy to peak force. At all energy levels, the C/PA6 system performed better than the C/SC-15 system. The load-time and energy-time curves for C/PA6 and C/SC-15 panels are shown in Figures 7 and 8, respectively. For the impact from 1.15 m on the carbon/SC-15 panel, the impactor totally perforated and remained embedded in the sample, maintaining a residual force on the load cell, which resulted in the force-time curve not returning to zero and the energy continuously increasing. Therefore, the calculations were truncated at the point of the impactor being embedded. At all energy levels, the damage to the C/PA6 system was lower than that of the C/SC-15 system. Figure 9 shows the curves for the C/PA6 and C/SC-15 panels at the maximum damage level on the same system of axis. The peak load, initiation energy (E_I), and propagation energy (E_P) are 13, 53, and 21% higher for the C/PA6 system as compared to the C/SC-15 system. The damage mode for both systems was found to be largely tensile face fracture, and damage was concentrated around the point of impact.

The C/PA6 composite was expected to be superior with respect to impact resistance, as the PA6 resin is tougher than the SC-15. During polymerization the carbon fibers provide nucleation sites for the spherulites of the nylon 6. This increases the interfacial bond strength [33,34]. The increase in interfacial bond strength increases the impact resistance of the composite.

Table 4. Average results of impact tests performed for C/PA6 and C/SC-15 composite systems

Drop Height (mm)	Energy to max load (J)		Maximum Load (kN)	
	C/PA6	C/SC-15	C/PA6	C/SC-15
460	22.1	18.2	7.3	6.2
710	25.2	22.4	6.9	6.4
1150	28.5	18.5	7.7	6.8

SUMMARY

The process developed for using vacuum assisted resin transfer molding (VARTM) for the infusion of nylon 6 resin, as reported in the previous work [1], was effective in infusing thicker panels (20 layers). Burn-out studies showed that a 7% higher fiber weight fraction was obtained for the carbon/PA6 system compared to the carbon/SC-15 system. The through-the-thickness crystallinity studies showed that there was a 3% higher degree of crystallinity in the midsection than the surfaces, which is a characteristic of the thermal history during processing.

The tensile tests yielded similar results for both composite systems for the modulus, with an 11% increase in the ultimate tensile strength for the carbon/PA6 system. The carbon/SC-15 system performed 21% better in flexure than the carbon/PA6 system. The failure in the carbon/PA6 system was more ductile. The SBSS was 6% lower for the carbon/PA6 than for the carbon/SC-15 composite. The lower values for both flexural and SBSS are possibly due to some moisture absorption by the PA6 resin. There was no particular care taken to keep the samples dry or dry them before testing.

The impact studies revealed that the peak load, initiation energy, and propagation energy are 13, 53, and 21% higher for the carbon/PA6 system as compared to the car-

bon/SC-15 system. The energy absorption characteristics were superior at all energy levels tested. This is especially important because the rubber toughened SC-15 resin has been especially developed to improve the impact capabilities of VARTM processed composite structures. This study demonstrates the viability of an alternative; i.e., a cost-effective thermoplastic such as nylon 6 can be processed identically and yield better impact properties.

ACKNOWLEDGEMENTS

The authors are grateful for the financial support for this effort provided by the Federal Transit Administration (FTA), Project AL-26-7001 and Southern Research Institute, Birmingham, Alabama. We acknowledge the technical contributions of Dr. Derrick R. Dean and his research group and Mr. Haibin Ning. The donation of materials by Bruggemann Chemical U.S., Inc., is also appreciated.

REFERENCES

1. Pillay, S., Vaidya, U.K. and Janowski, G.M. (2005). Liquid Molding of Carbon Fabric-reinforced Nylon Matrix Composite Laminates, *Journal of Thermoplastic Composites*, **18**: 509-527.
2. Thomason, J.L. and Vlug, M.A. (1996). Influence of Fiber Length and Concentration on the Properties of Glass Fibre-reinforced Polypropylene: 1. Tensile and Flexural Modulus. *Composites: Part A*, **27A**: 477-484.
3. Bush, S.F., Torres, F. G. and Methven, J. M. (2000). Rheological Characterization of Discrete Long Glass Fibre (LGF) Reinforced Thermoplastics. *Composites: Part A*, **31**: 1421-1431.
4. Brouwer, W.D., van Herpt, E.C.F.C., Labordus, M. (2003). Vacuum Injection Molding for Large Structural Applications, *Composites: Part A*, **34**: 551-558.
5. Williams, C., Summerscales, J. and Grove, S. (1996). Resin Infusion under Flexible Tooling (RIFT): A Review, *Composites: Part A*, **27A**: 517-524.

6. Zingraff, L., Bourban, P.E., Wakeman, M.D., Kohler, M. and Manson, J.A.E. (2002). Reactive Processing and Forming of Polyamide 12 Thermoplastic Composites, In: *23rd Europe SAMPE Conference Proceedings*, pp. 237-248.
7. Luise, A., Bourban, P.E. and Manson, J.A.E., (1999). *In Situ Polymerization of Polyamide 12 for Thermoplastic Composites*. ICCM-12, Paris.
8. Ciovacco, J. and Winckler, S.J. (2000). Cyclic Thermoplastic Properties and Processing, In: *45th International SAMPE Symposium*, Long Beach, CA.
9. Parton, Hilde and Verpoest, Ignass (2003). *Reactive Processing of Textile Reinforced Thermoplastics*, ICCM 14, San Diego, CA.
10. van Rijswijk, K., Vlasveld, D.P.N., Brsee, H.E.N. and Picken, S.J. (2003). Vacuum Injection of Anionic Polyamide 6, In: *Proceeding of ICCST 4*, Durban, South Africa.
11. Vlasveld, D.P.N., van Rijswijk, Bersee, H.E.N., Beukers, A. and Picken, S.J.N. (2003). *Process Considerations for Liquid Molding of Composites Based on Anionic Polyamide 6*, ICCM 14, San Diego, CA.
12. Sebenda, J. (1978). Recent Progress in the Polymerization of Lactams; Review, *Progress in Polymer Science*, **6**: 123-167.
13. Kim, K.J., Hong, D.S. and Tripathy, A.R. (1997). Kinetics of Adiabatic Copolymerization of ϵ -Caprolactam in the presence of Various Activators, *Journal of Applied Polymer Science*, **66**: 1195-1207.
14. Petrov, P., Jankova, K. and Mateva, R. (2003). Polyamide-6-b-Polybutadiene Block Copolymers: Synthesis and Properties, *Journal of Applied Polymer Science*, **89**: 711-717.
15. Murthy, N.S., Kagan, V.A. and Bray, R.G. (2003). Optimizing the Mechanical Performance in Semi-Crystalline Polymers: Roles of Melt Temperature and Sin-Core Crystalline Morphology of Nylon, *Journal of Reinforced Plastics and Composites*, **22**: 685-693.
16. Udipi, K., Dave, R.S., Kruse, R.L. and Stebbins, L.R. (1997). Polyamides from Lactams via Anionic Ring-opening Polymerization: 1. Chemistry and Some Recent Findings, *Polymer*, **38**: 927-938.
17. Udipi, K., Dave, R.S., Kruse, R.L. and Stebbins, L.R. (1997). Polyamides from Lactams via Anionic Ring-opening Polymerization: 1. Kinetics, *Polymer*, **38**:939-947.
18. Udipi, K., Dave, R.S., Kruse, R.L. and Stebbins, L.R. (1997). Polyamides from Lactams via Anionic Ring-opening Polymerization: 1. Rheology, *Polymer*, **38**: 949-954.

19. Joyce, R.M. and Ritter, D.M. (1941). U.S. Patent 2,251,519.
20. Hanford, W.E. and Joyce, R.M., (1948). Polymeric Amides from Epsilon-Caprolactam, *Journal of Polymer Science*, **3**: 167-172.
21. Reimschuessel, H.K. (1977). Nylon 6 Chemistry and Mechanisms, *Journal of Polymer Science: Macromolecular Reviews*, **12**: 65-139.
22. Sibal, P.W., Camargo, R.E. and Macosko, C.W. (1982). Designing Nylon 6 Polymerization for RIM, In: *Proceedings of the Second International Conference on Reactive Processing of Polymers*, pp. 97-125, Pittsburgh, Pennsylvania.
23. Mooij, H. (1991). *SRIM Nylon Composites, Advanced Materials: Cost Effectiveness, Quality Control, Health and Environment*, SAMPE/Elsevier Science Publishers, BV.
24. Gabbert, J.D. and Hedrick, R.M. (1984). Advances in Systems Utilizing NYRIM Nylon Block Copolymers for Reaction Injection Molding, *Polymer Process Engineering*, **4**: 359-373.
25. Gabbert, J.D. and Wohl, M.H., (1985). Nylon 6 RIM, *ACS Symposium Series*, pp. 135-162.
26. Dupre, C.R., Gabbert, J.D. and Hedrick, R.M., (1984). *Review of Properties and Processing Characteristics for Nylon Block Copolymer RIM*, Vol. 25, p. 296, Polymer Preprints, Division of Polymer Chemistry, America Chemical Society.
27. Gabbert, J.D., Garner, A.Y. and Hedrick, R.M. (July 1983). Reinforced Nylon 6 Block Copolymers, *Polymer Composites*, **4**: 196-199.
28. Magill, J.H. (1962). Crystallization Kinetics Study of Nylon 6, *Polymer*, **3**: 655-664.
29. van Rijswijk, I.K., Koppes, I.K., Bersee, H.E.N. and Beukers, A. (2004). *Processing Window for Vacuum Infusion of Fiber-reinforced Anionic Polyamide-6, FPCM -7*, pp. 71-76.
30. Murthy, N.S., Kagan, V.A. and Bray, R.G. (2003). Optimizing the Mechanical Performance in Semi-Crystalline Polymers: Roles of Melt Temperature and Sincore Crystalline Morphology of Nylon, *Journal of Reinforced Plastics and Composites*, **22**: 685-693.
31. Pyda, M. (ed.) (1994). ATHAS Data Bank, <http://web.utk.edu/~athas/databank/>
32. Fornes, T.D. and Paul, D.R. (2003). Crystallization Behavior of Nylon 6 Nanocomposites, *Polymer*, **44**: 3945-3961.

33. Ishak, Z.A.M. and Berry, J.P. (1994). Effect of Moisture Absorption on the Dynamic Mechanical Properties of Short Carbon Fiber Reinforced Nylon 6,6, *Journal of Polymer Composites*, **15**: 223-230.
34. Burton, R.H. and Folkes, M.J. (1983). Interfacial Morphology in Short Fiber Reinforced Thermoplastics, *Plastics and Rubber Processing and Applications*, **3**: 129-135.

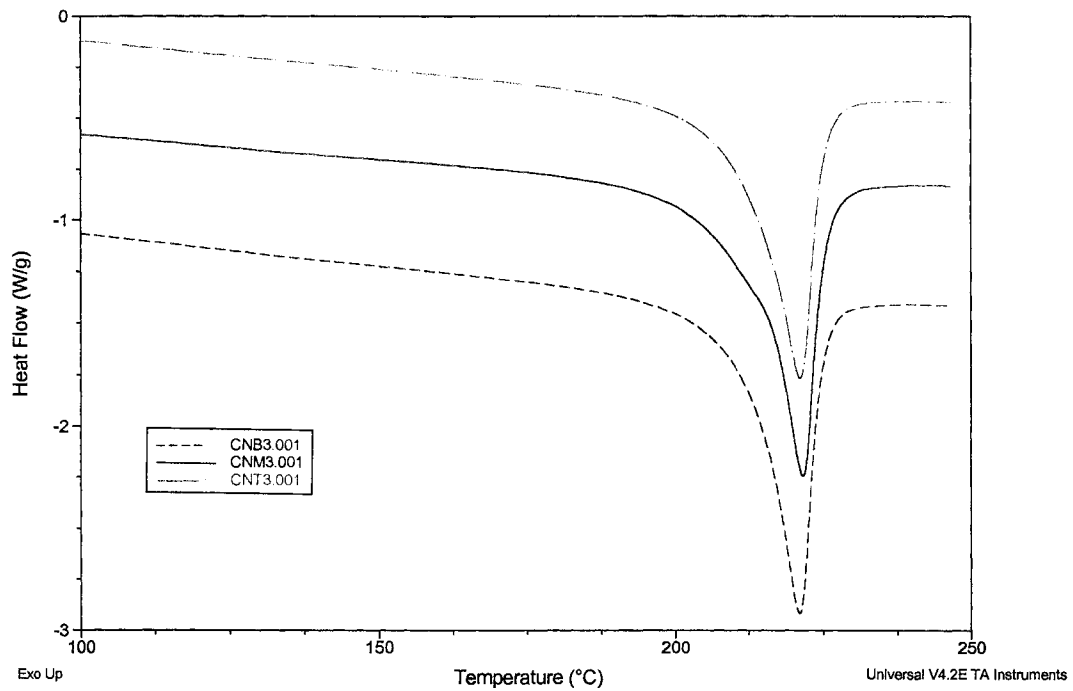


Figure 1. DSC thermograms of sections taken from the top, middle, and bottom (tool face) of carbon/nylon 6 composite panels.

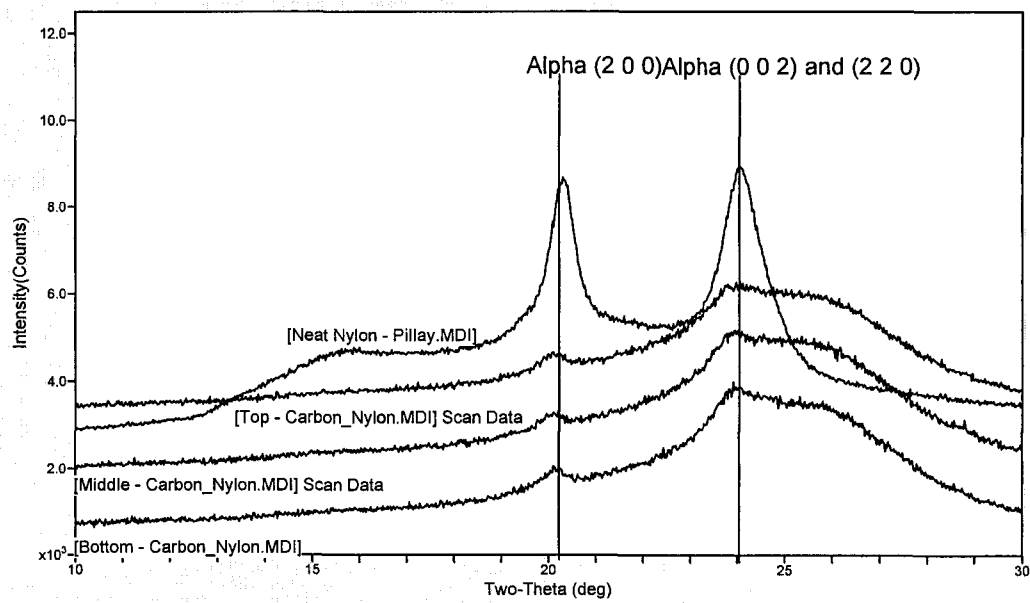


Figure 2. XRD scans of neat anionically polymerized nylon 6 and sections taken from the top, middle, and bottom (tool face) of carbon/nylon 6 composite panels.

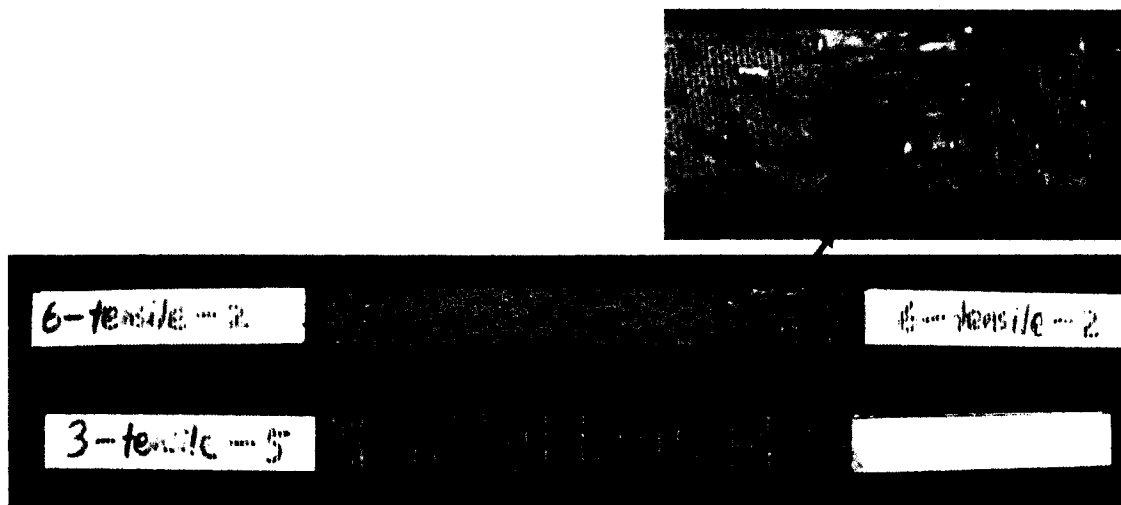


Figure 3. Typical failed sample in tension of carbon/PA6 composite sample. Failure occurred within the gage.



Figure 4. Typical failed sample in flexure of carbon/nylon 6 composite sample. Failure mode was tensile face fracture and fiber wrinkling and delamination on the compressive face, as observed by the inset.

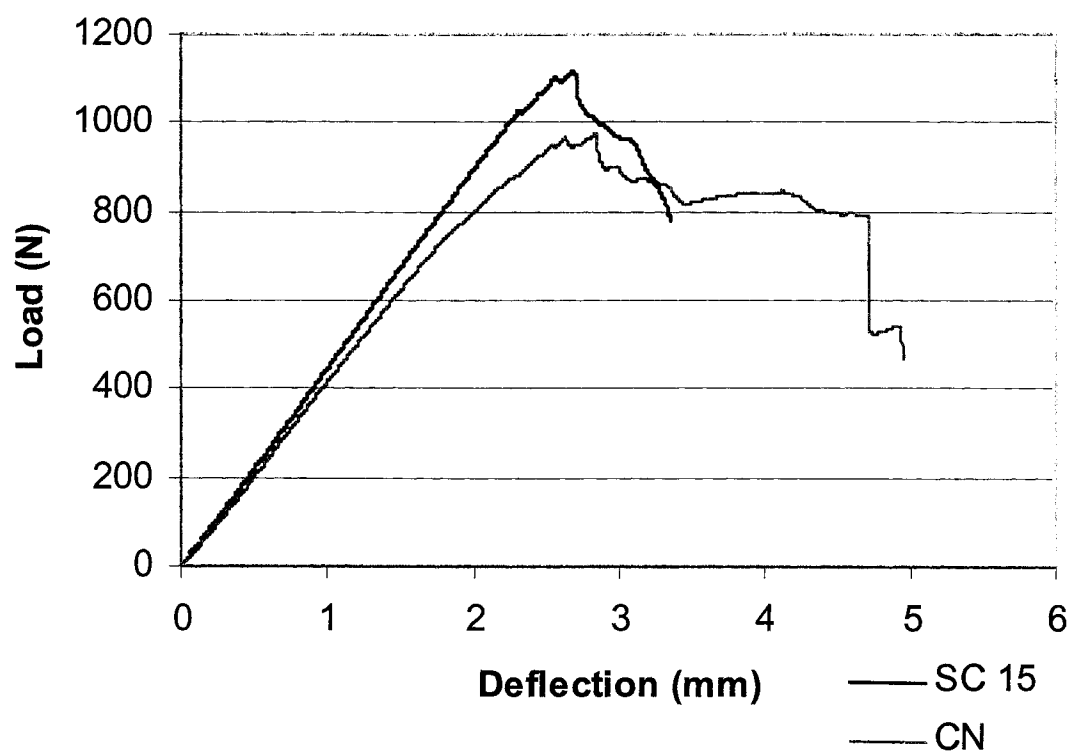


Figure 5. Load – deflection curve from flexure test, comparing carbon/nylon 6 to carbon/SC-15 composites. The ductile failure of the carbon/nylon 6 composite is clearly evident.

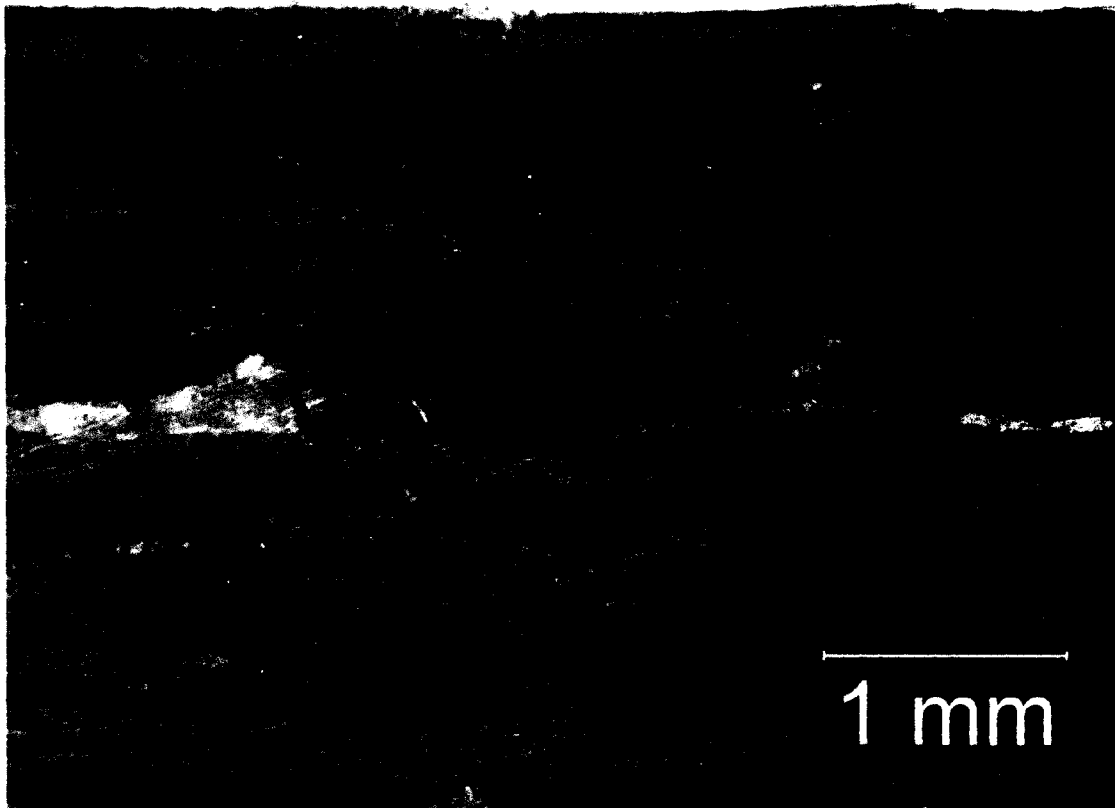


Figure 6. Typical failed sample after short beam shear test. Highlighted area shows the interlaminar shear crack at the midsection.

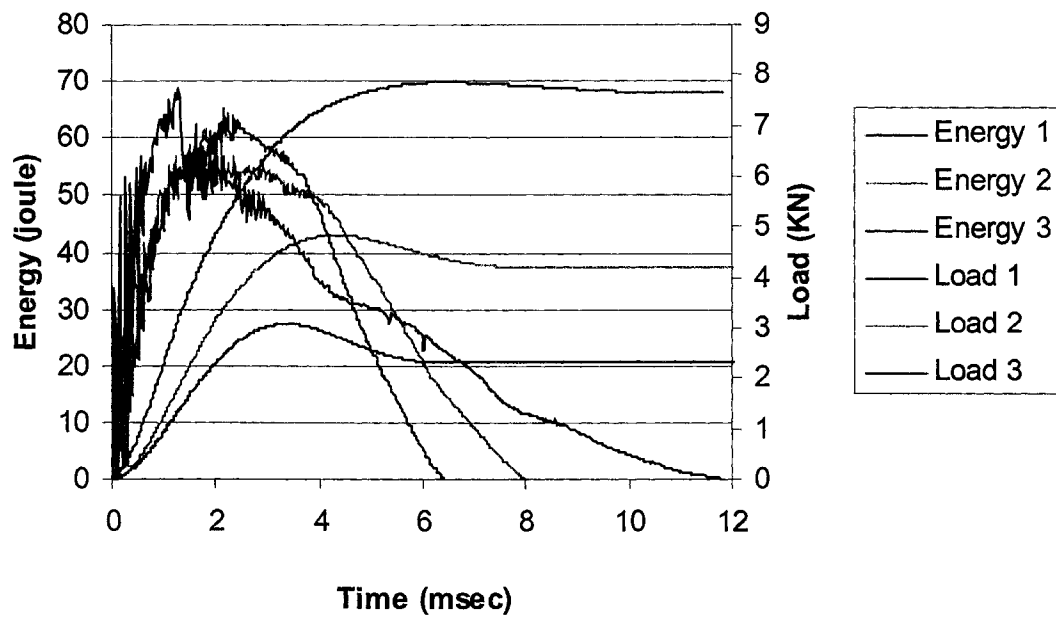


Figure 7. Typical force/energy – Time curve for carbon/PA6 composite samples for various energy levels. The impact heights of 0.46 m, 0.71 m, and 1.15 m are represented by levels 1, 2, and 3.

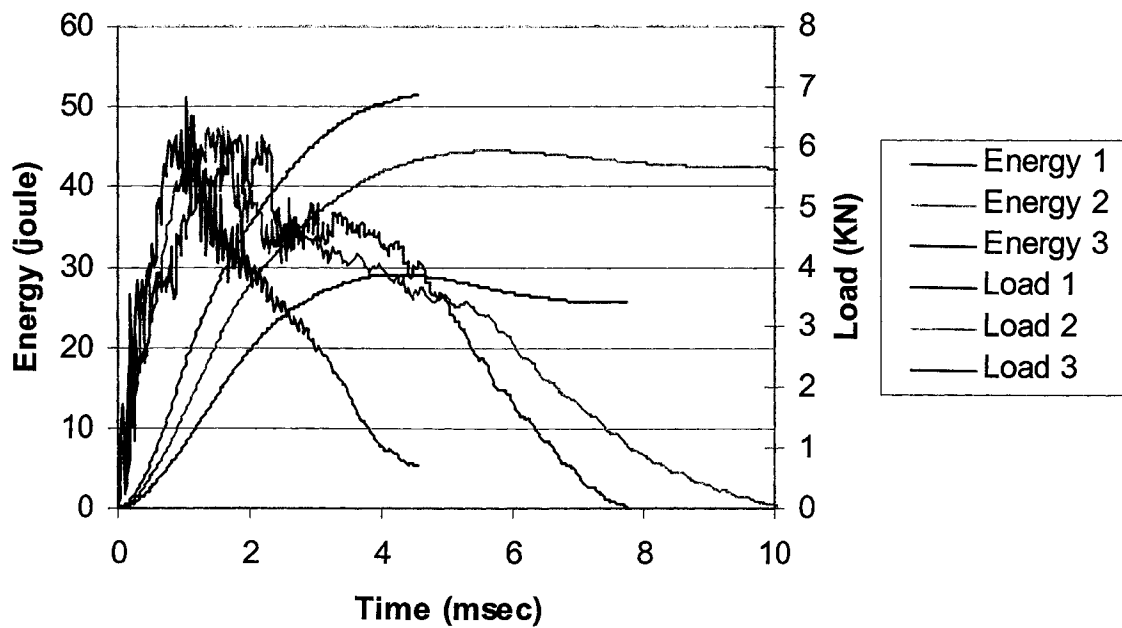


Figure 8. Typical force/energy – Time curve for carbon/SC-15 composite samples for various energy levels. The impact heights of 0.46 m, 0.71 m, and 1.15 m are represented by levels 1, 2, and 3.

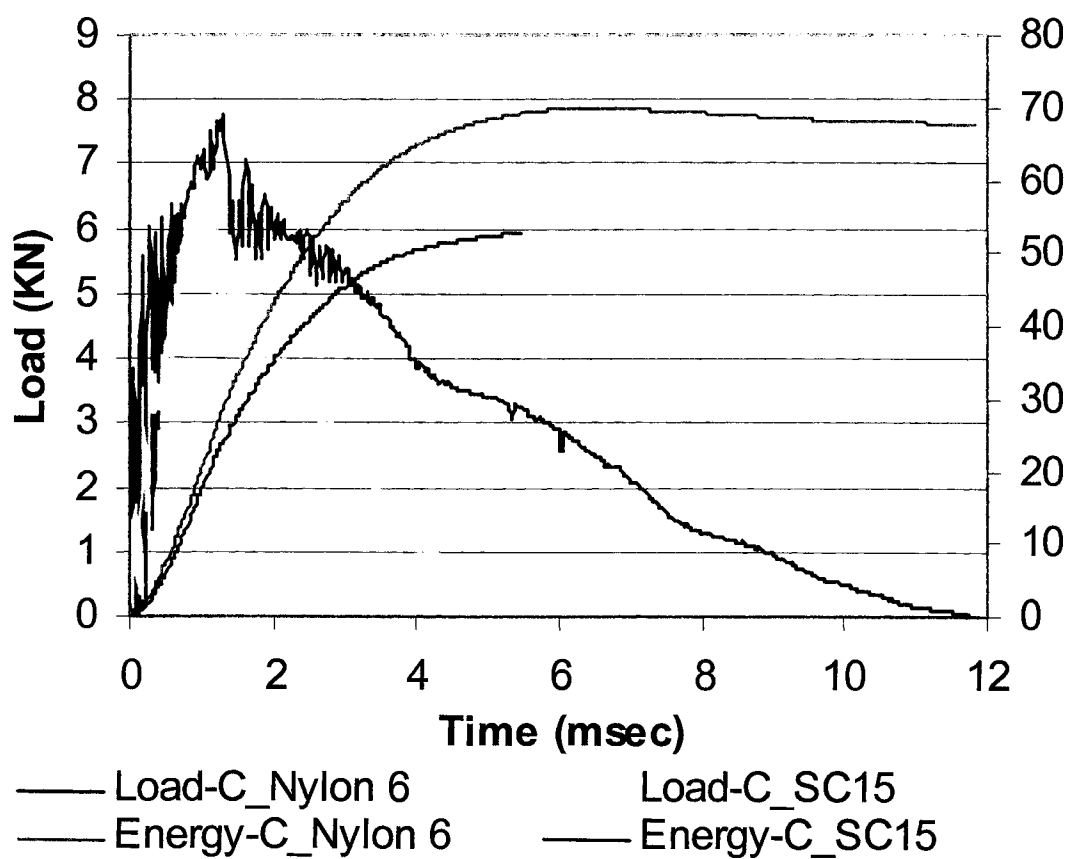


Figure 9. Force/energy – Time curve for carbon/nylon 6 and carbon/SC-15 composite samples at maximum energy level.

EFFECTS OF MOISTURE AND UV EXPOSURE ON LIQUID MOLDED CARBON
FABRIC-REINFORCED NYLON 6 MATRIX COMPOSITE LAMINATES

by

SELVUM PILLAY, UDAY K. VAIDYA, AND GREGG M. JANOWSKI

In preparation for *Composites Science and Technology*

Format adapted for dissertation

ABSTRACT

Liquid molding of thermoplastics has been limited by high resin viscosity, high temperature processing requirements, and a short processing window [1]. The processing parameters for vacuum assisted resin transfer molding (VARTM) developed by the authors and previously reported [2] have been adopted to process carbon/nylon 6 composite panels. The material used in this study was casting grade polyamide 6, ϵ -Caprolactam with a sodium-based catalyst and an initiator.

The present work addresses the effects of moisture and ultraviolet (UV) exposure on the static and dynamic mechanical properties of carbon fabric-reinforced, thermoplastic polyamide 6 (also referred to as nylon 6 and/or PA6) matrix panels processed using VARTM. The Bao and Yee dual diffusivity model [3] was applied to evaluate the moisture uptake for the C/PA6, fully immersed in distilled water at 100°C. The model shows good correlation with the experimental data in terms of the percentage of moisture absorption with respect to the square root of time. Scanning electron microscopy (SEM) results show that surface defects induced during processing result in matrix micro-cracks after moisture exposure and the fiber matrix interface is compromised. The flexural and SBSS is lowered by 45 and 65%, respectively, after exposure to moisture at 100°C. The impact resistance of the material is also lowered due to water ingress. However, the crystallinity and melting peaks are not affected.

UV exposure up to 600 h causes yellowing of the samples and an increase in crystallinity from 40 to 44%. The mechanical properties (flexure, SBSS, and low velocity impact resistance) are not affected by exposure to UV for up to 600 h.

INTRODUCTION

Polymer matrix carbon fiber-reinforced composites are widely used in a variety of applications, such as aerospace, mass transit, automotive, and sporting goods. Their use has become popular due to their attractive properties, including high strength to weight ratio, high specific stiffness, and corrosion resistance. However, their susceptibility to environmental degradation, especially hygrothermal aging and ultraviolet (UV) irradiation, depending on the application and formulation of the matrix, has been of major concern.

When exposed to humid environments, polymer-based composite structures can absorb moisture, which affects the long-term structural durability and properties of the composite [4,5]. Since high performance carbon fibers absorb little or no moisture compared to the matrix, the absorption is largely matrix dominated. Moisture penetration is largely dominated by diffusion. Other mechanisms that can contribute are capillarity and transport by micro-cracks [6]. The rate of moisture absorption depends largely on the type of matrix, orientation of the fibers with respect to the direction of diffusion, temperature of the water, and relative humidity [7]. Moisture absorption leads to changes in the thermophysical, mechanical, and chemical characteristics of the matrix by plasticization and hydrolysis [8-10]. Also, moisture wicking along the fiber-matrix interface degrades the fiber-matrix bond, which results in the loss of microstructural integrity. Matrix dominated properties such as interlaminar shear and impact resistance are most strongly affected.

Most polymers absorb solar UV radiation, which causes photolytic, photo-oxidative, and thermo-oxidative reactions that can degrade the polymer [11-13]. Polymer

matrix composite materials are susceptible to this degradation by virtue of the matrix and its importance in determining properties. The degradation of the material can range from mere discoloration to a significant loss of mechanical properties. Most plastics or polymer products that are used in outdoor applications use photo-stabilizers to prevent or minimize damage from UV exposure. The degradation mechanisms are quite complex and are usually dependent on the testing configuration and specific material being investigated [14]. This generally requires extensive experimental characterization of fundamental degradation mechanisms.

The wavelength of UV components of solar radiation incident on the earth's surface is under the 400 nm band. The energy provided by these UV photons falls within the range of the dissociation energies of polymer bonds, which are typically between 290-460 kJ/mole [15]. Thus, the chemical structure of the polymer is altered by photo oxidative reactions caused by the absorption of these UV photons, which leads to the deterioration in properties. Typically these reactions cause molecular chain scission and/or chain crosslinking. Chain scission lowers the molecular weight of the polymer, while crosslinking causes brittleness, which can lead to microcracking. The chain crosslinking caused by UV exposure can be advantageous and exploited, especially with thermoset resins, by using it as a curing agent [16].

If the polymer absorbs visible wavelengths, the photo-oxidative reactions can also cause the production of chromophoric chemical species, which may impart discoloration to the material. An autocatalytic degradation process is established if UV-absorbing chromophores are produced [14]. The formation of these groups provides a convenient means of monitoring the degradation process.

There has been substantial research conducted on moisture diffusion and UV exposure and the effects on carbon fiber-reinforced thermoset matrix composites [17-22]. Some studies have also been conducted on discontinuous fiber-reinforced thermoplastic composites [7]. However, little, if any, work has been reported on continuous carbon fiber-reinforced thermoplastic composites exposed to moisture or UV. The synergistic effects of the various elements of environmental (moisture and UV) exposure that are experienced by most composite materials can greatly affect the rate of degradation of the material.

The focus of this work is to understand the fundamental effects of moisture and UV exposure independently on carbon fabric-reinforced nylon 6 composites. A method for using VARTM to infuse carbon fabric preforms with poly-amide 6, a well-known thermoplastic resin that has been used extensively for casting applications, has been developed. The processing parameters, methodology, and limitations of using VARTM for nylon 6 matrix composites have been reported elsewhere [2]. The current study evaluates the effects of moisture and UV exposure on these composite materials and the effect on interlaminar shear strength, flexural strength, and low-velocity impact resistance.

Kinetics of Water Absorption

A basic study of the existing models of water absorption in composite materials was undertaken, to compare results of the experimental moisture uptake/diffusion data for the condition of the specimens fully immersed in distilled water at 100°C. A number of studies have been conducted on moisture diffusion in composites, and most agree that Fickian behavior adequately predicts the water ingress in these composites [7,23]. These

studies have also shown that the most aggressive condition for the composite was full immersion in water at 100° C. The equilibrium absorption was also reached in the minimum time, under 100 h for nylon 6/6 [7]. Most of these studies have been conducted for nonwoven (unidirectional and random chopped fiber) composite materials. Ishak and Berry [7] showed that Fickian absorption adequately modeled the moisture absorption of nylon 6/6 reinforced with short carbon fiber.

Equations 2 and 3 outline the model developed by Crank [24] for diffusion of a substance in one direction only. For an infinitely large plate of thickness h with single phase diffusion, M_t (mass of water absorbed at time t) by M_∞ (mass of water absorbed at saturation) is given by:

$$\frac{M_t}{M_\infty} = 1 - \frac{8}{\pi^2} \sum_{n=0}^{\infty} \frac{1}{(2n+1)^2} \times \text{EXP} \left[- \left(\frac{Dt}{h^2} \right) \pi^2 (2n+1)^2 \right] \quad (2)$$

This equation is a series solution to Fick's second law, which can then be resolved into two conditions of Dt/h^2 (Equations 3 and 4, respectively):

For $\frac{Dt}{h^2} > 0.05$ Equation 2 reduces to

$$\frac{M_t}{M_\infty} = 1 - \frac{8}{\pi^2} \text{EXP} \left[- \left(\frac{Dt}{h^2} \right) \pi^2 \right] \quad (3)$$

For $\frac{Dt}{H^2} \ll 0.05$ Equation (2) reduces to

$$\frac{M_t}{M_\infty} = \frac{4}{\pi^{1/2}} \left(\frac{Dt}{h^2} \right)^{1/2} \quad (4)$$

The diffusivity D can be calculated from the initial linear portion of the absorption curve from Equation (4).

The moisture absorption does not follow the previously described model for woven fabric composites. There have been limited studies on the mathematical modeling of moisture ingress on woven composites [3,25,26]. The transport of moisture in woven composite materials is very complicated, as it is influenced by the matrix material, weave architecture, residual stresses, and the fiber/matrix interface.

Whitney and Browning [26] studied the moisture diffusion of bidirectional graphite composites and proposed a residual stress-dependent model. The basis for the residual stress was the consideration that matrix shrinkage is restricted in both directions, hence large residual tensile stresses may develop after cure. As the diffusion of moisture progresses, the swelling of the matrix relieves the residual stress within the material and slows down the absorption. The linear dependency of diffusion on time proposed improved correlation with the experimental data; however, the fit still showed some discrepancy.

Bao and Yee [3] conducted an extensive study on the diffusion kinetics of moisture in both unidirectional and woven composites. They also found that the diffusion was non-Fickian for the woven composite. They conducted an extensive evaluation of the different models and fits with experimental data, and found that there were discrepancies with the experimental and predicted results. They had also evaluated the stress-dependent model proposed Whitney and Browning [26] and found that the correlation was limited at best. A closer study of the experimental absorption curves showed that there were two distinct linear regions before the equilibrium moisture was reached. They found that the moisture uptake was composed of two processes with different rates: a fast initial rate and

then a slower rate. They proposed the following dual diffusivity model, which is the sum of two Fickian processes with different diffusivities.

$$M_t = M_{\infty 1} \left\{ 1 - \exp \left[- 7.3 \left(\frac{D_1 t}{h^2} \right)^{0.75} \right] \right\} + M_{\infty 2} \left\{ 1 - \exp \left[- 7.3 \left(\frac{D_2 t}{h^2} \right)^{0.75} \right] \right\} \quad (5)$$

In this model, D_1 , $M_{\infty 1}$ and D_2 , $M_{\infty 2}$ are the diffusivity and equilibrium uptakes of the fast and slow processes, respectively.

EXPERIMENTAL

Carbon Fabric

The carbon fabric used in this study was supplied by US Composites and was a 4 harness satin weave, with a 3K tow size, and an areal density and thickness of 0.02 g/cm² and 0.254 mm, respectively. The fabric was washed in acetone to remove lubricants and sizing and then placed in a recirculating oven at 100°C for 1 h to remove any residual moisture and/or acetone.

Monomer, Activator, and Catalyst (PA6)

AP grade caprolactam monomer was used in this study. The monomer has low levels of moisture (<0.0015% by mass), a low melting point ($T_m = 69^\circ\text{C}$), and low viscosity (4.87 mPa·s at 100°C). Bruggolen C20, hexamethylene dicarbamoyl dicaprolactam, and Bruggolen C10, sodium caprolactamate, both especially developed for AP of caprolactam, were used as the activator and catalyst, respectively. The melt temperature of both C10 and C20 is 60°C. The monomer, catalyst, and activator were supplied by Bruggemann Chemical U.S., Inc., and were used without any further processing or puri-

fication. Due to the sensitivity to moisture of the catalyst and activator, they were stored and handled in a dry box with the relative humidity maintained at 8%.

Processing

Twenty 300 x 300 mm layers of the carbon fabric were laid onto the tool surface and bagged and sealed using high temperature film and tacky tape. A thermocouple was positioned at the surface of the top layer of the carbon to record and monitor the temperature. The tool temperature was then raised to 100°C, and a continuous vacuum of 1 atmosphere was applied to the system.

The viscosity of the resin is a function of the levels of catalyst and initiator, temperature, and time. Various combinations were investigated to achieve both full wet-out of the preform and full polymerization. The caprolactam was heated to 100°C until it was liquid. The catalyst and activator were then added, and the solution was brought to a molten state. The catalyst is sensitive to moisture, and the caprolactam oxidizes rapidly at these temperatures. Therefore, storage and processing must be done in a dry nitrogen environment. The resin was then infused into the preform via an infusion line. Once the resin reached the end of the preform, the infusion line was clamped off, and the temperature was raised to 150°C to polymerize the PA6. For further details on the process the reader is referred to [2].

Moisture Exposure

A significant number of studies have shown that the rate of moisture absorption by polymer matrix composite materials is dependent on the temperature, relative humid-

ity, diffusivity of water in the polymer, and weave architecture of the fabric [3,4,7,26]. These studies have also shown that the maximum (or equilibrium) moisture absorbed by a particular composite material is independent of temperature and relative. At higher temperatures and relative humidity, the maximum amount of moisture absorbed by the material will be reached in a significantly shorter time than exposure to a lower relative humidity and lower temperature.

Since the focus of this study was to evaluate the deterioration in mechanical properties of the carbon fabric-nylon 6 matrix composite, it was decided to expose the material to the most aggressive moisture condition, i.e., immersed in water at 100° C. The specimens were cut from the panels using a diamond saw blade and then polished with 600 grit silicon carbide paper to minimize cracking or debonding of the edges. The size of specimens for the different tests is shown in Table 1.

Table 1. Sample sizes prepared for different tests

Test	Sample Size (mm)
Low Velocity Impact (LVI)	100 x 100
Flexure	10 x 80
Short Beam Shear Strength (SBSS)	9 x 25
Moisture Absorption (ASTM D-570)	25 x 75

The specimens were then dried in a recirculating air oven at 70°C and periodically weighed on a high precision balance with a 0.1 mg resolution, until the weight had stabilized. The dry weight (W_d) of all the specimens was then recorded. The samples were then placed on a rack that prevented them from any contact with each other and fully submerged into a reaction vessel containing boiling water. The temperature of the water

was maintained at 100°C using a hot plate and oil bath to maintain even heating. The specimens were taken out at periodic intervals and weighed after excess moisture was wiped off. The percentage weight gain (Equation 1) was monitored as a function of the square root of time.

$$M = \frac{W_i - W_d}{W_d} \times 100 \quad (1)$$

Where M = percentage weight gain; W_i = weight of moist material at a specific time; and W_d = dry weight.

The weight gain was plotted against the square root of time until the equilibrium weight gain M_∞ was reached. The samples were then removed from the chamber. 50% of the samples were put into a container with water at ambient temperature and taken for testing and evaluation, while the rest were placed in a recirculating oven at 70°C to dry. The samples were periodically weighed until the weight had stabilized, indicating that all the moisture had been removed. The samples were placed in a desiccator and taken for testing and evaluation.

UV Exposure

Specimens were cut and prepared according to the dimensions provided in Table 1 for LVI, flexure, and SBSS tests. The specimens were then placed in RTR 200 UV exposure chamber with 12 fluorescent bulbs that provided UV irradiance at wavelengths of 200 to 400 nm within the chamber. These UV photons provide energy that is within the range of the dissociation energies of polymer bonds, which are typically between 290-460 kJ/mole. The specimens were removed at 100, 200, 300, 420, and 600 h of exposure and tested and evaluated.

RESULTS AND DISCUSSION

Moisture

Visual observation of the specimens that were exposed to moisture showed that there were areas of whitening of the matrix. The specimens seemed to have maintained structural integrity, and there was no evidence of complete breakdown of the matrix away from the fiber. SEM was conducted to ascertain the damage to the matrix and the fiber/matrix interface. Figure 1 shows cracks that were formed on the surface due to the effects of moisture and heat on the specimens. These were probably microcracks, which could not be seen by SEM prior to moisture exposure, that developed due to the residual stresses from the processing of the composite and which were expanded during exposure. Other processing anomalies, such as surface roughness, stacking faults in the weave, and misaligned fibers, could also contribute to cracks that opened during moisture exposure. Figure 2 shows the effect of the moisture attack on the fiber matrix interface. Figure 3 shows a SEM image of an as-processed sample, and it is evident that the fibers are well coated with the matrix and there is good adhesion of the matrix to the fiber.

UV Exposure

The specimens that were exposed to UV started to show discoloration after 300 h and, after 600 h of exposure, there was considerable yellowing of the specimens. There were no signs of chalking of the matrix or fibers that were exposed at the surface of the specimen. The specimens maintained their structural integrity and there were no visible signs of deterioration except for the yellowing. SEM microscopy showed that the fi-

ber/matrix interface was preserved and no cracks were evident on the surface of the specimens.

Water Absorption

Figure 4 shows the moisture absorption curves for the carbon/nylon 6 composites. Closer observation of the figure clearly indicates that for all samples sizes there is a definitive early stage of fast diffusion, followed by a slow (reduced) diffusion rate.

These results are in agreement with the model proposed by Bao and Yee. They showed that there were two distinct linear regions before the equilibrium moisture was reached in bismaleimide matrix woven carbon fiber composites,. Their study found that the moisture uptake was composed of two processes with different rates, a fast initial rate and then a slower rate, which compares well to what is observed in Figure 4. They proposed the dual diffusivity model (Equation 5), which is the sum of two Fickian processes with different diffusivities.

$$M_t = M_{\infty 1} \left\{ 1 - \exp \left[- 7.3 \left(\frac{D_1 t}{h^2} \right)^{0.75} \right] \right\} + M_{\infty 2} \left\{ 1 - \exp \left[- 7.3 \left(\frac{D_2 t}{h^2} \right)^{0.75} \right] \right\} \quad (5)$$

In the above model, D_1 , $M_{\infty 1}$ and D_2 , $M_{\infty 2}$ are the diffusivity and equilibrium uptakes of the fast and slow processes, respectively. As the absorption is described by the sum of two Fickian processes, Equation (4) can be used to determine diffusivity D_1 and D_2 can then be determined from Equation (5).

The curve fit using the Bao and Yee dual diffusion model [2] is shown in Figure 5 for the ASTM D-570 specimens. The dual diffusion model (Equation 5) shows very good correlation with the experimental data obtained in this study, with $R^2 = 0.99$. A Fickian

fit is also shown with $R^2 = 0.76$, which shows very poor correlation with the experimental data.

The bidirectional woven fiber arrangement (as in the carbon fabric used in this study) restricts matrix shrinkage in both directions, which could cause surface defects, as described earlier. These defects, especially near the surface, fill up with water very rapidly after immersion. However, this water does not change the local water concentration in the matrix; therefore, the water diffusion in the matrix is independent of the fast diffusion into the defects. Hence, the weight gains can be described by the sum of the two Fickian processes. The slow diffusion process corresponds to the diffusion in the matrix and represents the properties of the composite. The fast diffusion is more a function of the physical flaws of the composite, namely surface defects.

Crystallization Study

A TA Instruments Q100 differential scanning calorimeter (DSC) was used to characterize the thermal behavior of the samples exposed to moisture (M), specimens exposed to moisture and then dried (MD), and specimens as processed (D). The specimens were heated from 40 to 250°C at a rate of 10°C/min.

MOISTURE EXPOSURE

Figure 6 shows the DSC thermograms for the different specimens. A single peak at the melt temperature of 225°C for all three specimens was observed. The crystallinity was determined by comparing the experimental heat of fusion (ΔH) to the theoretical value for a 100% crystalline sample. ΔH was measured by integrating the area under the

peaks of the DSC thermograms. All three specimens yielded average ΔH values of 94 J/g, which translated into crystallinity values of 40%. Although various values have been reported in the literature for the theoretical ΔH , the value of 230 J/g, referenced from the ATHAS data bank [27], was used as it is the accepted value used by other researchers [28]. There is no apparent influence of moisture absorption on the position (temperature) and shape (crystallinity) of the melting peaks. Russell and Beaumont [29] also found that exposure to boiling water had no significant influence on the structure and morphology of the spherulites of nylon 6 moldings. It can be speculated that although there is plasticization of the matrix and possible changes to the crystal ordering during exposure to moisture, the heating during the DSC study causes the material to dry and recover sufficiently so that the thermograms are the unchanged.

UV EXPOSURE

Figure 7 shows the DSC thermograms of the specimens exposed to UV for 100 to 600 h. The melt temperatures (223°C) of the different specimens are within 1°C and fall well within the range of melt temperatures for nylon 6. The ΔH values for the specimens exposed to 100, 200, 300, 420, and 600 h of UV were 94, 97, 100, 101.5, and 103 J/g, respectively. This results in an increase in crystallization of 40 to 44%, using 230 J/g as the theoretical heat of fusion for 100% crystallinity. The exposure to UV light provides energy for the recrystallization of the nylon 6 polymer. Initial analysis of the data suggested that the heat generated from the exposure to UV caused annealing in the specimens; however, a cooling fan in the chamber maintains the temperature to under 40°C, which is too low to cause annealing. It is therefore postulated that the energy from the

UV causes molecular mobility and some recrystallization in the specimen. These specimens were taken from the surface of the exposed samples, as the depth of penetration of the UV is only within the top 50 to 60 microns of the sample. Therefore this result should not be overanalyzed with respect to predicting the overall effect to the composite structure.

FLEXURE TESTS

Three-point bend tests were conducted according to ASTM D 790M. Twelve samples of the dimensions 10 x 80 x 4 mm were prepared from the panels. Eight specimens were exposed to moisture and the remaining four were dried as per the preconditioning for the moisture tests. After exposure to moisture, four of the samples were also dried to allow some recovery. The support span was set at 64 mm, and the rate of cross-head motion was 1.7 mm/min.

Moisture Exposure

The results are summarized in Table 2. The average flexural modulus was lowered by 15% after exposure to moisture at 100°C. However, the modulus of the material was fully recovered after drying. The flexural strength was lowered by 45% after exposure to moisture and recovered to within 10% after drying. The mode of failure was a combination of tensile face fracture and wrinkling on the compressive face for the dry sample, similar to the failure shown in Figure 9. However, after exposure to moisture, the mode of failure was only wrinkling on the compressive face and delamination for both sets. The failure mode in the dry as-processed sample can be attributed to the high degree

of crystallinity of the nylon 6 due to the in situ anionic polymerization of the nylon 6 [2]. After exposure to moisture at 100°C, plasticization of the matrix occurs; this causes failure that is more typical of a thermoplastic composite. Figure 8 shows the typical failure for a sample exposed to moisture and then tested. The failure on the compressive face and subsequent delamination can be clearly observed.

UV Exposure

A total of 20 samples (4 at each time increment) were exposed to UV for 100, 200, 300, 420, and 600 h and tested as described previously. The results of the tests are summarized in Table 2. There was no significant change in the flexural properties after exposure to UV for up to 600 h. The maximum time of exposure (600 h) did not cause sufficient damage to the structure of the matrix. A significantly longer time of exposure is required before any change in the structure affects the flexural properties of the composite. A typical failed sample after exposure to UV for 600 h is shown in Figure 9. The mode of failure was a combination of tensile face fracture and wrinkling on the compressive surface. The flexural properties of the samples exposed to UV are lower than the values for the as-processed dried samples. These samples were not kept in a dry environment after processing, and it is assumed that some moisture was absorbed from the ambient room conditions.

Table 2. Average results of flexure tests performed for carbon/nylon 6 samples; M – samples exposed to moisture; MD- samples exposed to moisture, then dried; D- samples processed and then dried to remove any moisture

	Modulus (GPa)			Flexural Strength (MPa)		
	M	MD	D	M	MD	D
Mean	43.88	52.02	51.40	350.21	583.63	642.24
Standard Error	1.65	1.37	0.94	9.90	38.60	89.95
Minimum	39.44	48.52	48.92	327.47	472.17	475.08
Maximum	46.85	55.23	53.49	374.35	637.30	847.41

Table 3. Average results of flexure tests performed for carbon/nylon 6 samples, for various number hours of UV exposure.

Hours of exp.	Modulus (GPa)					Flexural Strength (MPa)				
	100	200	300	420	600	100	200	300	420	600
<i>Mean</i>	45.14	48.03	44.37	44.26	45.73	480.	548	457	467	511
<i>Standard Err.</i>	0.75	1.37	0.87	2.35	1.15	24.5	34	26	54	45
<i>Minimum</i>	43.65	45.53	41.92	38.67	42.62	440.	477	383	343	393
<i>Maximum</i>	47.20	51.91	45.68	49.49	48.00	551	641	503	582	607

Interlaminar Shear Stress

Short beam shear (SBS) tests were conducted according to ASTM D2344 to measure the interlaminar shear stress of the composites. The beams were loaded in three-point bending such that the dominant failure is shear. A variety of failure modes (bending, plastic indentation, and compressive) can occur that can skew the results, and care must be taken to examine the failed specimen to ensure that failure occurs at the midsection or neutral axis of the beam, which is indicative of shear failure. The tests do not purport to be absolute; however, they are a good indication for comparative analyses. The support span for the SBS test was 16 mm (4 x thickness), and the rate of cross-head motion was 1.0 mm/min.

MOISTURE ABSORPTION

The results are summarized in Table 3. The average short beam shear strength (SBSS) of the samples was 65% lower after exposure to moisture at 100°C. The material only recovered to 47% after drying. A typical photomicrograph of the tested samples is shown in Figure 10. It can be seen that the failure is between the laminar of the composite and at the midsection where the shear stress is at a maximum, and it can be assumed the SBSS is very close to the interlaminar shear strength. The radical loss after exposure to moisture is attributed to the plasticization of the matrix. The fiber matrix interface has also been degraded by moisture ingress, as shown in Figure 2. This was expected, as the interlaminar shear stress (ILSS) is a matrix dominated property. The material did have some recovery after drying; however, damage to the fiber matrix interface is irrecoverable.

UV EXPOSURE

A total of 20 samples (4 at each time increment) were exposed to UV for 100, 200, 300, 420, and 600 h and tested as described previously. The results of the tests are summarized in Table 4. There was no significant change in the ILSS properties after exposure to UV for up to 600 h. The maximum time of exposure (600 h) did not cause sufficient damage to the structure of the matrix. A significantly longer time of exposure is required before any change in the structure affects the ILSS properties of the composite. It should be noted that the SBSS values after exposure to UV are 24% lower than in the as-processed dried sample. It is assumed that the samples absorbed some moisture from

the ambient environment, as no special care was taken after processing to keep these samples in a dry environment.

Table 4. Average results of SBSS tests performed for carbon/nylon 6 samples; M – samples exposed to moisture; MD- samples exposed to moisture, then dried; D- samples processed and then dried to remove any moisture

	SBSS (MPa)		
	M	MD	D
Mean	22.98	35.45	66.41
Standard Error	0.32	0.67	0.61
Minimum	22.33	33.79	65.13
Maximum	23.79	37.03	68.03

Table 5. Average results of SBSS tests performed for carbon/nylon 6 samples, at various number hours of UV exposure.

Hours of Exp.	SBSS (MPa)				
	100	200	300	420	600
Mean	46.87	52.11	55.09	49.07	49.81
Standard Error	3.72	2.47	1.68	3.97	3.63
Minimum	36.26	48.44	50.24	43.52	40.98
Maximum	52.54	56.81	57.39	56.76	58.35

Impact

Low-velocity impact (LVI) tests were conducted to study the resistance to impact and damage initiation and propagation of the carbon/nylon 6 composite panels exposed to moisture and UV. An instrumented drop weight tower equipped with a load cell of capacity 1590 kg (3500 lbs) was used to conduct the tests. A hemispherical shaped tup of diameter 19.5 mm and mass 0.12 kg was used as the impactor. The total impactor mass,

including the tup, was 6.15 kg. The samples were clamped using a pneumatic assist mechanism, such that 76.2 mm diameter of the sample face was exposed to the impactor. Three impact heights, 0.46 m, 0.71 m, and 1.15 m, were chosen in order to capture the dominant failure modes of the plates from incipient to total failure and to analyze the energy absorption mechanism and damage progression. The force-time, energy-time, and load-deflection response of the samples were measured. Damage initiation and progression was monitored.

MOISTURE EXPOSURE

The failure modes of the three different types of samples, i.e., exposed to moisture (M), exposed to moisture then dried (MD), and as-processed and dried (D), were very different. The samples that were exposed to moisture showed a slight loss in stiffness, as the matrix became more plasticized and the fiber-matrix interfacial bond was compromised. This resulted in a more localized damage zone, as energy transfer/spread was mitigated. The recovered samples (MD) performed marginally better due to the matrix recovering some of its properties; however, the loss in the fiber matrix interface cannot be recovered. Figure 11 shows the force/energy – time profiles for the samples at the maximum drop height of 760 mm. The maximum energy absorbed by all three samples is approximately the same. However, the dry sample offers some rebound after impact. This implies that the sample is capable of absorbing more energy. The load profiles of the samples show that the failure in the moisture-exposed sample is quite catastrophic, as there is a sharp drop after the maximum load. The dry sample shows that there are damage interactions within the sample at the peak load. These interactions are load transfers

from matrix to fiber and delamination. The peak is not sharp, which implies that the sample is capable of withstanding a higher load. Inspection of the failed samples confirm these results, with the dry sample having a larger damage spread compared to the moisture exposed sample. SEM observation, as shown in Figure 12, shows that most of the fibers in the moisture exposed samples were not coated with the matrix, while Figure 13, the SEM image of the dry sample, shows that the fractured fibers are still well coated by the matrix. The main mode of failure for the dry samples was tensile face fracture with largely fiber breakage. The moisture exposed sample was a combination of fiber breakage and pull out. The fibers in the dry sample had multiple fractures compared to the moisture exposed samples. The sample exposed to 600 h of UV is shown in Figure 14; however, the failure in both dry and UV exposed samples are identical.

UV EXPOSURE

The samples that were exposed to UV for up to 600 h performed identically to the dry samples. The load/energy – time curve for a sample exposed to 600 h of UV is shown in Figure 15, which is identical to the profile for the dry sample shown in Figure 11. The SEM observation, shown in Figure 13, also shows no difference between the UV exposed samples and the dry samples.

SUMMARY

The equilibrium moisture content was reached after immersion in distilled water at 100°C for 100 h. SEM images showed that surface defects due to processing have been expanded and the fiber matrix interface was attacked by the water ingress. The dual

Fickian model for bidirectional composite developed by Bao and Yee [3] showed good correlation to the experimental results for water absorption.

DSC studies showed that the moisture ingress did not have any influence on the melting peaks or the crystallinity of the composite. The flexural properties are lowered by 45% due to water ingress; however, the material recovers to within 10% after drying. The SBSS, a matrix dominated property, is lowered by 65% due to water ingress and only recovers to 47% after drying. Low-velocity impact shows that the damage to the samples exposed to moisture performs much lower than the as-processed dry samples. The main contributing factor to the lowering of the mechanical properties is the plasticization of the matrix and the attack on the fiber matrix interface by the water.

Exposure to UV for up to 600 h caused yellowing of the samples. The crystallinity increased from 40 to 44% due to UV exposure. However, this was only on the surface of the samples. 600 h of exposure to UV did not have any effect on the flexural, inter-laminar shear strength or impact properties of the composite. The time of exposure will have to be significantly increased before the properties start to deteriorate.

REFERENCES

1. Sibal, P.W., Camargo, R.E. and Macosko, C.W. (1982). Designing Nylon 6 Polymerization for RIM, In: *Proceedings of the Second International Conference on Reactive Processing of Polymers*, pp. 97-125, Pittsburgh, Pennsylvania.
2. Pillay, S., Vaidya, U.K. and Janowski, G.M., (2005). Liquid Molding of Carbon Fabric-reinforced Nylon Matrix Composite Laminates, *Journal of Thermoplastic Composite Materials*, **18**: 509-527.
3. Bao, L.R. and Yee, A.F. (2002). Moisture Diffusion and Hygrothermal Aging in Bismaleimide Matrix Carbon Fiber Composites: part II-woven and Hybrid Composites, *Composites Science and Technology*, **62**: 2111-2119.

4. Shen, C.H. and Springer, G.S. (1977). Effects of Moisture and Temperature on the Tensile Strength of Composite Materials, *Journal of Composite Materials*, **11**: 2-16.
5. Shen, C.H. and Springer, G.S. (1977). Environmental Effects on the Elastic Moduli of Composite Materials, *Journal of Composite Materials*, **11**: 250-264.
6. Ishai, O., Environmental Effects on Deformation, Strength, and Degradation of Unidirectional Glass-fiber Reinforced Plastics. I. Survey, *Polymer Engineering and Science*, **15**: 486-490.
7. Ishak, Z.A.M. and Berry, J.P. (1994). Hygrothermal Aging Studies of Short Carbon Fiber Reinforced Nylon 6.6, *Journal of Applied Polymer Science*, **51**: 2145-2155.
8. Weitsman, Y.J. (1991). *Fatigue of Composite Materials*, Elsevier, New York.
9. Pitchard, G., (1999). *Reinforced Plastics Durability*, Woodhead Publishing Company, Cambridge, UK.
10. Zheng, Q. and Morgan, R.J. (1993). Synergistic Thermal-moisture Damage Mechanisms of Epoxies and Their Carbon Fiber Composites, *Journal of Composite Materials*, **27**: 1465-1478.
11. Rabek, J.F. (1995). *Polymer Photodegradation*, Chapman and Hall, London.
12. Scott, G. (1990). *Polymer Degradation and Stabilization*, Elsevier Applied Science, London.
13. Wypych, J. (1990). *Weathering Handbook*, Chemtec Publishing, Toronto, Canada.
14. Kumar, B.G., Singh, R.P. and Nakamura, T. (2002). Degradation of Carbon Fiber-reinforced Epoxy Composites by Ultraviolet Radiation and Condensation, *Journal of Composite Materials*, **36**: 2713-2733.
15. Ranby, B. and Rabek, J.F. (1975). *Photodegradation, Photo-Oxidation and Photostabilization of Polymers*, John Wiley and Sons, London.
16. Crivello, J.V., Narayan, R. and Sternstein, S.S. (1997). Fabrication and Mechanical Characterization of Glass Fiber Reinforced UV-cured Composites from Epoxidized Vegetable Oils, *Journal of Applied Polymer Science*, **64**: 2073-2087.
17. Whitcomb, J. and Tang, X. (2002). Micromechanics of Moisture Diffusion in Composites with Impermeable Fibers, *Journal of Composite Materials*, **36**: 1093-1101.

18. Suh, D.W. et al. (2001). Equilibrium Water Uptake of Epoxy/Carbon Fiber Composites in Hygrothermal Environmental Conditions, *Journal of Composite Materials*, **35**: 264-278.
19. Wan, Y.Z., et al (2002). Three-dimensionally Braided Carbon Fiber-Epoxy Composites, a New Type of Material for Osteosynthesis Devices. I. Mechanical Properties and Moisture Absorption Behavior, *Journal of Applied Polymer Science*, **85**: 1031-1039.
20. Trabocco, R.E. and Stander, M. (1976). Effect of Natural Weathering on the Mechanical Properties of Graphite/Epoxy Composite Materials, ASTM STP 602.
21. Phelps, H.R. and Long, Jr. E.R. (1980). Property Changes of a Graphite/Epoxy Composite Exposed to Nonionizing Space Parameters, *Journal of Composite Materials*, **14**: 334-341.
22. Giori, C. and Yamauchi, T. (1984). Effects of Ultraviolet and Electron Radiations on Graphite-Reinforced Polysulfone and Epoxy Resins, *Journal of Applied Polymer Science*, **29**: 237-249.
23. Shen, C.H. and Springer, G.S. (1976). Moisture Absorption and Desorption of Composite Materials, *Journal of Composite Materials*, **10**: 2-20.
24. Crank, J. (1975). *The Mathematics of Diffusion*, 2nd Edition, Oxford Press, London.
25. Bond, D.A. (2005). Moisture Diffusion in a Fiber-reinforced Composite: Part 1 – Non-Fickian Transport and the effect of Spatial Distribution, *Journal of Composite Materials*, In press
26. Browning, C.E., Husman, G.E. and Whitney, J.M. (1977). Moisture Effects in Epoxy Matrix Composites, ASTM Special Technical Publication, n617, pp. 481-496.
27. Pyda, M. (ed.) (1994). ATHAS Data Bank, <http://web.utk.edu/~athas/databank/>
28. Fornes, T.D. and Paul, D.R. (2003). Crystallization Behavior of Nylon 6 Nanocomposites, *Polymer*, **44**: 3945-3961.
29. Russel, D.P. and Beaumont, P.W.R. (1980). Structure and Properties of Injection-Molded Nylon-6: Part 1-Structure and Morphology of Nylon-6. *Journal of Materials Science*, **15**: 197-207.

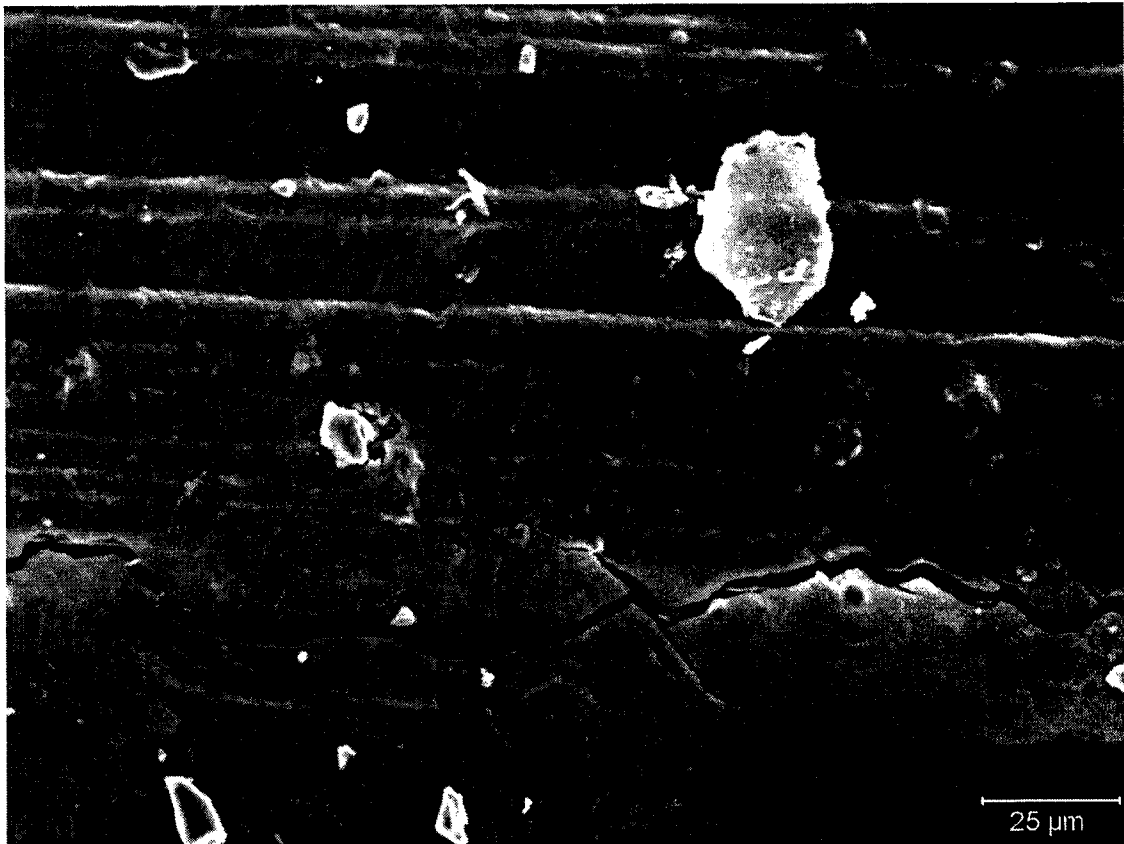


Figure 1. SEM image of carbon/nylon 6 composite surface cracks after exposure to water at 100°C for 100 h.

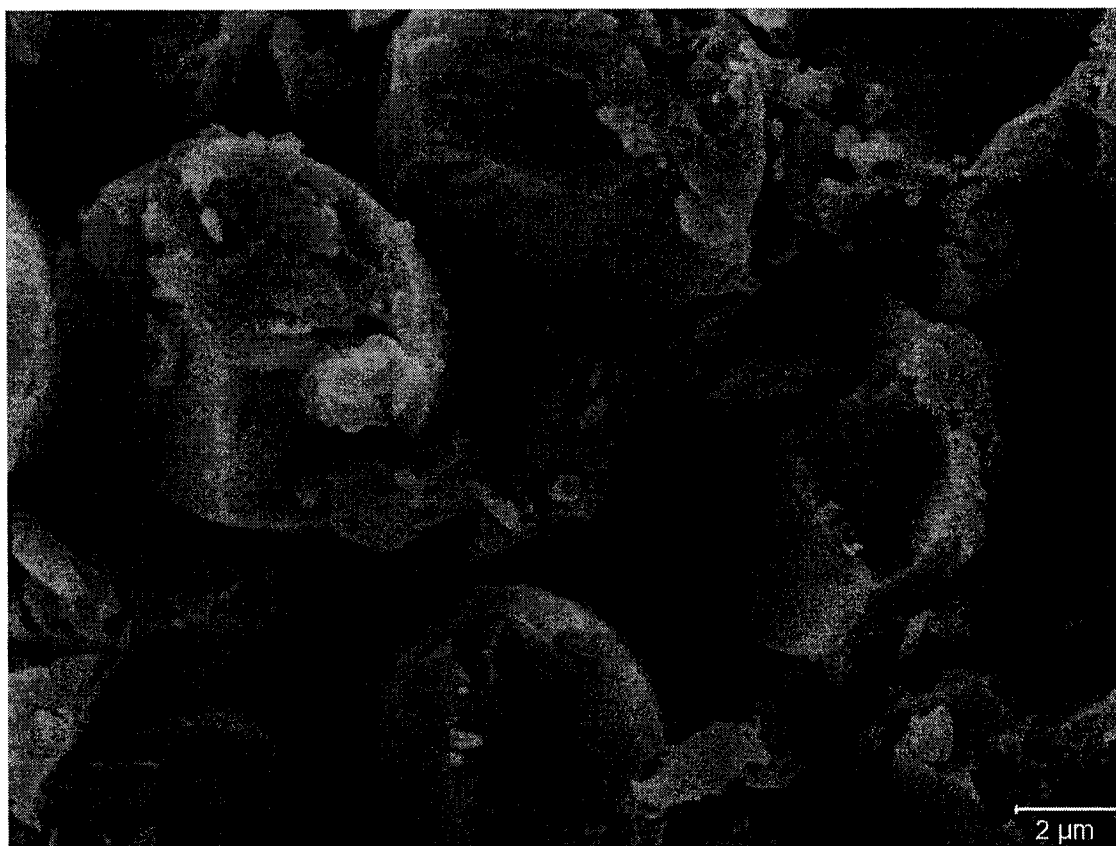


Figure 2. SEM image of carbon/nylon 6 composite showing fiber matrix interface degradation after exposure to water at 100°C for 100 h.

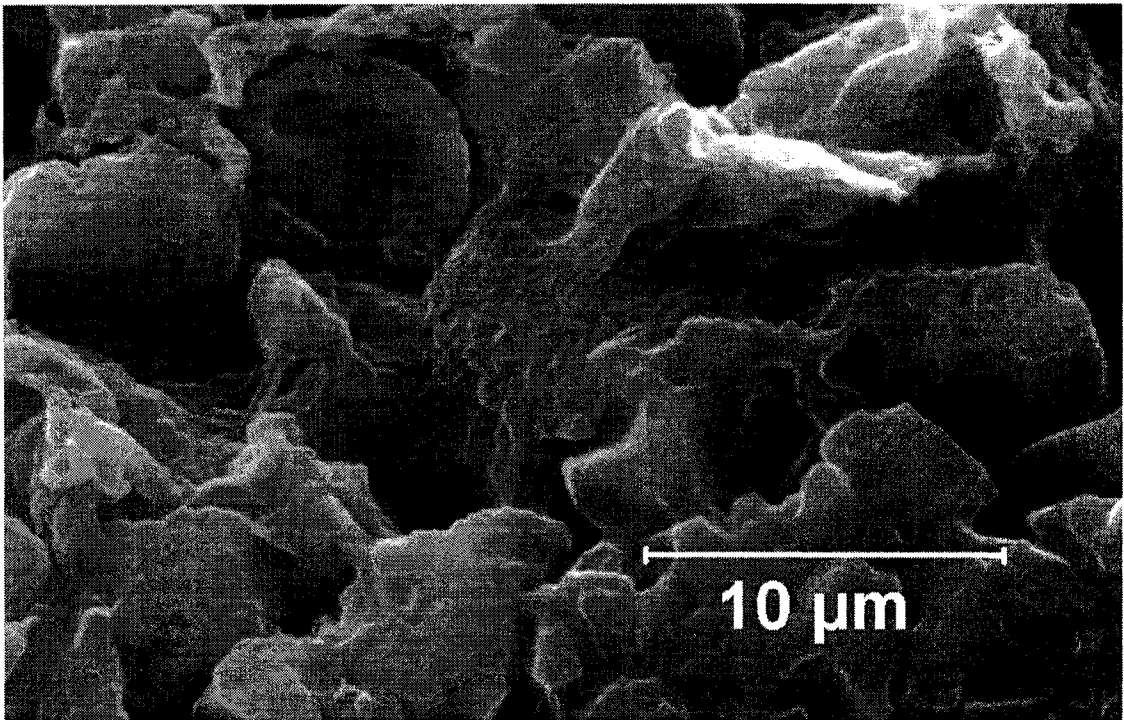


Figure 3. SEM image of carbon/nylon 6 composite showing the fiber matrix interface after processing. Very good wet-out at the filament level is achieved.

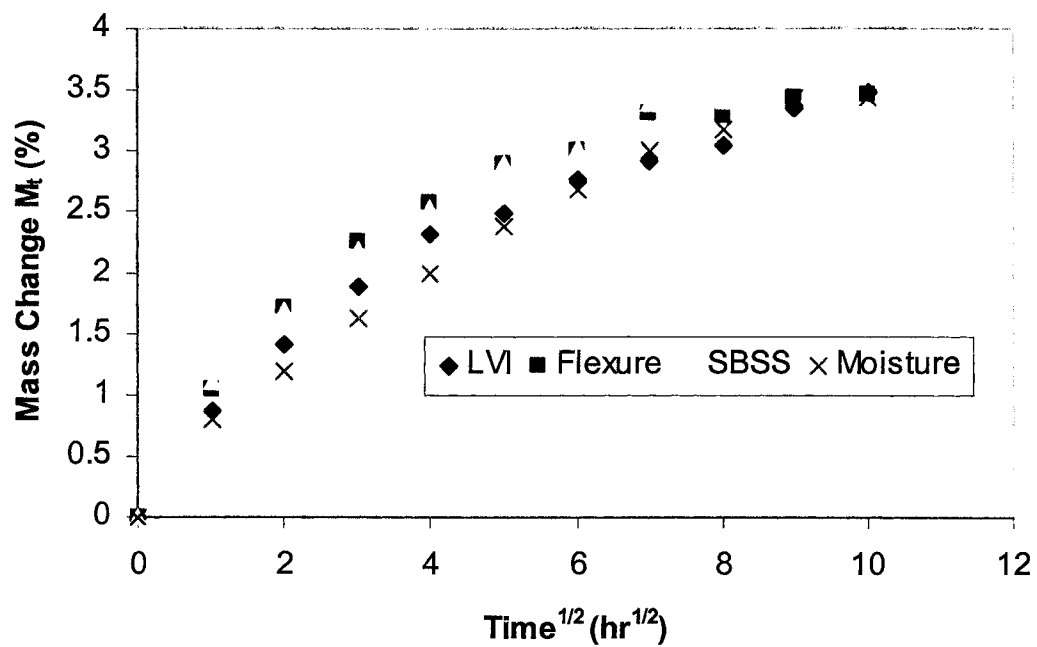


Figure 4. Curve showing percentage of water absorption against the square root of time for the different types of samples immersed in water at 100°C.

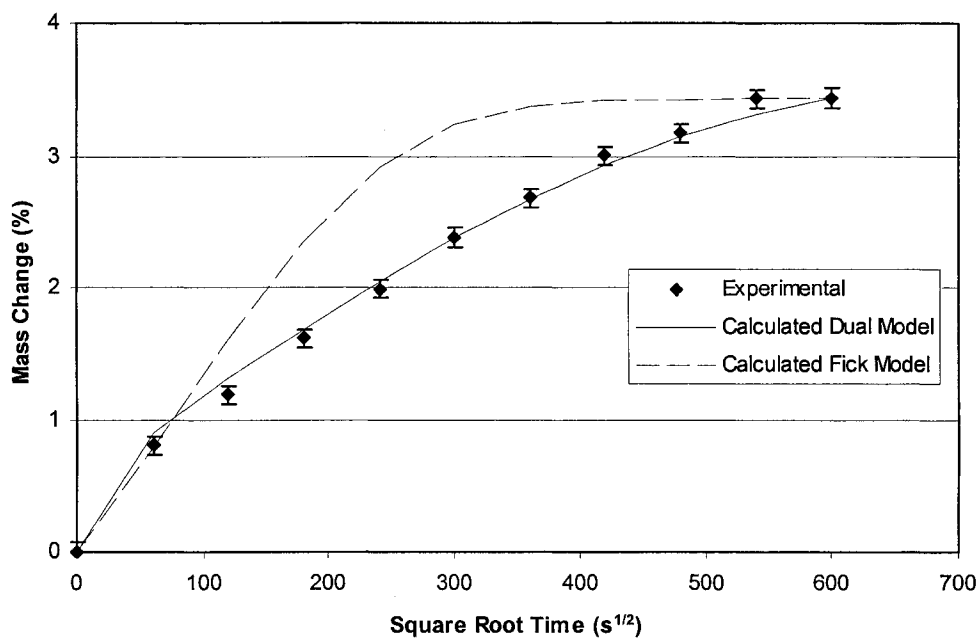


Figure 5. Curve showing percentage of water absorption against the square root of time for the ASTM D 570 samples immersed in water at 100°C compared to the dual diffusivity and Fickian models.

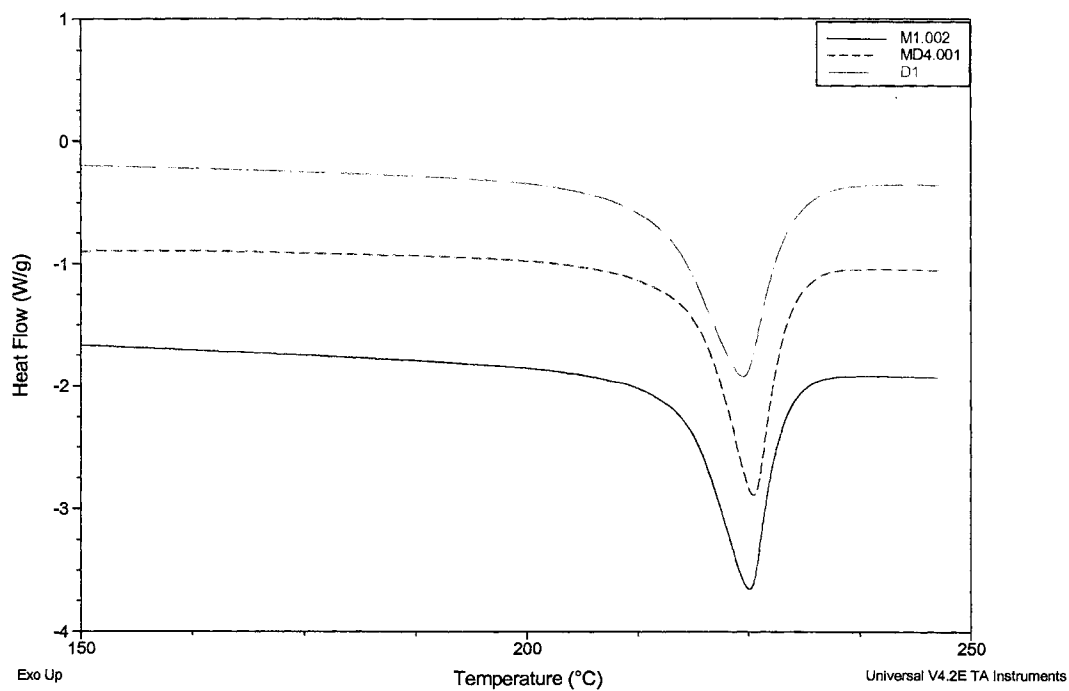


Figure 6. DSC thermograms for samples immersed in water at 100°C for 100 h, after recovery and dry samples.

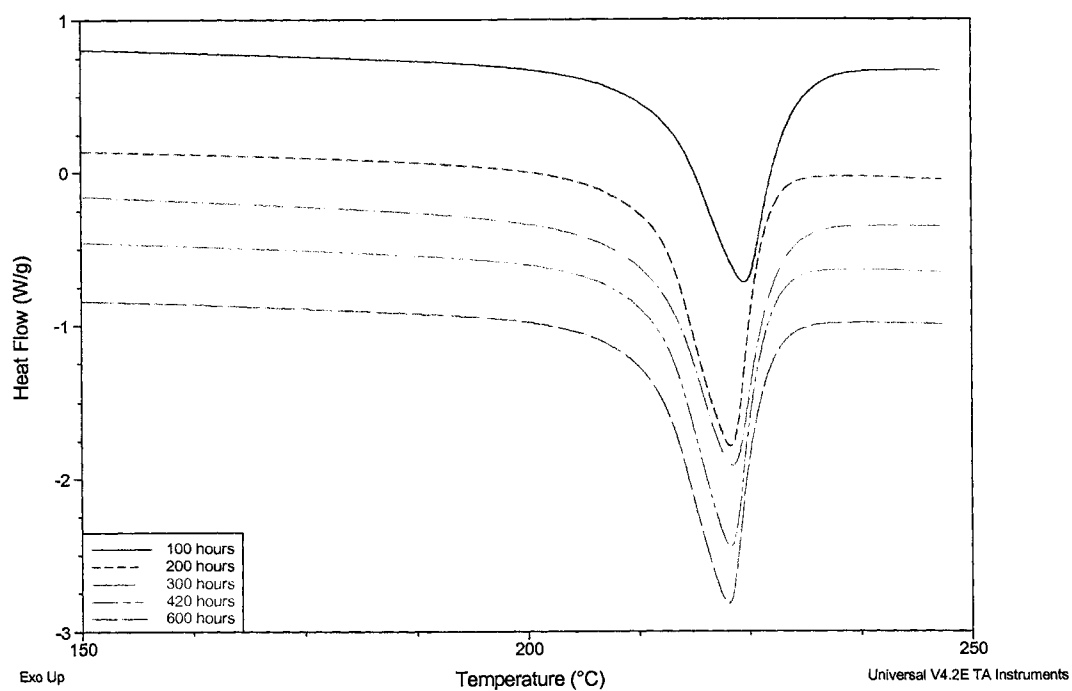


Figure 7. DSC thermograms for samples exposed to UV for 100, 200, 300, 420, and 600 h.

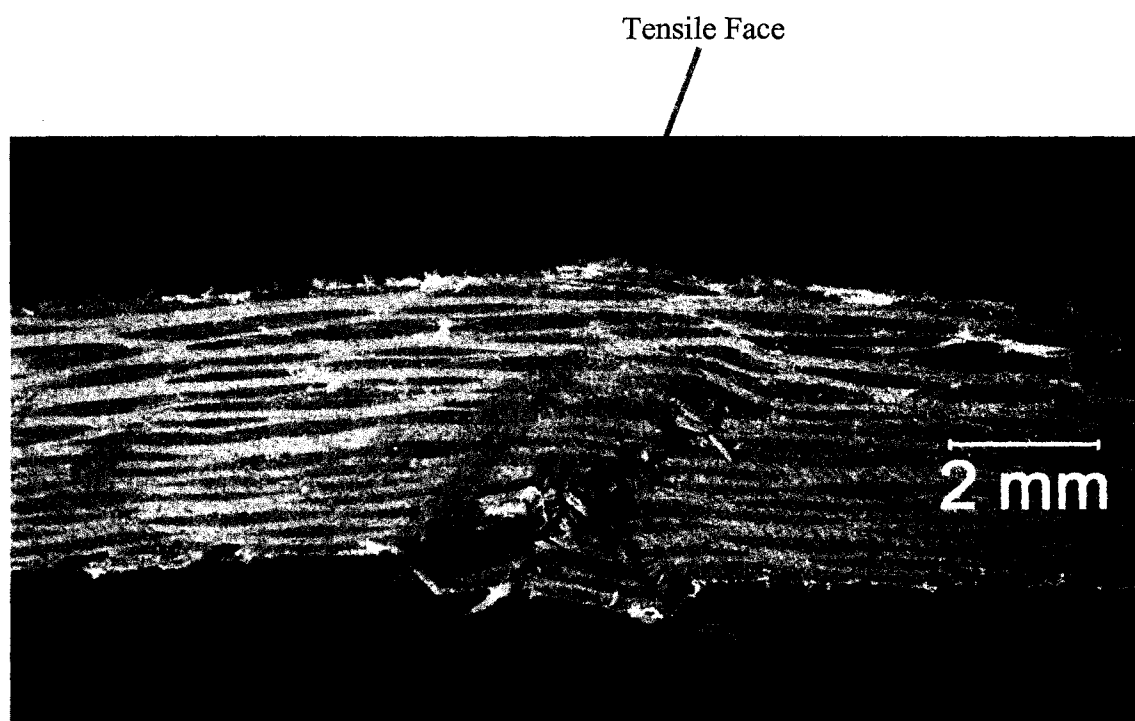


Figure 8. Typical failed carbon/nylon 6 sample tested in flexure after immersion in water at 100°C for 100 h.

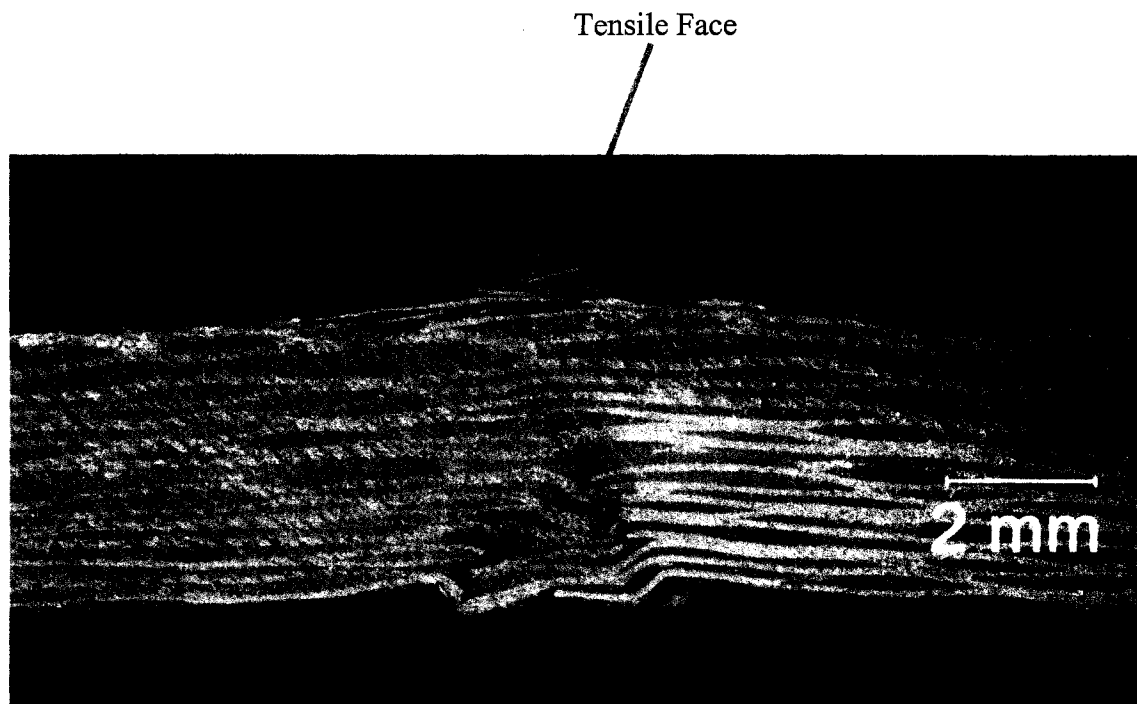


Figure 9. Typical failed carbon/nylon 6 sample tested in flexure after exposure to UV for 100 h. Mode of failure was a combination of tensile face fracture and fiber wrinkling on the compressive face.

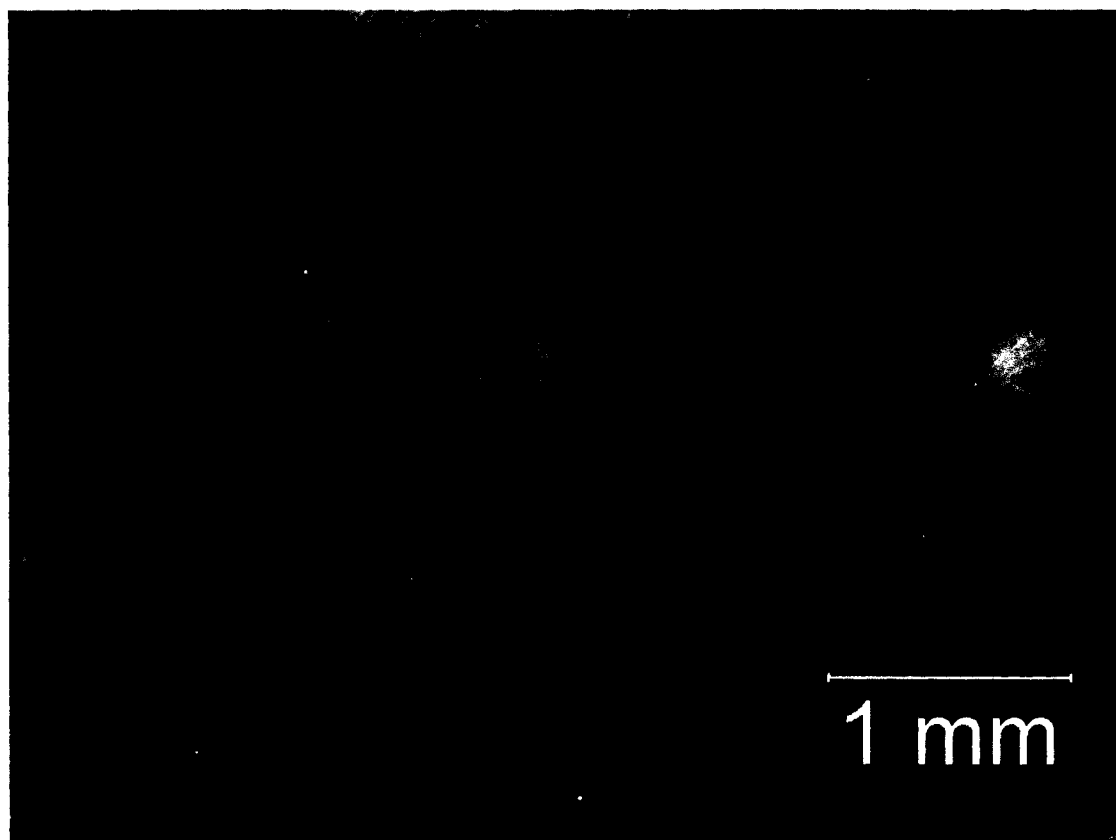


Figure 10. Typical failed SBSS sample, with initial failure crack at the midsection, as highlighted in the image.

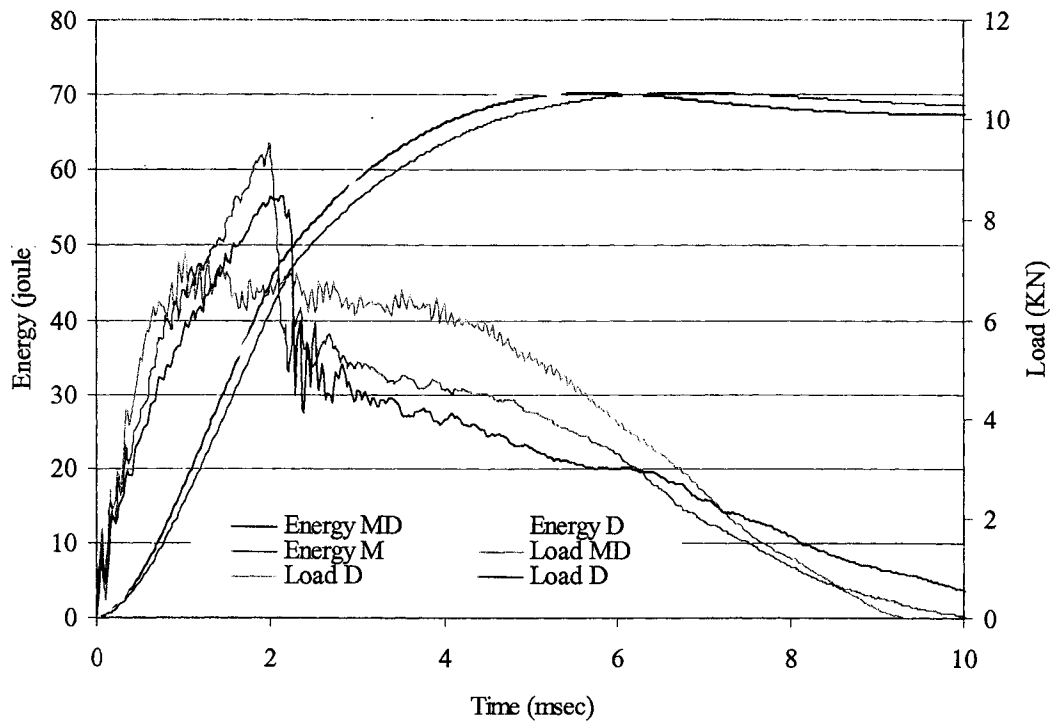


Figure 11. Typical force/energy – time curves for carbon/nylon 6 composite material exposed to moisture at 100°C; M- exposed to moisture, MD- exposed to moisture then dried, D- as processed and dried

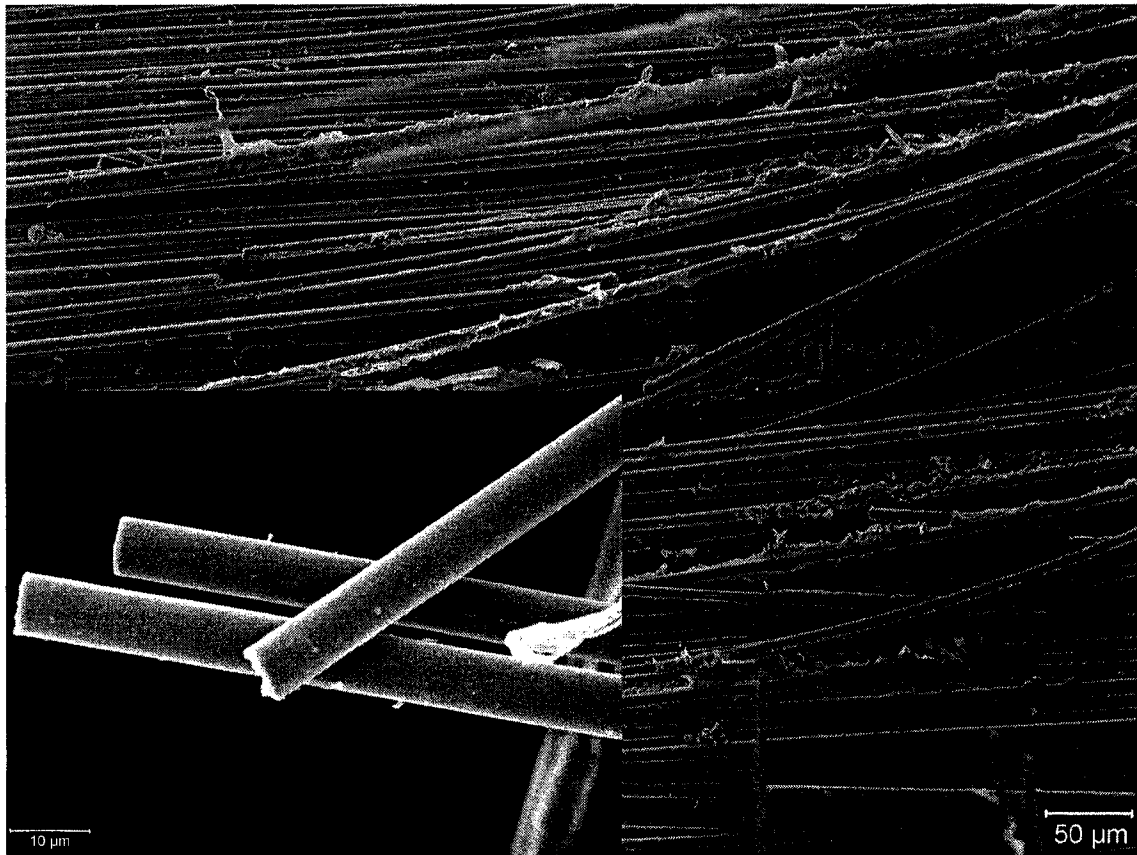


Figure 12. SEM image of moisture exposed sample after low-velocity impact test. Inset shows dry filaments, indicative of the fiber matrix interface attach by the moisture.

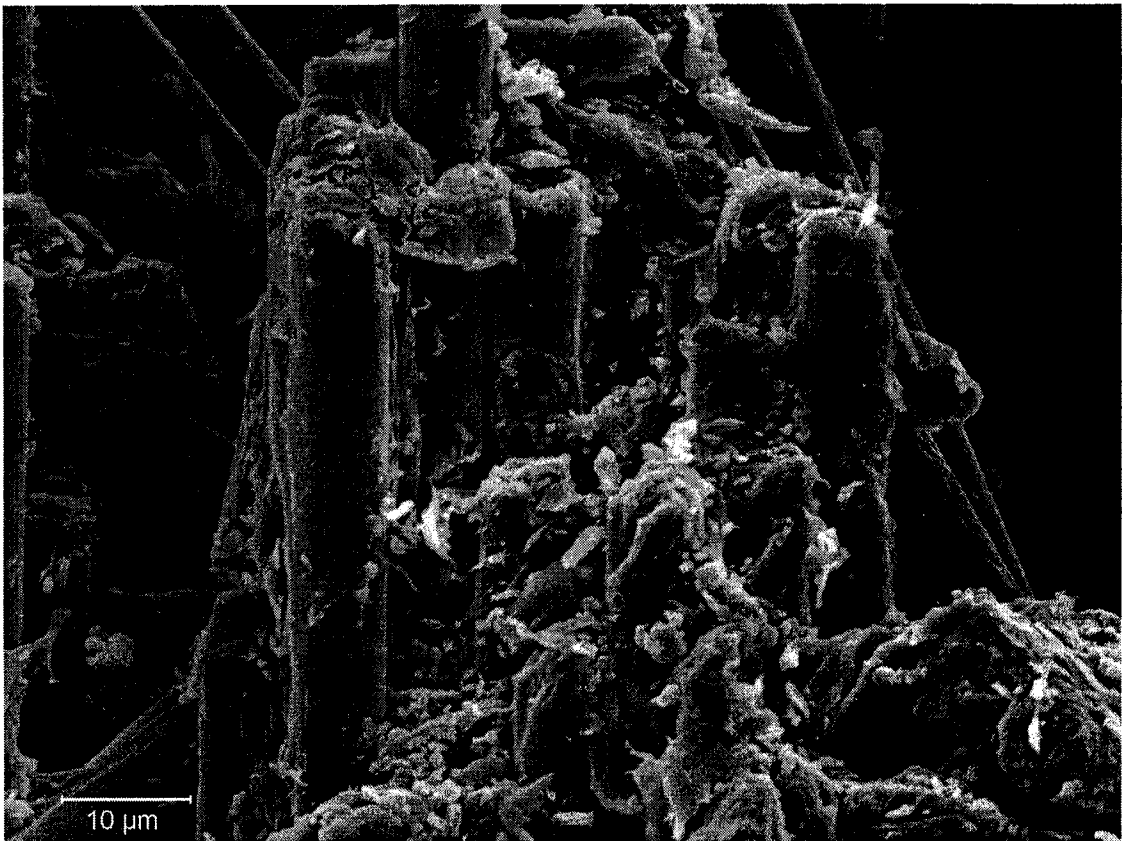


Figure 13. SEM image of as-processed, dry sample after low- velocity impact test. Failure mode is mainly due to fiber breakage, and matrix adhesion to the fiber is clearly evident.

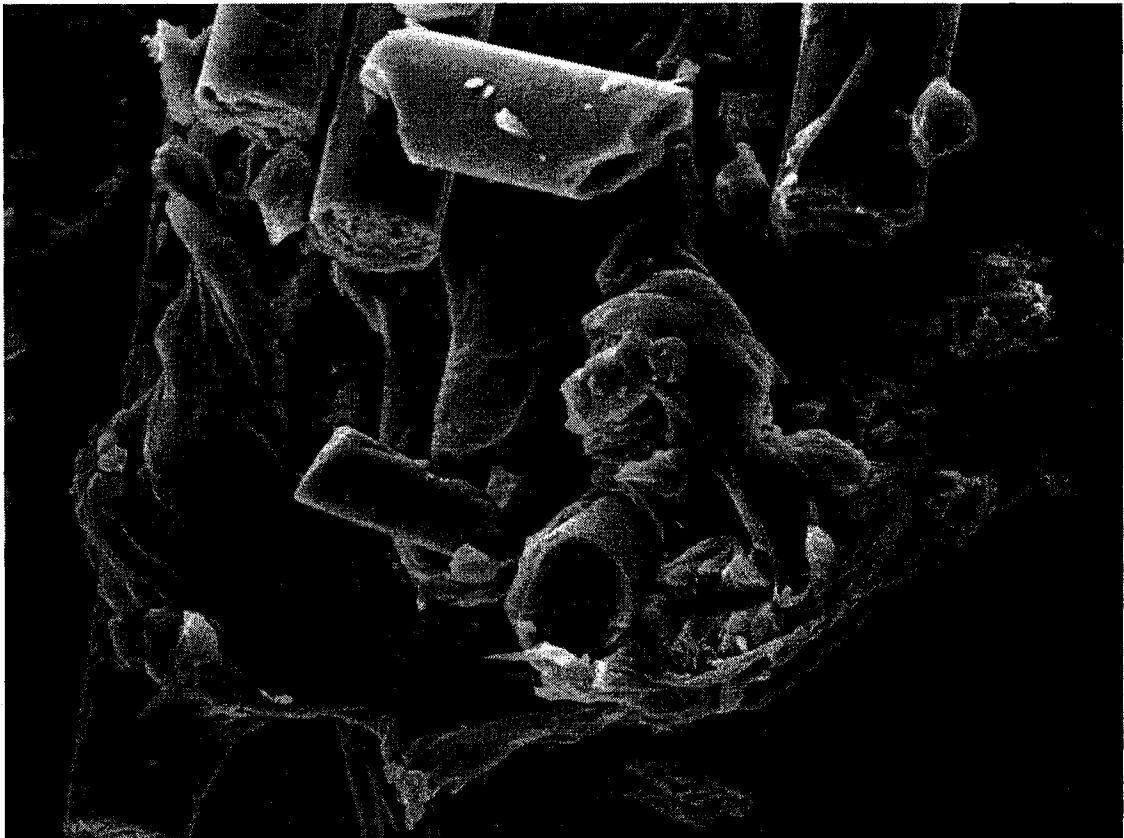


Figure 14. SEM image of sample exposed to 600 h of UV and then tested under low-velocity impact conditions. Failure mode is mainly due to fiber breakage, and matrix adhesion to the fiber is clearly evident.

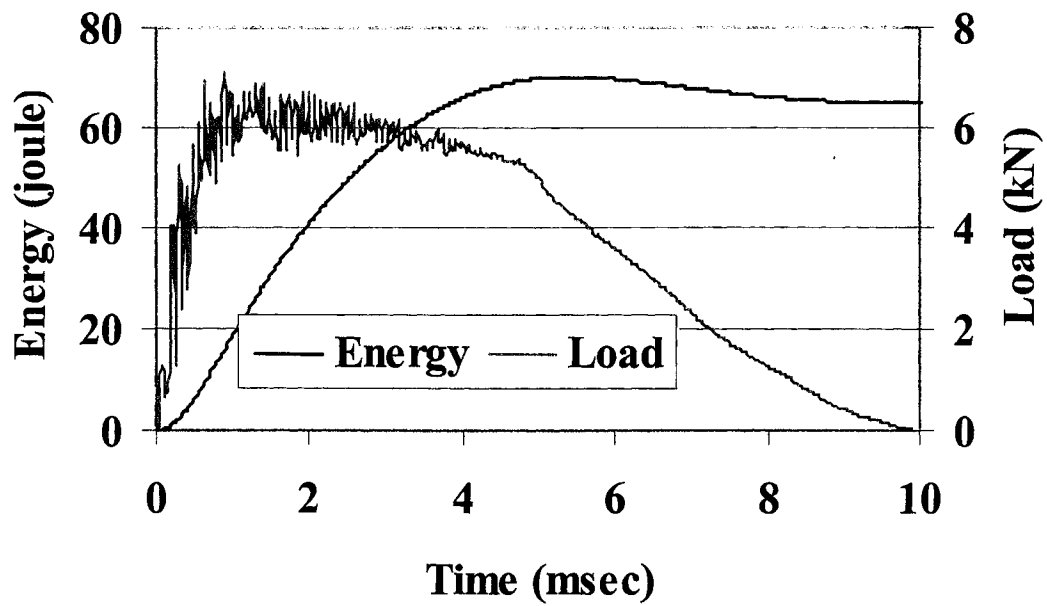


Figure 15. Typical force/energy – time curves for carbon/nylon 6 composite material exposed to UV for 600 h.

GENERAL SUMMARY

The aerospace, automotive, and mass transit sectors have steadily increased the use of composites for large-scale structures. The development of novel and cost effective technologies and materials has made composite structures a viable alternative to traditional materials. In this study a novel way to produce carbon-reinforced PA6 resin composite structures has been developed. The advantages of using a thermoplastic resin in the traditional thermoset domain can be exploited. It increases the alternatives that are available to engineers and designers of composite structures, especially where high toughness was a limiting constraint with thermoset resin structures.

VARTM, a method that is well established for thermosetting resin composites, was successfully modified and developed to infuse carbon fabric preforms with nylon 6, a thermoplastic resin. The methodology, processing parameters, and limitations were successfully established. Optical microscopy and SEM showed that good fiber impregnation was achieved at both the tow and filament levels.

The processing conditions developed yielded a relatively high (40-44%) degree of crystallinity of the nylon 6. A high (approximately 98%) degree of conversion from monomer to polymer was also achieved. A fiber weight percent of between 62 to 66%, with no visible (OM and SEM) void content, was achieved.

XRD and DSC studies showed that only the more stable α crystal structure was present and there were no peaks corresponding to the γ crystal structure. The tensile tests yielded similar results for both composite systems for the modulus, with an 11% increase

in the ultimate yield strength for the carbon/PA6 system. The carbon/SC-15 system performed 21% better in flexure than the carbon/PA6 system. The failure in the carbon/PA6 system was more ductile. The SBSS was 6% lower for the carbon/PA6 than for the carbon/SC-15 composite. This is possibly due to moisture absorption by the samples, as no particular care was taken to keep them dry or dry them before testing.

The main advantage of using thermoplastics over thermosets is the resistance to impact. The impact studies revealed that the peak load, initiation energy, and propagation energy were 13, 53, and 21% higher for the carbon/PA6 system as compared to the carbon/SC-15 system. The energy absorption characteristics were superior at all energy levels tested.

One of the major disadvantages of PA6 is its susceptibility to absorb moisture, which could reduce the properties of the structure. In this study the samples were immersed in boiling water until equilibrium uptake was reached, which is an exceptionally harsh condition. The equilibrium moisture content was reached after immersion in distilled water at 100°C for 100 h. SEM images showed that surface micro-cracks due to processing had expanded and the fiber matrix interface was attacked by the water ingress. The dual Fickian model for bidirectional composite developed by Bao and Yee [46] showed good correlation to the experimental results for water absorption.

DSC studies showed that the moisture ingress did not have any influence on the melting peaks or the crystallinity of the composite. The flexural properties are lowered by 45% due to water absorption; however, the material recovers to within 10% after drying. The SBSS, a matrix dominated property, is lowered by 65% due to water ingress, and only recovers to 47% after drying. Low-velocity impact shows that the damage to the

samples exposed to moisture performs much lower than the as-processed dry samples. The main contributing factor to the lowering of the mechanical properties is the plasticization of the matrix and the attack on the fiber matrix interface by the water.

Exposure to UV for up to 600 h caused yellowing of the samples. The crystallinity increased from 40 to 44% due to UV exposure. However, this was only on the surface of the samples. 600 h of exposure to UV did not have any effect on the flexural, interlaminar shear strength or impact properties of the composite. The time of exposure will have to be significantly increased before the properties start to deteriorate.

The main contribution of this study is to provide designers and engineers a thermoplastic material for large-scale composite structures. The comprehensive studies on the mechanical and thermal properties provide a good indication of the possible use of these materials, especially where toughness is a high requirement. The limitations with regard to environmental exposure are also presented to complete the study.

FUTURE WORK

The development of a process to use liquid molding techniques for infusion of thermoplastic resins offers several opportunities for future investigations. The following are some areas that could be further investigated:

- Infusion of other fabrics, such as glass and aramid, with PA6 resin.
- Investigation of other resins that can be polymerized in-situ.
- Addition of nanoclays and/or carbon nanotubes to improve barrier and mechanical properties.
- Investigation of the synergistic effects of the different environmental aspects that the composite has to withstand.

GENERAL LIST OF REFERENCES

1. Hartness, T., Husman, G., Koenig J., and Dyksterhouse J. (2001). The Characterization of Low Cost Fiber Reinforced Thermoplastic Composites Produced by the Drift Process, *Composites: Part A*, **32**: 1155-1160.
2. Composite Fabricators Association, www.cfa-hq.org.
3. Thomason, J.L. and Vlug, M.A. (1996). Influence of Fiber Length and Concentration on the Properties of Glass Fibre-reinforced Polypropylene: 1. Tensile and Flexural Modulus, *Composites: Part A*, **27A**: 477-484.
4. Bush, S.F., Torres, F. G. and Methven, J. M. (2000). Rheological Characterization of Discrete Long Glass Fibre (LGF) Reinforced Thermoplastics, *Composites: Part A*, **31**: 1421-1431.
5. Brouwer, W.D., van Herpt, E.C.F.C., Labordus, M. (2003). Vacuum Injection Molding for Large Structural Applications, *Composites: Part A*, **34**: 551-558.
6. Williams, C., Summerscales, J. and Grove, S., (1996). Resin Infusion under Flexible Tooling (RIFT): A Review, *Composites: Part A*, **27A**: 517-524.
7. Schlack, P. and German, Patent 748,253 (1938); U.S. Patent 2,241,321 (1941).
8. Joyce, R.M. and Ritter, D.M. (1941). U.S. Patent 2,251,519.
9. Hanford, W.E. and Joyce, R.M. (1948). Polymeric Amides from Epsilon-Caprolactam, *Journal of Polymer Science*, **3**:167-172.
10. Reimschuessel, H.K. (1977). Nylon 6 Chemistry and Mechanisms, *Journal of Polymer Science: Macromolecular Reviews*, **12**: 65-139.
11. Sibal, P.W., Camargo, R.E. and Macosko, C.W. (1982). Designing Nylon 6 Polymerization for RIM, In: *Proceedings of the Second International Conference on Reactive Processing of Polymers*, pp. 97-125, Pittsburgh, Pennsylvania.
12. Mooij, H. (1991). *SRIM Nylon Composites, Advanced Materials: Cost Effectiveness, Quality Control, Health and Environment*, SAMPE/Elsevier Science Publishers, BV.
13. Gabbert, J.D. and Hedrick, R.M. (1984). Advances in Systems Utilizing NYRIM Nylon Block Copolymers for Reaction Injection Molding, *Polymer Process Engineering*, **4**: 359-373.

14. Gabbert, J.D. and Wohl, M.H. (1985). Nylon 6 RIM, *ACS Symposium Series*, pp. 135-162.
15. Dupre, C.R., Gabbert J.D. and Hedrick R.M. (1984). *Review of Properties and Processing Characteristics for Nylon Block Copolymer RIM*, Vol. 25, p. 296, Polymer Preprints, Division of Polymer Chemistry, America Chemical Society.
16. Gabbert, J.D., Garner, A.Y., and Hedrick, R.M. (July 1983). Reinforced Nylon 6 Block Copolymers, *Polymer Composites*, **4**:196-199.
17. Zingraff, L., Bourban, P.E., Wakeman, M.D., Kohler, M. and Manson, J.A.E. (2002). Reactive Processing and Forming of Polyamide 12 Thermoplastic Composites, In: *23rd Europe SAMPE Conference Proceedings*, pp. 237-248.
18. Luise, A., Bourban, P.E. and Manson, J.A.E. (1999). *In Situ Polymerization of Polyamide 12 for Thermoplastic Composites*, ICCM-12, Paris.
19. Ciovacco, J. and Winckler, S.J. (2000). Cyclic Thermoplastic Properties and Processing, In: *45th International SAMPE Symposium*, Long Beach, CA.
20. Parton, Hilde and Verpoest, Ignass (2003). *Reactive Processing of Textile Reinforced Thermoplastics*, ICCM 14, San Diego, CA.
21. van Rijswijk, K., Vlasveld, D.P.N., Brsee, H.E.N. and Picken, S.J. (2003). Vacuum Injection of Anionic Polyamide 6, In: *Proceedings of ICCST 4*, Durban, South Africa.
22. Vlasveld, D.P.N., Van Rijswijk, Bersee, H.E.N., Beukers, A. and Picken, S.J.N. (2003). *Process Considerations for Liquid Molding of Composites Based on Anionic Polyamide 6*, ICCM 14, San Diego, CA.
23. Sebenda J. (1978). Recent Progress in the Polymerization of Lactams; Review, *Progress in Polymer Science*, **6**: 123-167.
24. Kim. K.J., Hong. D.S. and Tripathy. A.R. (1997). Kinetics of Adiabatic Copolymerization of ϵ -Caprolactam in the Presence of Various Activators, *Journal of Applied Polymer Science*, **66**: 1195-1207.
25. Petrov, P., Jankova, K. and Mateva, R. (2003). Polyamide-6-b-Polybutadiene Block Copolymers: Synthesis and Properties, *Journal of Applied Polymer Science*, **89**: 711-717.
26. Murthy, N.S., Kagan, V.A. and Bray, R.G. (2003). Optimizing the Mechanical Performance in Semi-Crystalline Polymers: Roles of Melt Temperature and Sin-Core Crystalline Morphology of Nylon, *Journal of Reinforced Plastics and Composites*, **22**: 685-693.

27. Udipi, K., Dave, R.S., Kruse, R.L. and Stebbins, L.R. (1997). Polyamides from Lactams via Anionic Ring-opening Polymerization: 1. Chemistry and Some Recent Findings, *Polymer*, **38**: 927-938.
28. Udipi, K., Dave, R.S., Kruse, R.L. and Stebbins, L.R. (1997). Polyamides from Lactams via Anionic Ring-opening Polymerization: 1. Kinetics, *Polymer*, **38**: 939-947.
29. Udipi, K., Dave, R.S., Kruse, R.L. and Stebbins, L.R. (1997). Polyamides from Lactams via Anionic Ring-opening Polymerization: 1. Rheology, *Polymer*, **38**: 949-954.
30. Muskat, I.E. (1950). U.S. Patent 2,495,640.
31. Gotch, T.M. (Nov., 1978). Improved Production Process for Manufacture of GRP on British Rail, *11th Reinforced Plastics Conference*, Brighton, pp. 33-39.
32. Gotch, T.M. (Nov., 1980). Developments and Potential of Vacuum Impregnation Techniques for GRP Manufacture, *12th Reinforced Plastics Conference*, Brighton, pp. 25-31.
33. Gotch, T.M. (May 1985). Low Investment Alternatives to Hand Layup GRP Production. Hands Off GRP II, *Conference Plastics and Rubber Institute*, Brighton, pp. 1-11.
34. Valentin, D., Paray, F. and Guetta, B. (1987). The Hygrothermal Behaviour of Glass Fibre Reinforced PA66 Composites: A Study of the Effect of Water Absorption on Their Mechanical Properties, *Journal of Materials Science*, **22**: 46-56.
35. Ishak, Z.A.M. and Berry, J.P. (1994). Effect of Moisture Absorption on the Dynamic Mechanical Properties of Short Carbon Fiber Reinforced Nylon 6,6, *Journal of Polymer Composites*, **15**: 223-230.
36. Lin, Chi-Wen (1993). Effects of Moisture Absorption on the Impact Behavior of Unidirectional Carbon Fiber Reinforced Nylon 6 Composite, *Advanced Composites 93: Proceedings of the International Conference on Advanced Composite Materials*, pp. 597-602.
37. Woldesenbet, E., Gupta, N., and Vinson, J.R. (2002). Determination of the moisture effects on impact properties of composite materials, *Journal of Materials Science*, **37**: 2693-2698.
38. Roy, S., Dharani, L.R., Gupta, V. and Xu, W. (2000). Modeling of Hygrothermal and Aging Effects in Textile Composites, Collection of Technical Papers – AIAA/ASME/ASCE/AHS/ASC Structures, *Structural Dynamics and Materials Conference*, 1 n III, pp. 1809-1819.

39. Pang, S.S., Li, G., Helms, J.E. and Ibekwe, S.I. (2001). Influence of Ultraviolet Radiation on the Low Velocity Impact Response of Laminated Beams, *Composites: Part B*, **32**: 521-528.
40. Anrady, A.L., Hamid, S.H., Hu, X. and Torikai, A. (1998). Effects of Increased Solar Ultraviolet Radiation on Materials, *Journal of Photochemistry and Photobiology B: Biology*, **46**: 96-103.
41. Yano, S. and Murayama, M. (1981). Photo-oxidation of Nylon 6 Above 300 nm, *Polymer Photochemistry*, **1**: 177-190.
42. Magill, J.H. (1962). Crystallization Kinetics Study of Nylon 6, *Polymer*, **3**: 655-664.
43. van Rijswijk, I.K., Koppes, I.K., Bersee, H.E.N. and Beukers, A. (2004). *Processing Window for Vacuum Infusion of Fiber-reinforced Anionic Polyamide-6*, FPCM -7, pp. 71-76.
44. Pyda, M. (ed.) (1994). ATHAS Data Bank, <http://web.utk.edu/~athas/databank/>
45. Fornes, T.D. and Paul, D.R. (2003). Crystallization behavior of nylon 6 nanocomposites, *Polymer*, **44**: 3945-3961.
46. Bao, L.R. and Yee, A.F. (2002). Moisture Diffusion and Hygrothermal Aging in Bismaleimide Matrix Carbon Fiber Composites: part II-Woven and Hybrid Composites, *Composites Science and Technology*, **62**: 2111-2119.

**GRADUATE SCHOOL
UNIVERSITY OF ALABAMA AT BIRMINGHAM
DISSERTATION APPROVAL FORM
DOCTOR OF PHILOSOPHY**

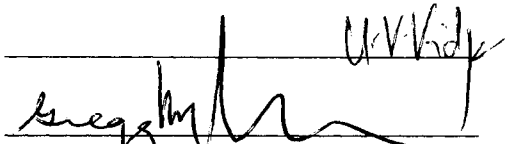
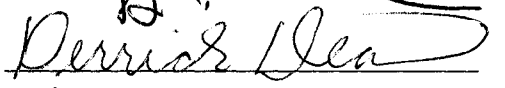
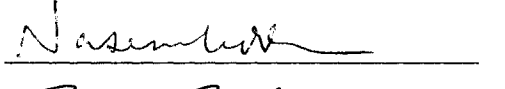


Name of Candidate Selvum Pillay

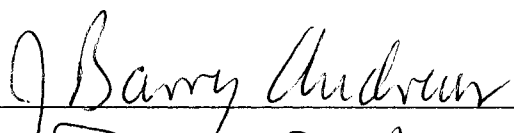
Graduate Program Materials Engineering

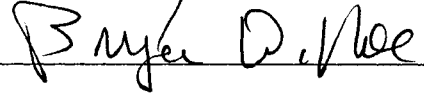
Title of Dissertation A Comprehensive Study of Woven Carbon Fiber
Reinforced Nylon 6 Composites

I certify that I have read this document and examined the student regarding its content. In my opinion, this dissertation conforms to acceptable standards of scholarly presentation and is adequate in scope and quality, and the attainments of this student are such that he may be recommended for the degree of Doctor of Philosophy.

Dissertation Committee:

Name	Signature
<u>Gregg M. Janowski</u> , Co-Chair	<u></u>
<u>Uday K. Vaidya</u> , Co-Chair	<u></u>
<u>Derrick R. Dean</u>	<u></u>
<u>Nasim Uddin</u>	<u></u>
<u>Mark L. Weaver</u>	<u></u>

Director of Graduate Program 

Dean, UAB Graduate School 

Date 12/22/05